

Vanessa Gomes Correia

**Green Synthesis of 2-Oxazoline-based Polymers
with Antimicrobial Activity using scCO₂**

Lisboa



FACULDADE DE
CIÊNCIAS E TECNOLOGIA
UNIVERSIDADE NOVA DE LISBOA

Green Synthesis of 2-Oxazoline-based Polymers with Antimicrobial Activity using scCO₂

Vanessa Gomes Correia

Thesis submitted to Faculdade de Ciências e Tecnologia - Universidade Nova de Lisboa
in partial fulfillment of the requirements for the obtention of the degree of
Master of Science in Biotechnology

Supervisor: Prof. Dr. Ana Aguiar-Ricardo

Monte da Caparica, 2009

ACKNOWLEDGMENTS

The successful development of this work was only possible due to many people that were around me and gave me all the support, help and bright advices that I needed at the right time.

Firstly, I would like to thank to my supervisor, Prof. Ana Aguiar Ricardo, who introduced me to the supercritical technology and alternative solvents and that latter gave me the opportunity of working on a supercritical lab. Thank you for providing me such an interesting and multidisciplinary work and for the precious orientations and advices!

I want to thank also to Dr^a Mariana Gomes de Pinho for receiving me at her lab at ITQB and for all the support, scientific sugestions and for providing me an *in vitro* side of the work.

To Dr^a Guilhermina Fragoso also my acknowledgments for receiving me at Instituto Superior de Ciências da Saúde Egas Moniz and for all the help.

To Dr. Vasco Bonifácio, thank you for being on my side in the lab and for giving me all the support I needed.

To Dr^a Teresa Casimiro for the always bright advices on the polymerization reactions and on *under pressure* issues!

To Prof. Susana Barreiros, my very special thank! Thank you for giving me the opportunity to be in this Master and in FCT!

To FCT's 510 lab team, thank you! To Mara (the one always with a smile! "Pfffff, there's a leak!"), Telma (the hyperactive supercritical of the lab), Eunice (the funny colleague and my partner at "fittings.ltd"), Rita (who provides *live music* in the lab all the time), Raquel (one of the younger members of the group but already great colleague) and Ricardo (the stronger and rupture disc-breaking man of the lab), thank you for being such good colleagues!

To ITQB's 506 lab team: a special thank to Ana Jorge and Pedro Matos! Both had a relevant role in the microbiology part of my work, always answering to my questions!

I would like to thank to Dr. Vivek Raje for the synthesis of bisoxazoline monomer, to Dr. João C. Lima to the advices in photoluminescence assays and to Dr^a Marta Andrade for the help in microwave-assisted polymerization. My acknowledgement also to laboratory of RMN at FCT-UNL and Analytical Services Laboratory of REQUIMTE.

Thank you also to all my friends and colleagues. You know who you are!

And finally, I want to thank to the special persons I carry in my heart: my parents Manuel and Paula, my sisters Nadine and Nádia, my brothers Manuel and Pedro and my grandparents Manuel and Ilda! You all know the important role you play in my life! And last but not the least, a special thanks to André for all the care and support.

ABSTRACT

Using a green methodology, 17 different poly(2-oxazolines) were synthesized starting from four different oxazoline monomers. The polymerization reactions were conducted in supercritical carbon dioxide under a cationic ring-opening polymerization (CROP) mechanism using boron trifluoride diethyl etherate as the catalyst. The obtained *living polymers* were then end-capped with different types of amines, in order to confer them antimicrobial activity. For comparison, four polyoxazolines were end-capped with water, and by their hydrolysis the linear poly(ethyleneimine) (LPEI) was also produced.

After functionalization the obtained polymers were isolated, purified and characterized by standard techniques (FT-IR, NMR, MALDI-TOF and GPC).

The synthesized poly(2-oxazolines) revealed an unusual intrinsic blue photoluminescence. High concentration of carbonyl groups in the polymer backbone is appointed as a key structural factor for the presence of fluorescence and enlarges polyoxazolines' potential applications.

Microbiological assays were also performed in order to evaluate their antimicrobial profile against gram-positive *Staphylococcus aureus* NCTC8325-4 and gram-negative *Escherichia coli* AB1157 strains, two well known and difficult to control pathogens. The minimum inhibitory concentrations (MIC)s and killing rates of three synthesized polymers against both strains were determined. The end-capping with *N,N*-dimethyldodecylamine of *living* poly(2-methyl-2-oxazoline) and poly(bisoxazoline) led to materials with higher MIC values but fast killing rates (less than 5 minutes to achieve 100% killing for both bacterial species) than LPEI, a polymer which had a lower MIC value, but took a longer time to kill both *E.coli* and *S.aureus* cells. LPEI achieved 100% killing after 45 minutes in contact with *E. coli* and after 4 hours in contact with *S.aureus*.

Such huge differences in the biocidal behavior of the different polymers can possibly underlie different mechanisms of action. In the future, studies to elucidate the obtained data will be performed to better understand the killing mechanisms of the polymers through the use of microbial cell biology techniques.

RESUMO

Utilizando uma metodologia alternativa, foram sintetizados 17 polioxazolinas a partir de quatro monómeros diferentes. As reacções de polimerização foram realizadas em dióxido de carbono supercrítico através de um mecanismo de polimerização catiónica via abertura de anel (CROP) e utilizando como iniciador o eterato de trifluoreto de boro. Os polímeros obtidos foram terminalmente funcionalizados com diferentes tipos de aminas, com o intuito de lhes conferir actividade antimicrobiana. Para comparação, foram também sintetizadas quatro polioxazolinas não funcionalizadas (terminação com água) e, através de hidrólise das polioxazolinas, foi produzido o polímero linear polietileneimina (LPEI).

Após a polimerização e funcionalização, os polímeros foram isolados, purificados e caracterizados pelas técnicas usuais (FT-IR, RMN, MALDI-TOF e GPC).

Os polímeros sintetizados revelaram uma fluorescência azul inesperada. A elevada concentração de grupos carbonilo na cadeia do polímero é apontada como o factor estrutural fundamental para a existência desta fluorescência intrínseca potenciando futuras aplicações das polioxazolinas.

Foram também efectuados ensaios microbiológicos de modo a avaliar o efeito antimicrobiano para as estirpes gram-positiva *Staphylococcus aureus* NCTC8325-4 e gram-negativa *Escherichia coli* AB1157, dois conhecidos e importantes microorganismos patogénicos. A concentração mínima inibitória (MIC) e as curvas de morte dos polímeros sintetizados foram determinadas para ambas as estirpes. A funcionalização com *N,N*-dimetildodecilamina dos *polímeros vivos* de poli(2-metil-2-oxazolina) e poli(bisoxazolina) originaram materiais com valor de MIC mais elevado e velocidades de morte mais rápidas (inferiores a 5 minutos para reduzir 100% a viabilidade de ambas as estirpes) enquanto que o LPEI, o polímero com valor de MIC mais baixo, reduz a viabilidade de *E.coli* e de *S.aureus* após 45 minutos e 4 horas em contacto com a estirpe, respectivamente.

Valores de MIC e tempos de acção tão distintos podem provavelmente ser justificados pela diferença ao nível dos mecanismos de acção do polímero. No futuro, serão desenvolvidos alguns estudos para elucidar estes mecanismos, nomeadamente através de técnicas de biologia celular e de microscopia de fluorescência.

ABBREVIATION LIST

BisOx – bisoxazoline monomer
CFU – Colony-Forming Units
CROP – Cationic Ring-Opening Polymerization
DABCO – 1,4 – diazabicyclo[2.2.2]octane
DDA – *N,N*-dimethyldodecylamine
DMF - dimethylformamide
E.coli – *Escherichia coli*
EtOx – 2-ethyl-2-oxazoline monomer
FT-IR – Fourier Transform Infrared
GPC – Gel Permeation Chromatography
HiP – High Pressure
IM – Inner Membrane
LPEI – Linear poly(ethyleneimine)
MALDI-TOF – Matrix Assisted Laser Desorption/Ionization Time-Of-Flight
MCHA – *N*-methylcyclohexylamine
MDA – *N*-methyldioctylamine
MeOTs – methyl *p*-toluenesulfonate
MetOx – 2-methyl-2-oxazoline monomer
MI – *N*-methylimidazole
MIC – Minimum Inhibitory Concentration
NMR – Nuclear Magnetic Resonance
OD – Optical Density
OM – Outer Membrane
PBisOx – poly(bisoxazoline)
PEtOx – poly(2-ethyl-2-oxazoline)
PG – peptidoglycan
PI – Propidium Iodide
PhOx – 2-phenyl-2-oxazoline monomer
PMetOx – poly(2-methyl-2-oxazoline)
PPhOx – poly(2-phenyl-2-oxazoline)
S.aureus – *Staphylococcus aureus*
scCO₂ – supercritical carbon dioxide
SCF – Supercritical Fluids
SEM – Scanning Electron Microscopy

CONTENTS

Acknowledgments.....	i
Abstract	iii
Resumo	iv
Abbreviation list	v
Contents	vi
Index of Figures	viii
Index of Tables	xii
Chapter 1 – 2-oxazoline-based polymer synthesis and functionalization	1
1.1 Overview.....	1
1.2 Introduction.....	1
1.2.1 Supercritical Fluids (SCF)	2
1.2.2 Polymerization and polymer processing in scCO ₂	4
1.2.3 Synthesis of 2-oxazoline-based polymers	6
1.2.4 End-capping of <i>living</i> poly(2-oxazoline)s	8
1.2.5 Linear poly(ethyleneimine), LPEI	9
1.3 Experimental Methods	10
1.3.1 Materials and Instrumentation	10
1.3.2 Polymer synthesis in scCO ₂	11
1.3.2.1 Experimental apparatus	11
1.3.2.2 Preparation of the <i>living polymers</i>	11
1.3.2.3 <i>Living polymer</i> end-capping with water	12
1.3.2.4 <i>Living polymer</i> end-capping with amines.....	13
1.3.2.5 Preparation of linear poly(ethyleneimine).....	13
1.3.3 Microwave-assisted synthesis of PMetOx	14
1.3.3.1 Preparation of the poly(2-methyl-2-oxazoline) <i>living polymer</i> ...	14
1.3.3.2 <i>Living polymer</i> end-capping with <i>N,N</i> -dimethyldodecylamine ...	14
1.4 Results and Discussion.....	16
1.4.1 Synthesized 2-oxazoline-based polymers	16
1.4.2 Polymer characterization.....	17
1.4.3 Scanning electron microscopy, SEM.....	27
1.4.4 Intrinsic blue photoluminescence	28
1.5 Conclusion	34

1.6 References	35
Chapter 2 – Characterization of the antimicrobial effect of functionalized 2-oxazoline-based polymers	38
2.1 Overview.....	38
2.2 Introduction.....	38
2.2.1 Mechanisms of resistance of antimicrobial agents	39
2.2.2 Mechanisms of action of antibacterial agents.....	39
2.2.3 Pathogenic relevance of <i>E.coli</i> and <i>S.aureus</i>	44
2.2.4 Characterization of antimicrobial effect	44
2.3 Experimental Methods	49
2.3.1 Bacterial strains and growth conditions	49
2.3.2 Disc diffusion technique	49
2.3.3 MIC determination.....	49
2.3.4 Killing curves.....	50
2.3.5 Fluorescence microscopy	50
2.4 Results and Discussion.....	51
2.4.1 Disc diffusion technique	51
2.4.2 MIC determination.....	53
2.4.3 Killing curves.....	56
2.4.4 Fluorescence microscopy	61
2.5 Conclusion.....	65
2.6 References	66
Future Work.....	69
Appendix Section.....	71

INDEX OF FIGURES

Chapter 1

- Figure 1.1** Schematic pressure-temperature phase diagram of a pure substance showing the supercritical fluid (SCF) region. The triple point (T) and critical point (C) are marked. The diagram also shows the variation in density of the substance in the different regions (adapted from ref. 4) 2
- Figure 1.2** Schematic phase diagram of CO₂ with snapshots of the observed changes from a liquid-gas equilibrium to the supercritical region (adapted from ref. 5)..... 4
- Figure 1.3** General method for the synthesis of polymers in scCO₂. The monomer and initiator are added to a high-pressure cell and CO₂ is introduced. The reactor is heated, a supercritical phase occurs and polymerization starts. After polymerization is complete, polymer precipitates and CO₂ is released from the high pressure cell. (adapted from ref. 4) 5
- Figure 1.4** Schematic representation of the experimental apparatus. 1- CO₂ cylinder; 2 – high pressure pump; 3 – line filter; 4- check valve; 5 – high pressure transducer; 6 – rupture disc; 7 – thermostatted bath; 8 – syringe; 9 – HPLC high-pressure valve; 10- high pressure visual cell; 11- immersible stirrer; 12 – schlenk; 13 – vent; V1 to V12 – HIP high pressure valves; V4 and V5 – gas inlet (argon or nitrogen) or vacuum exit; V9 – vacuum exit (adapted from ref. 1) 11
- Figure 1.5** Green synthesis of 2-oxazoline-based polymers and its functionalization by amine end-capping..... 12
- Figure 1.6** Chemical structures of the amines used in living polymer end-capping 13
- Figure 1.7** Chemical structure of DABCO..... 13
- Figure 1.8** Real apparatus of LPEI preparation 14
- Figure 1.9** Microwave assisted synthesis of poly(2-methyl-2-oxazoline) followed by end-capping with N,N-dimethyldodecylamine..... 15
- Figure 1.10** SEM micrographs of LPEI powder obtained by acid hydrolysis of PMetOx-DDA 27
- Figure 1.11** SEM micrographs of LPEI after liophilisation of their aqueous solution 28
- Figure 1.12** Left glass vial: pure water. Right glass vial: strong fluorescence phenomenon of PMetOx-DDA_{mw} in aqueous solution under UV lamp..... 28

Figure 1.13 Absorption spectra of the synthesized 2-methyl-2-oxazoline-based polymers	29
Figure 1.14 Fluorescence emission spectra of the 2-methyl-2-oxazoline-based polymers	30
Figure 1.15 Absorption spectra of the synthesized 2-ethyl-2-oxazoline-based polymers	30
Figure 1.16 Fluorescence emission spectra of 2-ethyl-2-oxazoline-based polymers	31
Figure 1.17 Absorption spectra of synthesized 2-phenyl-2-oxazoline-based polymers ...	31
Figure 1.18 Fluorescence emission spectra of the 2-phenyl-2-oxazoline-based polymers	32
Figure 1.19 Absorption spectra of synthesized the bisoxazoline-based polymers	32
Figure 1.20 Fluorescence emission spectra of the bisoxazoline-based polymers.....	33

Chapter 2

Figure 2.1 Chemical structures of the main phospholipid components of bacterial membranes.(adapted from ref. 4).....	40
Figure 2.2 Molecular composition of gram positive and gram-negative bacteria. Main differences in evidence: peptidoglycan thickness and the presence of outer membrane (OM) in gram-negative bacteria (adapted from ref. 5)	40
Figure 2.3 Structural differences between the E.coli and the S.aureus peptidoglycans. The basic unit of the petidoglycan is composed by β -1,4-linked N-acetylglucosamine (GlcNAc) and N-acetylmuramic acid (MurNAc). (adapted from ref. 7)	41
Figure 2.4 Models of transmembrane channel formation. Antimicrobial agent associates to the membrane surface (A) and accumulates (B). Once a critical antimicrobial agent/lipid ratio is reached, an insertion into the membrane is observed, with the formation of barrel-stave type pore (C) or formation of localized toroidal pores (D). (adapted from ref. 10).....	42
Figure 2.5 Model of membrane disruption by the carpet mechanism. The antimicrobial agent binds (A) and accumulates (B) in the membrane surface. Continued accumulation and covering (“carpeting”) of the bilayer (C) leads to a detergent-like disintegration (D) (adapted from ref. 10)	43
Figure 2.6 Proposed mechanism of membrane disruption by the polymers in the literature (adapted from ref.12)	43

Figure 2.7 Typical bacterial growth curve at constant temperature conditions with three main phases shown. n_0 represents the initial population density, n_{max} the maximum population density, μ_{max} the maximum specific growth rate and λ the lag parameter (adapted from 20)	46
Figure 2.8 Schematic diagram that illustrates some approaches used in the assessment of bacterial viability (adapted from ref. 25)	47
Figure 2.9 Chemical structure of PI	47
Figure 2.10 Disc diffusion test. Two polymers showing antimicrobial activity (with inhibition zones well defined) and two polymers that do not impair bacterial growth are shown in the image.....	53
Figure 2.11 MIC of the water soluble 2-oxazoline-based polymers and also of two polymers referred in the literature, for E.coli and S.aureus	54
Figure 2.12 Bacterial growth after the addition of the polymers. The decrease in the optical density (600 nm) of E.coli in the presence of PmetOx-DDA and PBisOx-DDA after 4 and 10 minutes and stabilization of the bacterial growth during 45 minutes in the presence of LPEI can be seen. Time t=0 minutes represents the addition of the polymer. Assays were done in duplicate (1 and 2 for each polymer).....	57
Figure 2.13 Number of viable cells per mL after the addition of the polymers. The reduction in the number of viable E.coli in the presence of PmetOx-DDA and PBisOx-DDA during 10 minutes and LPEI during 45 minutes of assay can be seen in a logarithmic scale. PmetOx-DDA and PBisOx-DDA assays are overlapped in the graph, showing identical behaviour. The value of the initial viable cells (10^8 cells) is an estimated value. Time t=0 minutes represents the addition of the polymer. Assays were done in duplicate (1 and 2 for each polymer)..	58
Figure 2.14 Bacterial growth after the addition of the polymers. The reduction in the optical density (600 nm) of S.aureus in the presence of PmetOx-DDA and PBisOx-DDA after 4 and 10 minutes and the stabilization of the bacterial growth during 240 minutes in the presence of LPEI can be seen. Inset shows PmetOx-DDA and PBisOx-DDA assays in detail. Time t=0 minutes represents the addition of the polymer. Assays were done in duplicate (1 and 2 for each polymer)	59
Figure 2.15 Number of viable cells per mL after the addition of the polymers. The reduction in the number of viable S.aureus in the presence of PmetOx-DDA and PBisOx-DDA during 10 minutes and of LPEI during 240 minutes of assay can be seen in a logarithmic scale. PmetOx-DDA and PBisOx-DDA assays are overlapped in the graph, showing identical behaviour. The value of the initial viable cells (10^8 cells) is an estimated value. Inset shows	

PMetOx-DDA and PBisOx-DDA assays in detail. Time t=0 minutes represents the addition of the polymer. Assays were done in duplicate (1 and 2 for each polymer) 60

Figure 2.16 Fluorescence labeling with propidium iodide for assessment of cell viability. **A** and **B**: cells of E.coli AB1157 visualized by phase-contrast and fluorescence microscopy using Texas Red filter, respectively, in the absence of any polymer. **C** and **D**: same cells incubated with PMEtOx-DDA during 5 minutes. **E** and **F**: same cells incubated with PBisOx-DDA **4a** during 5 minutes. **G** and **H**: same cells incubated with LPEI during 30 minutes. Dead cells are seen as fluorescent on right panels 62

Figure 2.17 Fluorescence labeling with propidium iodide for assessment of cell viability. **A** and **B**: cells of S.aureus NCTC 8325-4 visualized by phase-contrast and fluorescence microscopy using Texas Red filter, respectively, in the absence of any polymer. **C** and **D**: same cells incubated with PMEtOx-DDA during 5 minutes. **E** and **F**: same cells incubated with PBisOx-DDA during 5 minutes. **G** and **H**: same cells incubated with LPEI during 240 minutes. Dead cells are seen as fluorescent on right panels 63

Appendix Section

Appendix 1 $^1\text{H-NMR}$ spectrum (400 MHz, CDCl_3) of PMetOx-DDA	72
Appendix 2 $^1\text{H-NMR}$ spectrum (400 MHz, D_2O) of LPEI	73
Appendix 3 FT-IR spectrum (NaCl) of PMetOx-DDA	74
Appendix 4 FT-IR spectrum (NaCl) of LPEI	75
Appendix 5 MALDI-TOF spectrum (dithranol) of PMetOx-DDA _{mw}	76
Appendix 6 MALDI-TOF spectrum (dithranol) of LPEI	77

INDEX OF TABLES

Chapter 1

Table 1.1 Temperature and pressure critical conditions of some substances (adapted from ref. 2)	3
Table 1.2 Effect of temperature, pressure and monomer/initiator ratio in the polymerization reaction of 2-substituted-2-oxazoline in scCO ₂ (adapted from ref. 1).....	7
Table 1.3 Schematic representation of the synthesized 2-oxazoline-based polymers.....	16

Chapter 2

Table 2.1 Evaluation of the presence or absence of antimicrobial activity determined by disc diffusion technique (see polymers reference in table 1.3) Results of each polymer were identical to all 7 microorganism tested. ✓=presence of an inhibition halo; ✕= no inhibition halo present	51
Table 2.2 MIC determination of water soluble 2-oxazoline-based polymers.....	53

Chapter 1 – 2-OXAZOLINE-BASED POLYMER SYNTHESIS AND FUNCTIONALIZATION

1.1 OVERVIEW

This section describes the green synthesis of 2-oxazoline-based polymers and their functionalization using scCO₂ technology.

The synthetic method consists in a cationic ring opening polymerization (CROP), using boron trifluoride etherate (BF₃.Et₂O) as the catalyst. The polymerization is performed using CO₂ as the solvent under supercritical conditions. The pressure, temperature and monomer to catalyst feed ratio of the polymerizations was based on previously established conditions.¹ The CROP methodology produces *living polymers* which allows the end-capping of poly(2-oxazolines) with different types of amines. This functionalization allow the tuning of the polymers antimicrobial activity, a goal of the present work that will be later investigated (chapter 2).

The aim of this chapter is to investigate whether a scCO₂-based process can be successfully employed in the synthesis of antimicrobial 2-oxazoline-based polymers and also to obtain a library of amine end-capped polyoxazolines.

Characterization and analysis of the polymers will be performed using FT-IR, NMR, GPC and MALDI-TOF along with microbiological techniques (chapter 2).

1.2 INTRODUCTION

This section describes the production of 2-oxazoline-based polymers which are potentially suitable for use as antimicrobial materials. The chosen methodology takes advantage of the unique properties of scCO₂.

The process that was used to produce 2-oxazoline-based polymers generates well defined polymers of narrow average molecular weight distributions by using an alternative synthesis. Since no organic solvents are employed it constitutes a greener approach and a cleaner process to the environment.

This is important as long as the environment issues concerns are growing nowadays and industries are looking forward to have new and cleaner alternatives relatively to the existing processes.

1.2.1 Supercritical fluids (SCF)

The use of supercritical fluids has been investigated continuously in recent years since they exhibit interesting physical properties.

The definition of a supercritical fluid usually begins with a phase diagram, which defines the critical temperature and pressure of a substance (figure 1.1).

For a pure substance, the critical point marks the end of the vapour-liquid coexistence curve. Above that critical point (with defined temperature and pressure), neither liquid or gas phases exist; instead, a poorly defined phase, known as a supercritical region, occurs. Then, a homogeneous and opalescent system without a phase separation takes place. Such fluids have the gas-like characteristic of compressibility, diffusivity and low viscosity, and the liquid-like characteristic of high density and solubilization power. The SCF characteristics can be tuned by simply changing the pressure or temperature, being this possibility a great advantage in several processes.^{2,3}

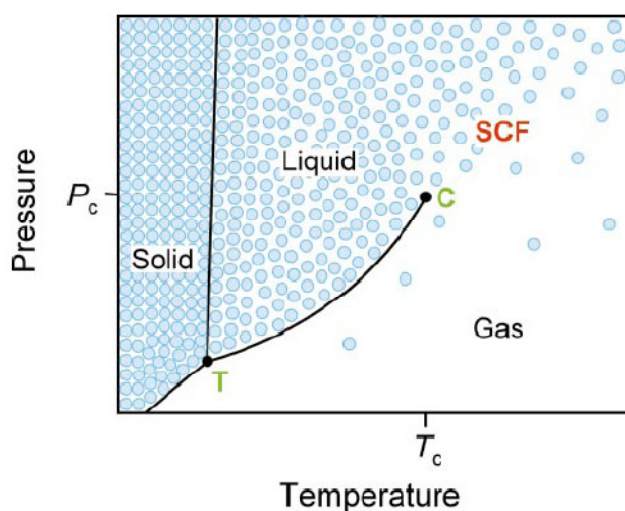


Figure 1.1 Schematic pressure-temperature phase diagram of a pure substance showing the supercritical fluid (SCF) region. The triple point (T) and critical point (C) are marked. The diagram also shows the variation in density of the substance in the different regions (adapted from ref. 4).

All pure substances can form SCF above their respective critical points but higher values of temperature and pressure can limit some processes, being of particularly importance the correct choice of what SCF should be used (table 1.1).

Table 1.1 Temperature and pressure critical conditions of some substances (adapted from ref. 2).

Solvent	T _c / °C	P _c / bar
Carbon dioxide	31.0	73.8
Ethane	32.3	48.7
Methanol	239.6	80.9
<i>n</i> -hexane	234.5	30.1
Water	374.3	221

In particular, supercritical CO₂ (scCO₂) is the most used, being frequently promoted as a green solvent with many advantages over conventional solvents. ScCO₂ is a non-flammable, non-toxic, chemically inert and readily accessible solvent and simple depressurization results in its removal. In addition, its physical properties can be tuned by manipulation of the temperature and pressure.^{5,6}

ScCO₂ has been receiving increasing attention as a reaction medium in alternative to common and environmentally unattractive organic solvents. Although carbon dioxide is a greenhouse gas, it is an abundant material in the environment and can be extracted from the atmosphere, be used as an alternative solvent and later released again to the environment, completely clean from any chemicals used in the process. However, commercial CO₂ later on employed in a process is usually not captured from the atmosphere, but in fact obtained as a byproduct of the commercial ammonia process. This process can be considered as a process that prevents pollution once it avoids the emission of CO₂ to the atmosphere.⁷

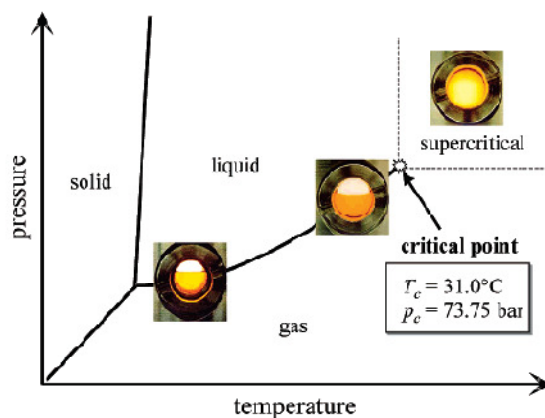


Figure 1.2 Schematic phase diagram of CO₂ with snapshots of the observed changes from a liquid-gas equilibrium to the supercritical region (adapted from ref. 5).

1.2.2 Polymerization and polymer processing in scCO₂

Supercritical fluids have a great potential in polymer processing, providing some key advantages when compared to the conventional methods. Although there are significant costs associated with polymer processing under high pressures, the advantages of this type of polymerization add significant value to the final processed products.²

ScCO₂ and its distinctive properties allowed it to emerge as the most extensively studied supercritical fluid for polymerization reactions.

One of the key advantages of the use of scCO₂ in polymerizations is the weak ability of interaction between CO₂ and the functional groups in polymers. For polymerization reactions performed in supercritical fluids, the mass transfer for mixing reactants plays an important role in the entire process, in order to allow proper contact between monomer and catalyst, having, then, a significant influence on the yield and selectivity of a large range of chemical processes.²

Another advantage is the “solvent-free” nature of scCO₂ that makes it an ideal choice for the processing of pharmaceutical and biomedical materials, materials that are under a strong control over product integrity and presence of harmful solvent residues. By that reason, scCO₂ has stimulated several studies, since industries are becoming increasingly more aware of environmental issues.

Carbon dioxide is also a good solvent for most non-polar and some polar molecules of low molar mass but it is a poor solvent for most high molar mass polymers under mild conditions (<100 °C, <350 bar), being the only polymers that show good solubility in CO₂ under this

conditions, fluoropolymers and silicones.⁸ This fact generally permits the precipitation of the polymer in high pressure reactor. Consequently, polymers can be isolated from the reaction media by simple depressurization (with removal of unreacted monomer and catalyst), resulting in a dry clean product (figure 1.3).⁸ This feature corresponds to a potential cost and energy saving since it decreases the energy used and eliminates purification steps (drying and purification) required in polymer manufacturing to remove the solvent.⁸

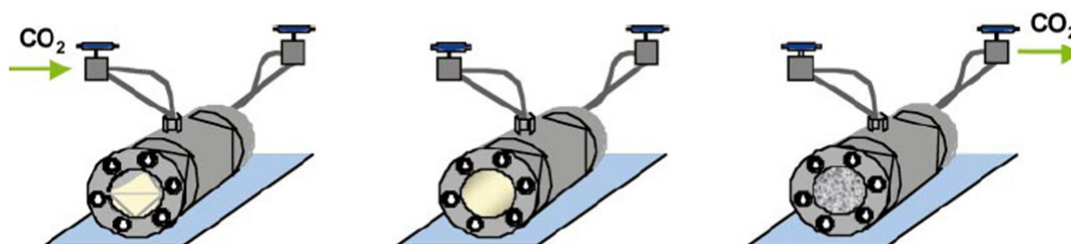


Figure 1.3 General method for the synthesis of polymers in scCO₂. The monomer and initiator are added to a high-pressure cell and CO₂ is introduced. The reactor is heated, a supercritical phase occurs and polymerization starts. After polymerization is complete, polymer precipitates and CO₂ is released from the high pressure cell. (adapted from ref.4)

Classification of polymerization reactions. Polymerizations can be classified as chain growth and step-growth polymerizations. The main types of chain-growth polymerization include free-radical, cationic, anionic, and metal-catalyzed reactions. The majority of polymerizations in scCO₂ are focused on free-radical polymerizations, but there are a number of reports in the areas of cationic and metal-catalyzed reactions.⁸

In this work it was used a chain growth polymerization through a cationic ring opening mechanism and for that reason this is the type in focus here.

Cationic polymerizations are a challenging area in polymer science. *Living* cationic polymerization methods have been developed in order to produce polymers with a high control of molecular weight, molecular weight distribution, reactivity and end group functionalization by stabilization of the active carbocation through nucleophilic interactions. This stabilization is generally achieved by association of a nucleophilic counterion or with a Lewis base since it avoid side reactions. Studies have shown that CO₂ is inert in this type of polymerization.⁸

1.2.3 Synthesis of 2-oxazoline-based polymers

There are many publications describing the polymerization of polyoxazolines. Polyoxazolines of various architectures and chemical functionalities can be prepared in a *living* and controlled manner via cationic ring-opening polymerization (CROP). Monomers substituted in the 4- and 5-position are more difficult to polymerize due to steric hinderance,⁹ the reason why 2-substituted oxazolines were chosen in this work.

Oxazoline-based polymers are biodegradable, relatively non-toxic and generally water soluble. Due to their versatility and ability to form functional materials, this class of polymer are interesting candidates for use in a large number of applications, such as smart materials, membrane structures, drug carriers, synthetic vectors for DNA or RNA delivery and antimicrobial agents.⁹

Although, 2-oxazoline-based polymers have not found widespread commercial application due, in part, to their polymerization times ranges (reactions times can vary from several hours to several days).⁹ This disadvantages can be overcome with the use of supercritical fluid or microwave technologies. These methods lead to less side reactions and maintain the *living* character of the reaction, using a higher temperature and pressure.

The polymerization starts with a nucleophilic attack of the lone pair of the nitrogen of the 2-oxazoline ring onto an activated 2-oxazoline monomer (oxazolinium species formed by coordination of the 2-oxazoline monomer with the initiator). The nucleophilic attack of the second monomer unit onto the formed oxazolinium species leads to the ring opening by cleavage of the C–O bond. Due to the absence of chain-transfer or termination reactions under the appropriate conditions, the polymerization occurs in a *living* manner until all monomer is consumed or an end-capping agent is added.¹⁰

The interest in this class of polymers is increasing due to their particular characteristics and extensive applications in chemistry, biochemistry and pharmacology.¹¹ In this work, four different 2-oxazoline monomers were used; three are commercially available (2-methyl-2-oxazoline, 2-ethyl-2-oxazoline and 2-phenyl-2-oxazoline) and one was synthesized (bis-oxazoline, that leads to a branched polyoxazoline).

Conventional synthesis of 2-oxazoline-based polymers. Conventional polymerization of 2-substituted-2-oxazoline has been widely described in the literature. In a typical procedure, a solution of 2-substituted-2-oxazoline in acetonitrile and the initiator methyl *p*-

toluenesulfonate (MeOTs) is heated at 60 °C with stirring. The polyoxazoline is obtained as white powder, after purification by reprecipitation in diethyl ether and drying under vacuum.¹²

It is important to develop green alternatives to this process of synthesis due to the current shortage of acetonitrile, a common solvent used on a manufacturing scale in several processes, and mainly to avoid the use of organic solvents and purification steps.

Synthesis of 2-oxazoline-based polymers in scCO₂. The synthesis of 2-substituted-2-oxazolines in scCO₂ was already described in literature for three different monomers using boron trifluoride etherate (BF₃.OEt₂) as initiator. The effect of temperature, pressure and initial monomer/initiator molar ratio on the yield, average molecular weight and polydispersity of the synthesized polymers was also investigated. It was obtained, in all reactions, low molecular weight polymers in high yield (over 80%) with narrow molecular weight distribution. 2-Methyl- and 2-ethyl-2-oxazolines polymers were found to be water soluble while poly(2-phenyl-2-oxazoline) is only soluble in organic solvents.¹ This method was the one used in this work.

The table 1.2 describes the effect of such parameters in the polymerization reaction of 2-substituted-2-oxazoline in scCO₂ and summarizes some of the conditions used in the experimental part of this work.

Table 1.2 Effect of temperature, pressure and monomer/initiator ratio in the polymerization reaction of 2-substituted-2-oxazoline in scCO₂ (adapted from ref.1).

Monomer	T _c / °C	p _c / Mpa	[M]/[I]	Yield (%)
MeOx	60	16	15	94
	60	20	15	80
	70	16	15	93
EtOx	60	16	12	90
	70	17	12	94
	70	21	12	97
PhOx	60	16	10	95
	60	20	10	99
	70	16	10	99

Microwave-assisted synthesis of 2-oxazoline-based polymers. In the last decade, microwave irradiation has been developed to provide an effective alternative energy source

for conventional reactions and processes, leading to an exponential increase of publications in this area.

Microwaves are electromagnetic radiation with frequencies between 300 GHz and 300 MHz (with a wavelength in the range of 1 mm to 1 m) and have been widely used in heating materials for industrial and domestic purposes.¹³ Microwave irradiation, considered an environmentally-friendly process, offers some advantages over conventional heating, such as instantaneous and rapid bulk heating, direct heating, high temperature homogeneity and energy saving. This technology can provide an improvement in reaction rate, yield and selectivity of a certain process and it is nowadays widely used in polymerizations and polymer processing. Microwave irradiation is then a fast and effective method for polymerization, being with no doubt an alternative methodology.¹⁴

This type of polymerization can be used to obtain polymers with a higher molecular weight, when compared to the supercritical technology, maintaining the *living* character of the reaction as well as the possibility of further functionalization.

1.2.4 End-capping of *living* poly(2-oxazolines)

Most of the studies related with antimicrobial activity are based in compounds and materials possessing quaternary ammonium salts in their structure (although biguanide, phosphonium and sulphonium salts have also been used) since its antimicrobial activity has been known for decades.^{15,16}

The urgent need of antimicrobial materials has stimulated research in the last years in order to face the spreading of microbial infections and the increasing microbial resistance to antibiotics. The polymerization of 2-substituted-2-oxazoline *via* a *living* cationic ring-opening mechanism provides an extraordinary control of the morphology of the polymers as well as their later functionalization in order to obtain an ammonium-type end-capping.^{17,18}

In this work, the obtained *living polymers* were later end-capped with different types of amines (linear, branched, cyclic, acyclic, aliphatic and aromatic) producing the desired quaternary ammonium functionalization.

1.2.5 Linear poly(ethyleneimine), LPEI

Poly(ethyleneimine) is a polymer which contains nitrogen free groups in the backbone. Therefore, its functional backbone (with secondary amine groups) offers many possibilities for further chemical modifications.¹⁹ Moreover, it possesses a high number of advantages, such as chelating agent, good water solubility, and good physical and chemical stability.²⁰ Concerning biochemistry and medicine, further research involving PEI could throw light upon certain biological processes and bring interesting results for the treatment of diseases and infections.²⁰

Under normal physiological conditions (pH from 6.8 to 7.4), PEI is charged but has the capacity to protonate in certain acidic subcellular environments. Its potency as a gene delivery vector could be due to a direct charge-based interaction with the various biological barriers, such as negatively charged membranes that any polymeric drug delivery vehicle must traverse, which can result ultimately in destabilization of the membranes. It is also possible that PEI can influence indirectly a particular cell or subcellular compartment, for example, by acting as a proton sponge that causes ion influx and ultimately leads to membrane rupture.²¹

Linear PEI (LPEI) has been synthesized via the cationic ring-opening polymerization of *N*-(2-tetrahydropyranyl)aziridine²² or through an acid or base-catalysed hydrolysis of unsubstituted or 2-substituted-2-oxazolines.²³

Therefore, LPEI can also be synthesized by the hydrolysis of 2-substituted-2-oxazoline polymerized in scCO₂ leading this way to a low molecular weight linear polymer. Its use as an antimicrobial agent has been already described in the literature, being used in modified membranes,²⁴ as nanoparticles²⁵ and as a ligand.²⁰ However, its mechanism of action has not been yet described and the characterization of its effect has been not deeply studied.

1.3 EXPERIMENTAL METHODS

1.3.1 Materials and Instrumentation

The monomers 2-methyl-2-oxazoline (MetOx), 2-ethyl-2-oxazoline (EtOx) and 2-phenyl-2-oxazoline (PhOx), the initiator boron trifluoride diethyl etherate ($\text{BF}_3 \cdot \text{OEt}_2$), diethyl ether, as well as methylimidazole, 1,4-diazabicyclo[2.2.2]octane and methyl tosylate were purchased from Sigma-Aldrich. *N,N*-dimethyldodecylamine and *N*-methylcyclohexylamine were purchased from Fluka. *N*-methyldioctylamine was purchased from Acros Organics. All monomers and amines were used without further purification. Acetonitrile was purchased from Scharlau Chemie. The monomer Bisoxazoline (BisOx) was synthesized as described in the literature.²⁶ Carbon dioxide was supplied by Air Liquide with a purity of 99,998%.

The infrared spectra were obtained using a FT-IR “Nicolet Nexus” equipment. The NMR spectra were acquired in a Bruker ARX 400 spectrometer. The MALDI-TOF mass spectrometry was performed on a AUTOFLEX Bruker apparatus using dithranol as the matrix. The samples were prepared by mixing aqueous solutions of the polymer (10^{-4} M) and matrix in a typical ratio 1:1 (v/v). Average molecular weight of the polymer samples were determined by Gel Permeation Chromatography (GPC) using a KNAUER system with an evaporative light scatter detector from Polymer laboratories using dimethylformamide (DMF) as the eluent (temperature of the evaporator: 175 °C, temperature of the nebulizator: 85 °C, eluent rate flow: 1.8 mL min⁻¹). Two Polypore columns were used in series. MALDI-TOF mass spectrometry was carried out at Riaidt in Spain. All the other polymer analyses were carried out at REQUIMTE, Associated Laboratory.

The polymerization reaction in a microwave was performed in a screw capped quartz reaction vial specially designed for the single-mode microwave system Synthewave 402 (Prolabo).

1.3.2 Polymer synthesis in scCO₂

1.3.2.1 Experimental apparatus.

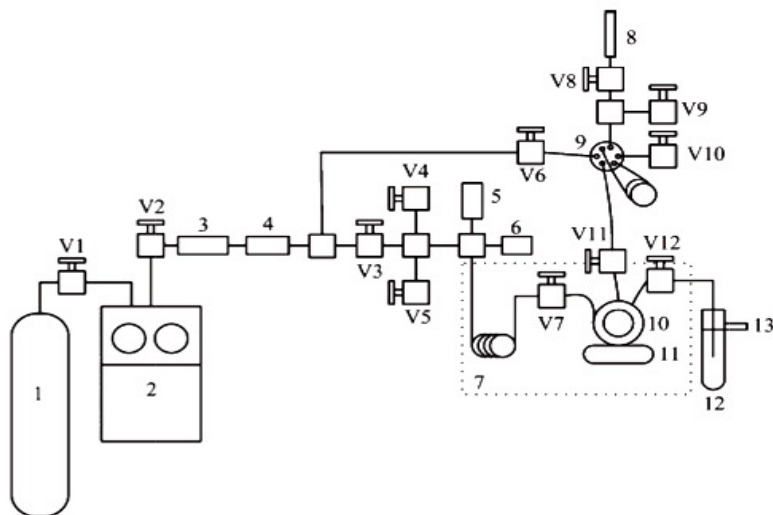


Figura 1.4 Schematic representation of the experimental apparatus. 1- CO₂ cylinder; 2 – high pressure pump; 3 – line filter; 4- check valve; 5 – high pressure transducer; 6 – rupture disc; 7 – thermostatted bath; 8 – syringe; 9 – HPLC high-pressure valve; 10- high pressure visual cell; 11- immersible stirrer; 12 – schlenk; 13 – vent; V1 to V12 – HIP high pressure valves; V4 and V5 – gas inlet (argon or nitrogen) or vacuum exit; V9 – vacuum exit (adapted from 1).

1.3.2.2 Preparation of the *living* polymers. Polymerization reactions were carried out in a 11 mL stainless-steel reactor equipped with two aligned sapphire windows in both tops stamped with Teflon o-rings. Four different 2-substituted oxazoline monomers were studied (MetOx, EtOx, PhOx and BisOx) and boron trifluoride etherate (BF₃.Et₂O) was used as the initiator. The monomer/initiator ratio used to each polymerization was, respectively: [M]/[I]=15 (MetOx), [M]/[I]=12 (EtOx), [M]/[I]=10 (PhOx) and [M]/[I]=7,5 (BisOx), according to the results previously reported in the literature.¹

The reactor cell was charged with the 2-substituted oxazoline, the initiator, a magnetic stirring bar, and then immersed in a thermostated bath. For polymerizations performed at 60 °C a water bath was used, for higher temperatures, 70°C, an oil bath was chosen. Carbon dioxide was introduced in the reactor in order to achieve the desired reaction pressure (from 16 to 20 MPa). After 20 hours of reaction, the pressure was slowly released and the reactor

reached the room temperature. Inside the reactor, and according to the adopted conditions of temperature and pressure, a viscous foam or a solid, was obtained – the so called *living polymer*. The *living polymer* allows the functionalization by end-capping with different molecules and, later, the determination of its antimicrobial susceptibility (figure 1.5).

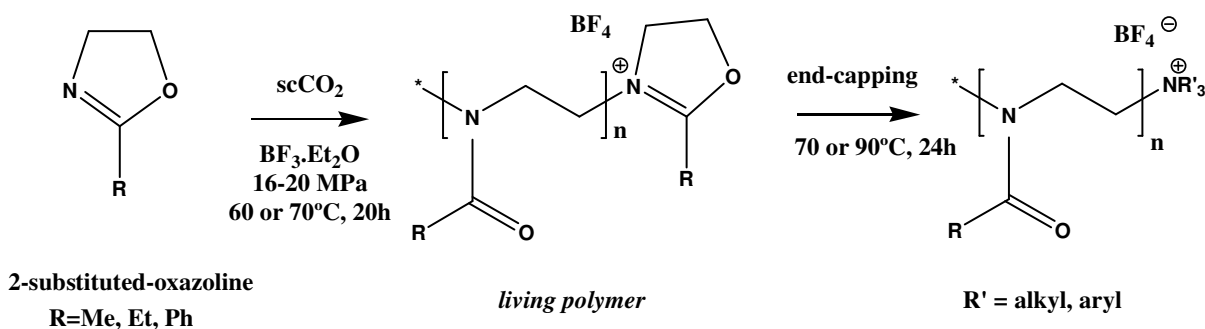


Figure 1.5 Green synthesis of 2-oxazoline-based polymers and its functionalization by amine end-capping.

1.3.2.3 Living polymer end-capping with water. Termination of the *living polymer* can be performed with the addition of a tenfold excess of water in relation to the added amount of initiator. The mixture was kept at room temperature under stirring during one hour. To purify the final polymer, an extraction with diethyl ether is performed. The aqueous phase, where the polymer is present, is then evaporated, dried in vacuum and the final pure product is easily obtained.

1.3.2.4 Living polymer end-capping with amines. Functionalization of the *living polymer* can be performed with the addition of a tenfold excess of amine to relation of the amount of initiator. The mixture was kept at 70 °C (or 90 °C in the case of PPhOxs) under stirring during 24 hours (figure 1.6). When the final polymer was a solid, it was washed with diethyl ether and dried in vacuum. Oily polymers were purified by extraction with diethyl ether and water, once the polymer is miscible in water. Finally, the aqueous phase is evaporated to dryness.

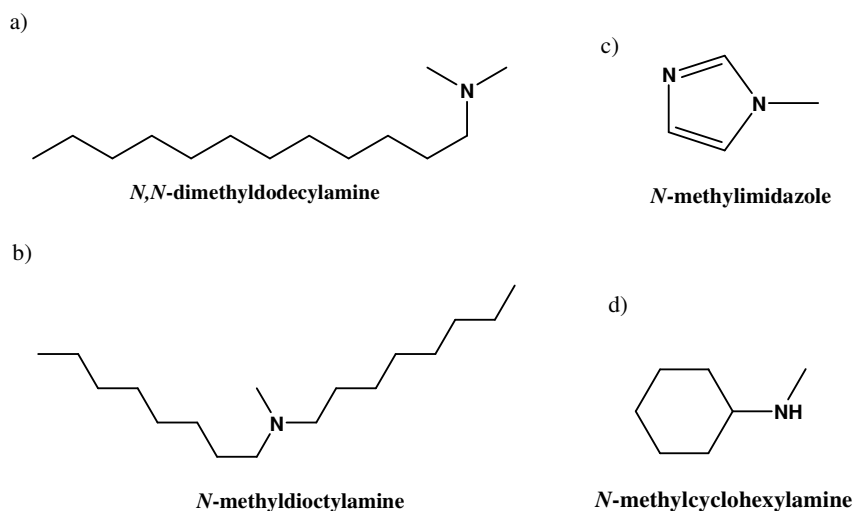
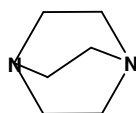


Figure 1.6 Chemical structures of the amines used in *living polymer* end-capping.

Functionalization of the *living polymer* can also be performed with the dropwise addition of DABCO (figure 1.7) in acetonitrile solution (0,1 g/mL of acetonitrile), taking into account that DABCO is also in a tenfold excess to the relation of the amount of the initiator.²⁷ The mixture was kept at room temperature under stirring during 1 hour. The final product, in the presence of an excess of diethyl ether, precipitated and become an oil. Diethyl ether and acetonitrile were removed and the final product was dried in vacuum. The final product was obtained as a white solid.



1,4-diazabicyclo[2.2.2]octane

Figure 1.7 Chemical structure of DABCO.

1.3.2.5 Preparation of Linear Poly(ethyleneimine) hydrochloride. LPEI was prepared by hydrolysis of poly(2-methyl-2-oxazoline) end-capped with *N,N*-dimethyldodecylamine ($M_w=1248$ g/mol, $PD=1.13$) in a 5M HCl (hydrochloric acid) solution under reflux (100 °C) for 9 hours (figure 1.8). After this period the polymer precipitates as the hydrochloride salt. The mixture is then filtered off, washed with acetone and dried in vacuum.²⁸ LPEI is obtained as a white solid.



Figure 1.8 Real apparatus of LPEI preparation.

1.3.3 Microwave-assisted synthesis of PMeOx

1.3.3.1 Preparation of the poly(2-methyl-2-oxazoline) *living polymer*. A solution of the monomer 2-methyl-2-oxazoline in acetonitrile was prepared. The polymerization was initiated by methyl tosylate considering a ratio [monomer]:[initiator]= 60:1. The solution contained the following quantities of monomer/initiator/solvent (all entries in grams), in that order: (2.0/0.0729/3.0535). The reaction occurred in a single mode microwave system at 140 °C and during 9 minutes (figure 1.9).¹⁴ The polymer was obtained as a dark green oil.

1.3.3.2 *Living polymer* end-capping with *N,N*-dimethyldodecylamine. Functionalization of the *living polymer* can be performed with the addition of a tenfold excess of amine to relation of the amount of initiator. The mixture was kept at 70 °C under stirring and during 24 hours (figure 1.9). The polymer was washed with diethyl ether and become a viscous brown solid. After being dried in vacuum, the polymer became an orange solid.

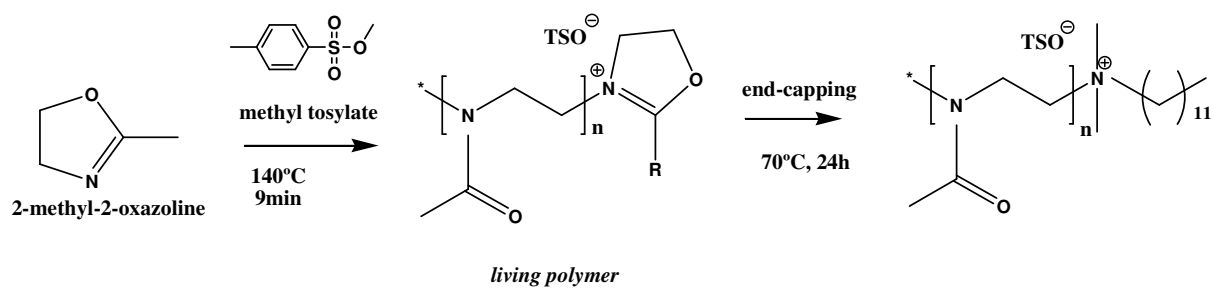


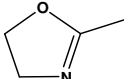
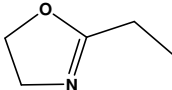
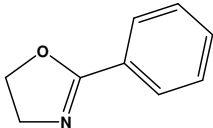
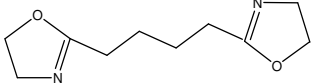
Figure 1.9 Microwave assisted synthesis of poly(2-methyl-2-oxazoline) followed by end-capping with *N,N*-dimethyldodecylamine.

1.4 RESULTS AND DISCUSSION

1.4.1 Synthesized 2-oxazoline-based polymers

The table 1.3 summarizes all the synthesized polymers.

Table 1.3 Schematic representation of the synthesized 2-oxazoline-based polymers.

2-oxazoline monomer	End-capping	Polymer reference
 2-methyl-2-oxazoline	<i>N,N</i> -dimethyldodecylamine	PMetOx-DDA
	<i>N</i> -methyldioctylamine	PMetOx-MDA
	Water	PMEtOx-OH
	<i>N,N</i> -dimethyldodecylamine	PMetOx-DDA _{mw}
 2-ethyl-2-oxazoline	<i>N,N</i> -dimethyldodecylamine	PEtOx-DDA
	<i>N</i> -methyldioctylamine	PEtOx-MDA
	DABCO	PEtOx-DABCO
	<i>N</i> -Methylimidazole	PEtOx-MI
	<i>N</i> -methylcyclohexylamine	PEtOx-MCHA
	Water	PEtOx-OH
 2-phenyl-2-oxazoline	<i>N,N</i> -dimethyldodecylamine	PPhOx-DDA
	<i>N</i> -methyldioctylamine	PPhOx-MDA
	Water	PPhOx-OH
 Bis-oxazoline	<i>N,N</i> -dimethyldodecylamine	PBisOx-DDA
	<i>N</i> -methyldioctylamine	PBisOx-MDA
	Water	PBisOx-OH

The LPEI, also synthesized, was prepared by acid hydrolysis of poly(2-methyl-2-oxazoline) end-capped with *N,N*-dimethyldodecylamine (PMetOx-DDA).

1.4.2 Polymer characterization

Polymers were characterized using FT-IR, $^1\text{H-NMR}$, $^{13}\text{C-NMR}$, GPC and MALDI-TOF techniques, as long as they were soluble in the required solvents.

NMR as well as FT-IR spectroscopies are useful to identify the functional groups present in the polymers. The NMR analysis, provided not only information about the structure of the polymers and purity but also enable us to determine the molecular weights of the obtained polymers through the integration of the signals of the polymer backbone relative to the signals of the amine end-capping. These techniques allowed us also to conclude if the end-capping was successfully achieved.

GPC and MALDI-TOF will be important in the determination of the molecular weights of the polymers.

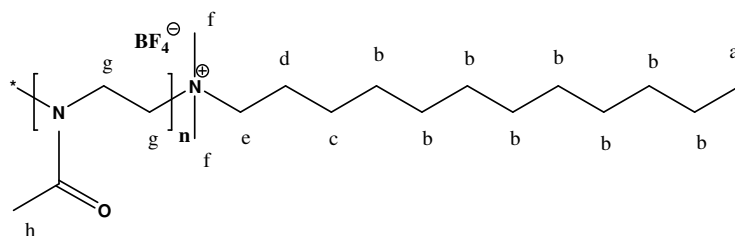
Poly(2-methyl-2-oxazoline) end-capped with *N,N*-dimethyldodecylamine (PMetOx-DDA). Yellow solid. Water soluble. Hygroscopic. Yield: 68 %.

FT-IR: $\nu_{\text{max}}/\text{cm}^{-1}$ 1738 (w, HO(C=O)N-), 1634 (s, Me(C=O)N-)

$^1\text{H-NMR}$ (400MHz, CDCl_3) δ/ppm = 0.87 (3H, t, $J=6.3$ Hz, Ha), 1.24 (16H, bs, Hb), 1.71 (2H, bs, Hc), 2.13 (3H, bs, Hh), 3.01 (2H, t, $J=8.0$ Hz, Hd), 3.15 (2H, bs, He), 3.44 (10H, bs, Hg+Hf, overlapped signals) $^{13}\text{C-NMR}$ (400MHz, CDCl_3) δ/ppm = 14.10, 21.15, 22.65, 24.48, 26.44, 29.80, 29.35, 29.56, 31.86, 43.49, 44.95, 47.05, 47.84, 58.63, 170.88 (C=O), 171.62 (C=O)

GPC: M_n = 17 235 g/mol M_w/M_n = 1.13

MALDI-TOF (after hydrolysis): M_n = 1248 g/mol n = 12



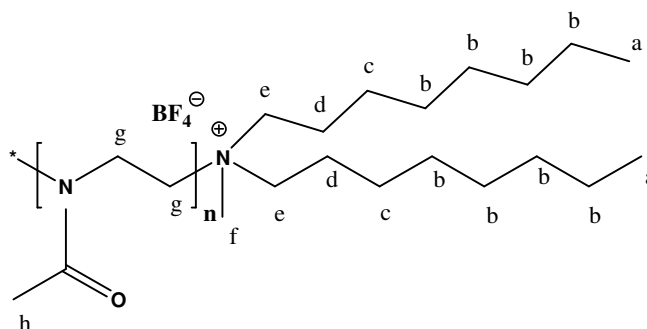
Poly(2-methyl-2-oxazoline) end-capped with *N*-methyldioctylamine (PMetOx-MDA). Yellow solid. Water soluble. Hygroscopic. Polymer insoluble in dimethylformamide. Yield: 66 %.

FT-IR: $\nu_{\text{máx}}/\text{cm}^{-1}$ 1731 (w, HO(C=O)N-), 1636 (s, Me(C=O)N-)

$^1\text{H-NMR}$ (400MHz, $(\text{CD}_3)_2\text{SO}$) δ/ppm = 0.85 (6H, t, 6.68Hz, Ha), 1.26 (12H, bs, Hb), 1.54 (4H, bs, Hc), 1.98 (3H, bs, Hh), 2.88 (2H, t, $J=7.6$ Hz, Hd), 3.07 (2H, s, He), 3.34 (7H, bs, Hg+Hf, overlapped signals) **$^{13}\text{C-NMR}$ (400MHz, $(\text{CD}_3)_2\text{SO}$) δ/ppm =** 13.94, 20.84, 22.04, 23.76, 26.01, 28.46, 31.15, 42.85, 44.10, 46.01, 46.72, 55.26, 170.19 (C=O) $M_n=1305$ g/mol $n=12$

GPC: n.a.

MALDI-TOF: n.a.



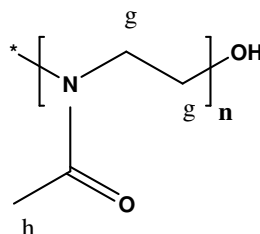
Poly(2-methyl-2-oxazoline) end-capped with water (PMetOx-OH). Yellow oil. Water soluble. Yield: 43%.

FT-IR: $\nu_{\text{máx}}/\text{cm}^{-1}$ 3460 (w, OH), 1735 (w, HO(C=O)N-), 1634 (s, Me(C=O)N-)

$^1\text{H-NMR}$ (400MHz, CDCl_3) δ/ppm = 2.14 (3H, bs, Hh), 3.45 (2H, bs, Hg) **$^{13}\text{C-NMR}$ (400MHz, CDCl_3) δ/ppm =** 20.54, 46.44, 104.85, 173.31 (C=O)

GPC: $M_n=17384$ g/mol $M_w/M_n=1.24$

MALDI-TOF: n.a.



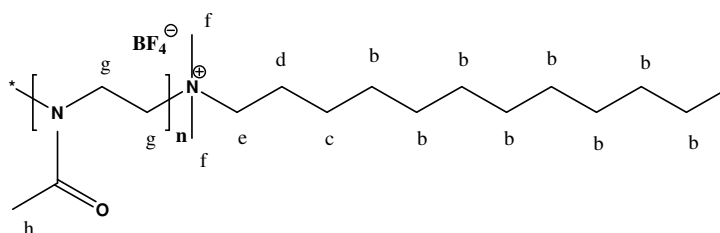
Poly(2-methyl-2-oxazoline) end-capped with *N,N*-dimethyldodecylamine, synthesized in microwave (PMetOx-DDA_{mw}). Orange solid. Water soluble. Hygroscopic. Yield: 96 %.

FT-IR: $\nu_{\text{máx}}/\text{cm}^{-1}$ 1710 (w, HO(C=O)N-), 1622 (s, Me(C=O)N-)

$^1\text{H-NMR}$ (400MHz, CDCl_3) δ/ppm = 0.86 (3H, bs, Ha), 1.24-1.17 (18H, m, Hb+Hc), 2.14 (3H, bs, Hh), 3.03 (4H, Hd+He), 3.44 (10H, bs, Hg+Hf, overlapped signals) **$^{13}\text{C-NMR}$ (400MHz, CDCl_3) δ/ppm =** 15.24, 21.17, 43.50, 45.33, 46.74, 47.56, 170.70 (C=O), 171.36 (C=O) **M_n :** 4988 g/mol **n :** 56

GPC: M_n = 26194 g/mol M_w/M_n = 1.30

MALDI-TOF: M_n = 2098 g/mol n = 22



Poly(2-ethyl-2-oxazoline) end-capped with *N,N*-dimethyldodecylamine (PEtOx-DDA).

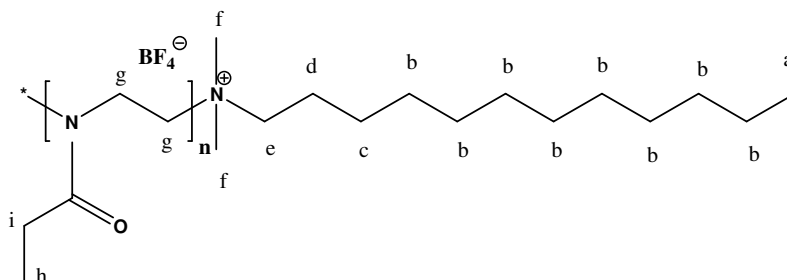
Yellow solid. Water soluble. Hygroscopic. Yield: 61 %.

FT-IR: $\nu_{\text{máx}}/\text{cm}^{-1}$ 1738 (w, HO(C=O)N-), 1637 (s, Et(C=O)N-)

$^1\text{H-NMR}$ (400MHz, CDCl_3) δ/ppm = 0.85 (3H, t, $J=6.6$ Hz, Ha), 1.08 (3H, bs, Hh), 1.22 (16H, bs, Hb), 1.70 (2H, bs, Hc), 2.27-2.38 (2H, bs, Hi), 3.04 (2H, t, $J=7.5$ Hz, Hd), 3.14 (2H, bs, He), 3.42 (10H, bs, Hg+Hf, overlapped signals) **$^{13}\text{C-NMR}$ (400MHz, CDCl_3) δ/ppm =** 9.30, 9.42, 14.04, 22.59, 24.34, 25.87, 26.33, 27.03, 29.02, 29.29, 29.40, 29.50, 31.81, 43.45, 45.32, 45.77, 46.93, 58.59, 174.00 (C=O), 174.72 (C=O) **M_n :** 1572 g/mol **n :** 13

GPC: M_n = 11 745 g/mol M_w/M_n = 1.15

MALDI-TOF: n.a.



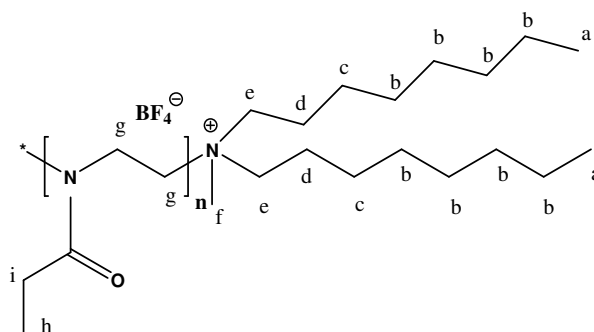
Poly(2-ethyl-2-oxazoline) end-capped with *N*-methyldioctylamine (PEtOx-MDA). Yellow solid. Water soluble. Hygroscopic. Yield: 66 %.

FT-IR: $\nu_{\text{máx}}/\text{cm}^{-1}$ 1741 (w, HO(C=O)N-), 1634 (s, Et(C=O)N-)

$^1\text{H-NMR}$ (400MHz, $(\text{CD}_3)_2\text{SO}$) δ/ppm = 0.85 (6H, t, 6.68Hz, Ha), 1.03 (3H, bs, Hh) 1.26 (12H, bs, Hb), 1.56 (4H, bs, Hc), 2.30 (4H, bs, Hi), 2.95 (4H, t, $J=7.6$ Hz, Hd), 3.07 (7H, s, He+Hf, overlapped signals), 3.34 (4H, bs, Hg) **$^{13}\text{C-NMR}$ (400MHz, $(\text{CD}_3)_2\text{SO}$) δ/ppm =** 9.42, 13.94, 22.05, 23.52, 24.97, 25.96, 28.46, 31.16, 42.84, 44.45, 45.89, 55.13, 173.20 (C=O) $M_n=$ 1374 g/mol $n=$ 11

GPC: $M_n=$ 15 573 g/mol $M_w/M_n=$ 1.07

MALDI-TOF: n.a.



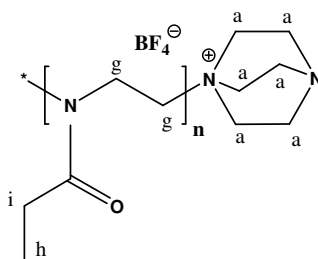
Poly(2-ethyl-2-oxazoline) end-capped with DABCO (PEtOx-DABCO). White solid. Water soluble. Yield: 79 %.

FT-IR: $\nu_{\text{máx}}/\text{cm}^{-1}$ 1718 (w, HO(C=O)N-), 1631 (s, Et(C=O)N-)

$^1\text{H-NMR}$ (400MHz, CDCl_3) δ/ppm = 1.11 (3H, bs, Hh), 2.29-2.41 (2H, bs, Hi), 2.82 (12H, s, Ha), 3.46 (2H, bs, Hg) **$^{13}\text{C-NMR}$ (400MHz, CDCl_3) δ/ppm =** 9.44, 25.91, 29.40, 29.66, 30.89, 43.65, 45.24, 46.88, 52.76, 173.93 (C=O), 174.61 (C=O) $M_n=$ 1315 g/mol $n=$ 12

GPC: $M_n=$ 9499 g/mol $M_w/M_n=$ 1.12

MALDI-TOF: n.a.



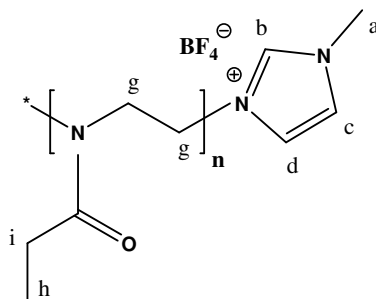
Poly(2-ethyl-2-oxazoline) end-capped with *N*-Methylimidazole (PETox-MI). Orange oil. Water soluble. Yield: 85 %.

FT-IR: $\nu_{\text{máx}}/\text{cm}^{-1}$ 1743 (w, HO(C=O)N-), 1620 (s, Et(C=O)N-)

$^1\text{H-NMR}$ (400MHz, CDCl_3) δ/ppm = 1.07 (3H, bs, Hh), 2.25-2.35 (2H, bs, Hi), 3.41 (4H, bs, Hg), 3.69 (3H, s, Ha), 6.89 (2H, bs, Hd), 7.04 (2H, bs, Hc), 7.55 (2H, s, Hb) **$^{13}\text{C-NMR}$ (400MHz, CDCl_3) δ/ppm =** 9.37, 25.85, 33.48, 42.28, 43.71, 45.31, 120.30, 128.31, 137.54, 173.93 (C=O), 174.61 (C=O) $M_n=790$ g/mol $n=7$

GPC: $M_n=13\,924$ g/mol $M_w/M_n=1.08$

MALDI-TOF: $M_n=790$ g/mol $n=7$



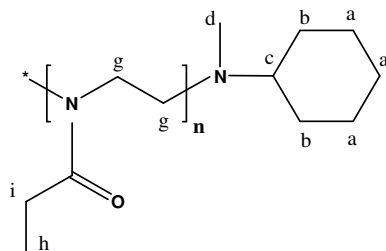
Poly(2-ethyl-2-oxazoline) end-capped with *N*-methylcyclohexylamine (PETox-MCHA). Orange oil. Water soluble. Yield: 86 %.

FT-IR: $\nu_{\text{máx}}/\text{cm}^{-1}$ 1726 (w, HO(C=O)N-), 1657 (s, Et(C=O)N-)

$^1\text{H-NMR}$ (400MHz, CDCl_3) δ/ppm = 0.83-1.29 (6H, m, Ha), 1.09 (3H, bs, Hh), 1.63-2.01 (4H, m, Hb), 2.25-2.40 (2H, bs, Hi), 2.58 (3H, s, Hd), 2.70 (1H, s, Hc), 3.43 (4H, bs, Hg) **$^{13}\text{C-NMR}$ (400MHz, CDCl_3) δ/ppm =** 9.30, 9.42, 14.04, 22.59, 24.34, 25.87, 26.33, 27.03, 29.02, 29.29, 29.40, 29.50, 31.81, 43.45, 45.32, 45.77, 46.93, 174.00 (C=O), 174.72 (C=O) $M_n=821$ g/mol $n=7$

GPC: $M_n = 10\,776$ g/mol $M_w/M_n = 1.11$

MALDI-TOF: n.a.



Poly(2-ethyl-2-oxazoline) end-capped with water (PEtOx-OH). Orange oil. Water soluble.
Yield: 70%.

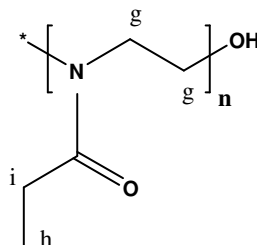
FT-IR: $\nu_{\text{max}}/\text{cm}^{-1}$ 3418 (w, OH), 1738 (w, HO(C=O)N-), 1626 (s, Et(C=O)N-)

$^1\text{H-NMR}$ (400MHz, CDCl_3) $\delta/\text{ppm} =$ 1.08 (3H, bs, Hh), 2.37 (2H, bs, Hi), 3.41 (4H, bs, Hf)

$^{13}\text{C-NMR}$ (400MHz, CDCl_3) $\delta/\text{ppm} =$ 9.40, 25.89, 44.16, 45.41, 46.46, 46.91, 174.07 (C=O), 174.73 (C=O)

GPC: $M_n = 8482$ g/mol $M_w/M_n = 1.15$

MALDI-TOF: n.a.



Poly(2-phenyl-2-oxazoline) end-capped with *N,N*-dimethyldodecylamine (PPhOx-DDA). Orange solid. Methanol and chloroform soluble. Yield: 99 %.

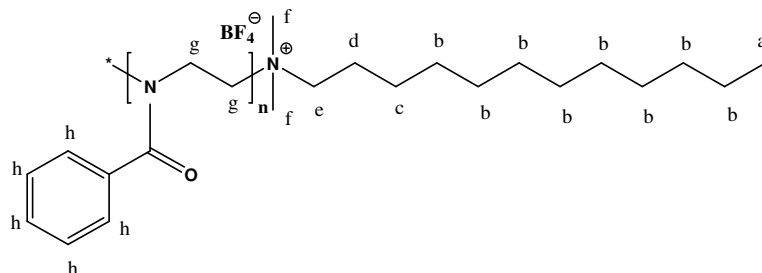
FT-IR: $\nu_{\text{max}}/\text{cm}^{-1}$ 1717 (w, HO(C=O)N-), 1634 (s, Ph(C=O)N-)

$^1\text{H-NMR}$ (400MHz, CDCl_3) $\delta/\text{ppm} =$ 0.87 (3H, t, $J = 6.3$ Hz, Ha), 1.24 (16H, s, Hb), 1.55 (2H, bs, Hc), 3.06 (2H, bs, Hd), 3.10 (2H, bs, He), 3.35 (10H, bs, Hg+Hf, overlapped signals),

7.08-7.35 (5H, bs, Hh) **$^{13}\text{C-NMR}$ (400MHz, CDCl_3) $\delta/\text{ppm} =$** 14.06, 22.63, 25.50, 26.73, 29.27, 29.39, 29.55, 31.85, 44.11, 126.29, 126.93, 128.64, 129.60, 171.74 (C=O) $M_n = 1116$ g/mol $n = 6$

GPC: $M_n = 8\,184$ g/mol $M_w/M_n = 1.12$

MALDI-TOF: n.a.



Poly(2-phenyl-2-oxazoline) end-capped with N-methyldioctylamine (PPhOx-MDA).

Orange solid. Methanol and chloroform soluble. Yield: 88 %.

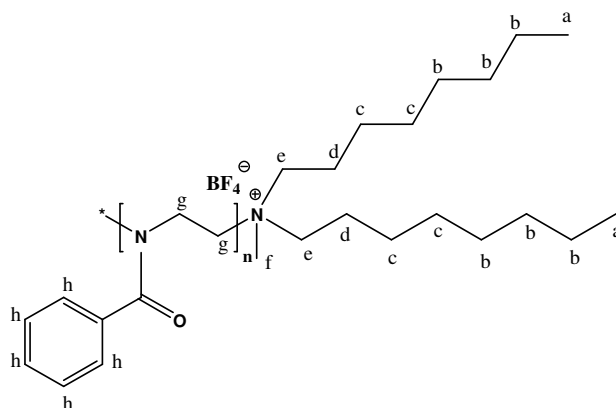
FT-IR: $\nu_{\text{máx}}/\text{cm}^{-1}$ 1726 (w, HO(C=O)N-), 1630 (s, Ph(C=O)N-)

$^1\text{H-NMR}$ (400MHz, CDCl_3) $\delta/\text{ppm} =$ 0.87 (3H, t, $J = 6.88$ Hz, Ha), 1.25 (12H, bs, Hb), 1.69 (4H, bs, Hc), 2.99 (11H, bs, Hd+He+Hf, overlapped signals), 2.99-3.53 (4H, bs, Hg), 7.08-7.33 (5H, bs, Hh) **$^{13}\text{C-NMR}$ (400MHz, CDCl_3) $\delta/\text{ppm} =$** 14.03, 22.54, 23.68, 26.39, 28.95, 31.59, 42.32, 46.25, 125.55, 126.34, 127.19, 127.85, 128.67, 129.48, 135.57, 172.13 (C=O)

$M_n = 1321$ g/mol $n = 7$

GPC: $M_n = 12\,036$ g/mol $M_w/M_n = 1.13$

MALDI-TOF: n.a.



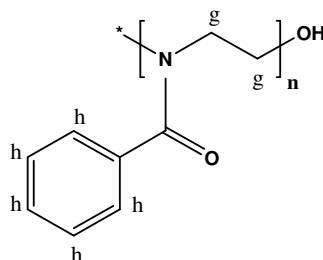
Poly(2-phenyl-2-oxazoline) end-capped with water (PPhOx-OH). Orange oil. Methanol and chloroform soluble. Yield: 99%

FT-IR: $\nu_{\text{máx}}/\text{cm}^{-1}$ 3368 (w, OH), 1714 (w, HO(C=O)N-), 1644 (s, Ph(C=O)N-)

$^1\text{H-NMR}$ (400MHz, CDCl_3) δ/ppm = 3.44-3.49 (4H, bs, Hg), 7.03-7.29 (5H, bs, Hh) $^{13}\text{C-NMR}$ (400MHz, CDCl_3) δ/ppm = 46.99, 126.26, 126.99, 127.83, 128.39, 128.66, 129.47, 172.28 (C=O), 173.41 (C=O)

GPC: M_n = 5875 g/mol M_w/M_n = 1.14

MALDI-TOF: n.a.



Poly(bisoxazoline) end-capped with *N,N*-dimethyldodecylamine (PBisOx-DDA). Brown solid. Water soluble. Yield: 67 %.

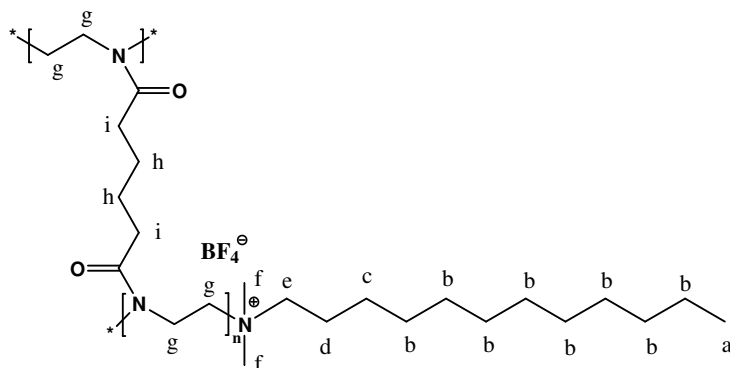
FT-IR: $\nu_{\text{max}}/\text{cm}^{-1}$ 1744 (w, HO(C=O)N-), 1652 (w, N-(C=O))

$^1\text{H-NMR}$ (400MHz, CD_3OD) δ/ppm = 0.89 (3H, t, J = 6.2 Hz, Ha), 1.29-1.37 (16H, bs, Hb), 1.62 (4H, bs, Hh), 1.70 (2H, bs, Hc), 2.22 (4H, bs, Hi), 3.02 (2H, t, J =5.3 Hz, Hd), 3.07-3.11 (2H, bs, He), 3.26-3.30 (14H, bs, Hg+Hf, signals overlapped with the signal of the solvent)

$^{13}\text{C-NMR}$ (400MHz, CD_3OD) δ/ppm = 14.41, 17.08, 23.71, 26.63, 27.42, 30.18, 30.45, 30.47, 30.61, 30.71, 33.04, 36.66, 42.80, 42.93, 43.43, 61.60, 176.18 (C=O) M_n = 786 g/mol n = 3

GPC: M_n = 4 897 g/mol M_w/M_n = 1.05

MALDI-TOF: n.a.



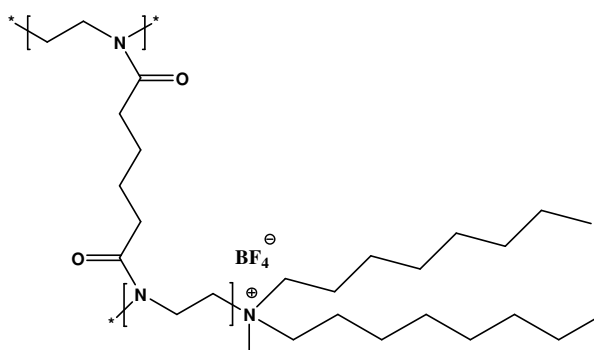
Poly(bisoxazoline) end-capped with *N*-methyldioctylamine (PBisOx-MDA). Orange solid. Slightly soluble in water and methanol. Polymer insoluble in chloroform, dimethyl sulfoxide and dimethylformamide.

FT-IR: $\nu_{\text{máx}}/\text{cm}^{-1}$ 1735 (w, HO(C=O)N-), 1654 (s, N-(C=O))

$^1\text{H-NMR}$: n.a. **$^{13}\text{C-NMR}$:** n.a.

GPC: n.a.

MALDI-TOF: n.a.



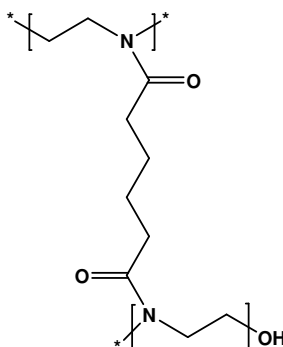
Poly(bisoxazoline) end-capped with water (PBisOx-OH). Yellow solid. Slightly water and methanol soluble. Polymer insoluble in chloroform, dimethyl sulfoxide and dimethylformamide. Yield: 67%.

FT-IR: $\nu_{\text{máx}}/\text{cm}^{-1}$ 3384 (w, OH), 1737 (w, HO(C=O)N-), 1636 (s, N-(C=O))

$^1\text{H-NMR}$: n.a. **$^{13}\text{C-NMR}$:** n.a.

GPC: n.a.

MALDI-TOF: n.a.



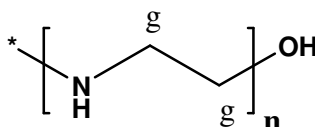
Linear Poly(ethyleneimine) hydrochloride (LPEI). White solid. Water soluble. Polymer insoluble in dimethylformamide. Yield: 74 %.

FT-IR: $\nu_{\text{máx}}/\text{cm}^{-1}$ 3420 (s, **NH**), 2659 (s, **CH**)

$^1\text{H-NMR}$ (400MHz, D_2O) δ/ppm = 3.48 (4H, s, Hg) $^{13}\text{C-NMR}$ (400MHz, D_2O) δ/ppm = 43.83

GPC: n.a.

MALDI-TOF: M_n = 548 g/mol n = 12



FT-IR spectroscopy allowed the identification of the main functional groups of all polymers. The amide carbonyl absorption band was found in the spectra of all polymers (with exception of LPEI) with values from 1620 to 1657 cm^{-1} . LPEI showed its typical absorption bands at 3420 cm^{-1} (NH) and 2659 cm^{-1} (CH). The partial insertion of CO_2 in the polymer chain, that is already reported,¹ was also observed for all polymers. This was confirmed by the absorption bands ranging from 1710 to 1743 cm^{-1} . The OH functional groups were also observed in the polymers end-capped with water with absorption bands from 3368 to 3460 cm^{-1} .

To determine the molecular weight of each polymer, NMR spectroscopy, GPC and MALDI-TOF techniques were used.

The M_n values determined by GPC were higher than the expected. This result can be explained by the use of polystyrene standards for the calibration of the GPC curves (with a minimum value around 1260 g/mol).

MALDI-TOF analysis, when performed, showed to be more reliable than GPC and to be consistent with the results of NMR analysis. In the case of PMetOx-DDA_{mw}, the difference obtained by different techniques, could be justified by the higher polydispersity obtained by the microwave-assisted synthesis (PDI= 1.30). Therefore, the polymer obtained should be a mixture of polymers with a range of molecular weights and consequently can justify the lower n value obtained by MALDI-TOF analysis.

NMR analysis is the most reliable technique to determine the molecular weight of the end-capped polymers. The end-capping with different amines only occurs in one of the chain

ends. In the case of polymers end-capped with water, this calculation was not possible because the signals of OH functional group usually cannot be visualized in the NMR spectrum. In the case of branched PBisOx-DDA, the end-capping with the amine could have occurred in more than one end-chain. Therefore, it can only be concluded that, to each branch of the polymer that was end-capped, the calculated n value was 3, and consequently the polymer can have a higher molecular weight.

In addition, the analysis of the NMR spectra allows us to conclude that the end-capping was successfully performed in all *living polymers*. The NMR signals of the different 2-oxazoline-based polymers and the end-capping amines are consistent with data reported in the literature. It was also possible to conclude from the NMR spectra of LPEI that the complete hydrolysis of both oxazoline's acetyl groups and the amine end-capping has been achieved (see appendix 2).

Therefore, the synthesis of 2-oxazoline-based polymers in scCO_2 generates well defined *living polymers*, with low polydispersity (PDI= 1.05 to 1.15) and low molecular weight ($n=6$ to 13); these polymers can be later selectively end-capped. Yields from 68 to 99% were obtained.

On the other hand, the polymerization of PMetOx-DDA_{mw} by a microwave-assisted synthesis showed a yield of 96% but with a higher PDI.

1.4.3 Scanning electron microscopy, SEM

SEM micrographs were only obtained for LPEI since polyoxazolines are highly hygroscopic solids or oils (figures 1.10 and 1.11).

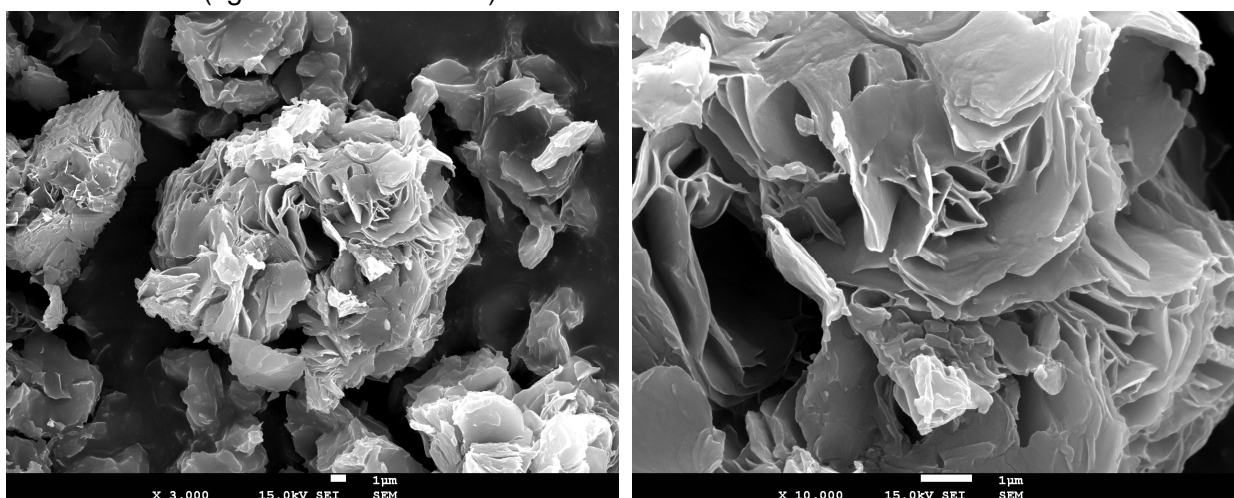


Figure 1.10 SEM micrographs of LPEI powder obtained by acid hydrolysis of PMetOx-DDA.

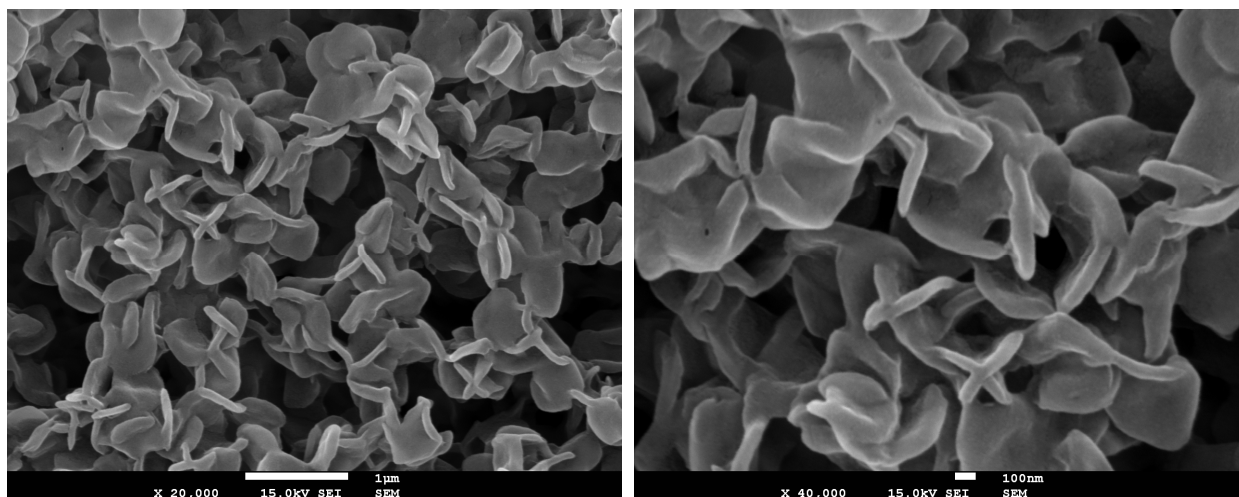


Figure 1.11 SEM micrographs of LPEI after liophilisation of their aqueous solution.

LPEI shows a well defined and characteristic microstructure. The differences observed in the SEM micrographs may be related to the process of liophilisation, in which the freezing of the aqueous solution of the polymer leads to an unusual star shaped morphology (figure 1.11).

1.4.4 Intrinsic blue photoluminescence

A strong blue photoluminescence was observed from the synthesized polymers, even after a careful and extensive purification procedure. This unexpected result was already described in the literature for dendrimers^{29,30} and hyperbranched polymers.^{31,32,33} Carbonyl groups that exist in the core of the polymer are appointed as a key structural factor for the presence of fluorescence.³² This is a surprising result, because there are no fluorophores in this type of polymers, and this behavior is unexpected for linear polymers.



Figure 1.12 Left glass vial: pure water. Right glass vial: strong fluorescence phenomenon of PMetOx-DDA_{mw} in aqueous solution under UV lamp.

The fluorescence emission intensity of 2-oxazoline-based polymers with different molecular weights and end-capping molecules was also measured. The samples were prepared in order to assure an absorbance equal to 0.1 to ensure that self-quenching processes were not present.

- **2-methyl-2-oxazoline-based polymers**

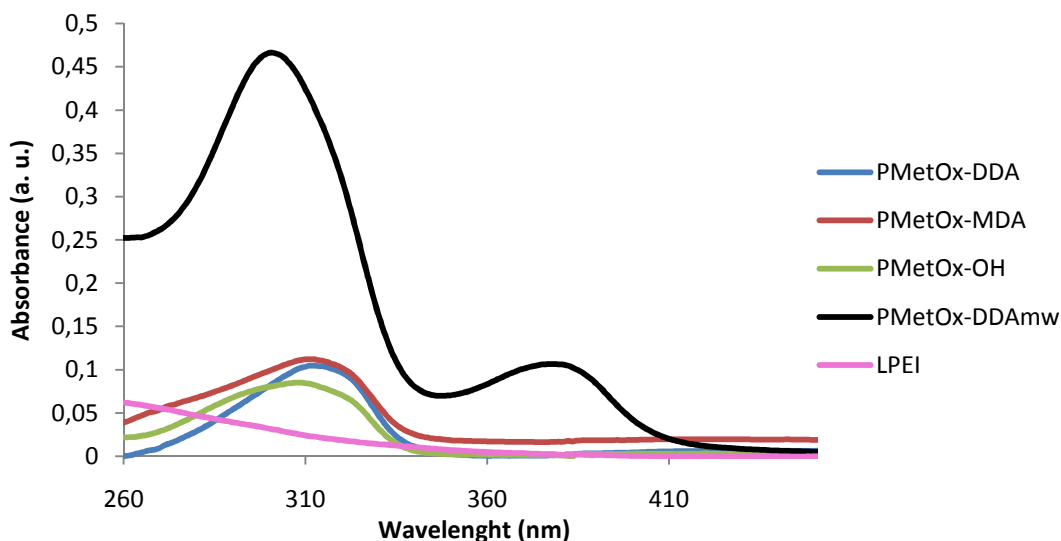


Figure 1.13 Absorption spectra of the synthesized 2-methyl-2-oxazoline-based polymers.

Comparing the 2-methyl-2-oxazoline-based polymers with different end-capping molecules (figure 1.13), it can be observed that similar absorbance spectra were obtained for the polymers synthesized in $scCO_2$ with an absorption maximum at 308-312 nm. In PMetOx-DDA_{mw} two absorption bands were present. Excitation of the maximum of both bands was performed in order to evaluate their emission spectra. It was found that both led to the same emission band although with different intensities. The band at 378 nm led to the most intense emission band.

The LPEI showed no absorption band, supporting the idea that the carbonyl groups are essential to the existence of an intrinsic fluorescence in the polymers (figure 1.13).

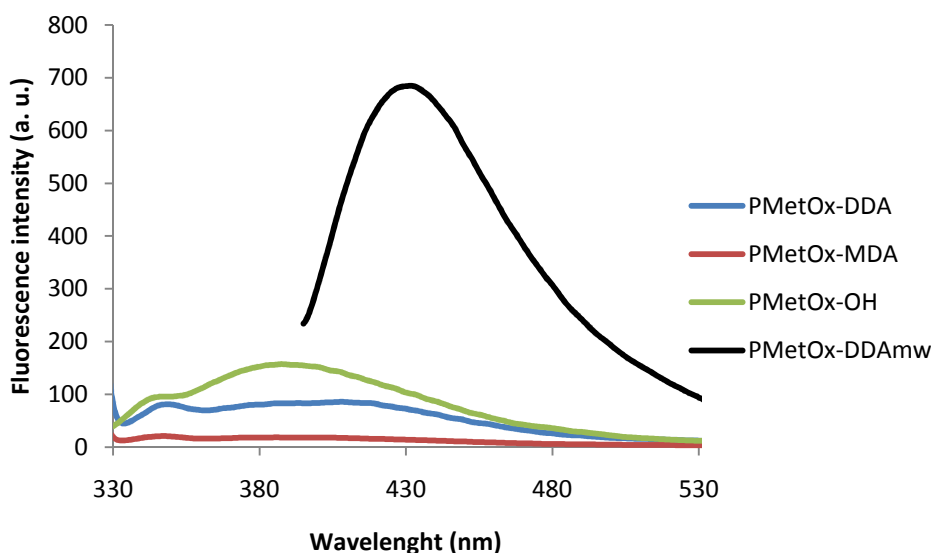


Figure 1.14 Fluorescence emission spectra of the 2-methyl-2-oxazoline-based polymers.

Comparing the relative intensity of polymers fluorescence (figure 1.14), it was found that polymers synthesized in supercritical media showed again a more similar behavior with an emission band around 390 nm. On the other hand, PMetOx-DDA_{mw}, showed a more intensive band at 430 nm. The different polymerization conditions can justify the differences observed. The fluorescence intensity increases with the molecular weight, resulting from a possible enhanced rigidity of the molecular architecture and/or from a more quantity of carbonyl groups present in the polymer backbone.

- **2-ethyl-2-oxazoline-based polymers**

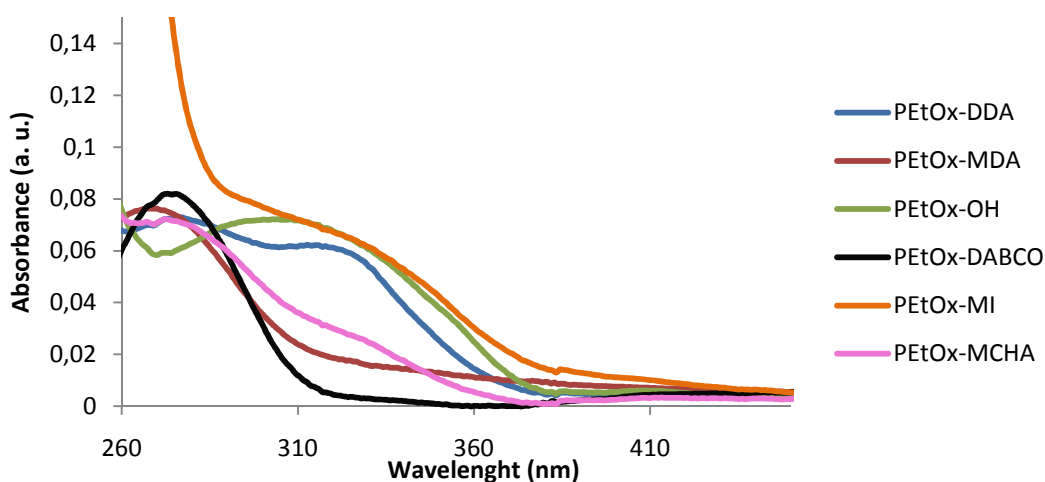


Figure 1.15 Absorption spectra of the synthesized 2-ethyl-2-oxazoline-based polymers.

Comparing now the 2-ethyl-2-oxazoline-based polymers with different end-capping molecules (Figure 1.15), it can be observed that some polymers have their absorption band from 267 to 276 nm.

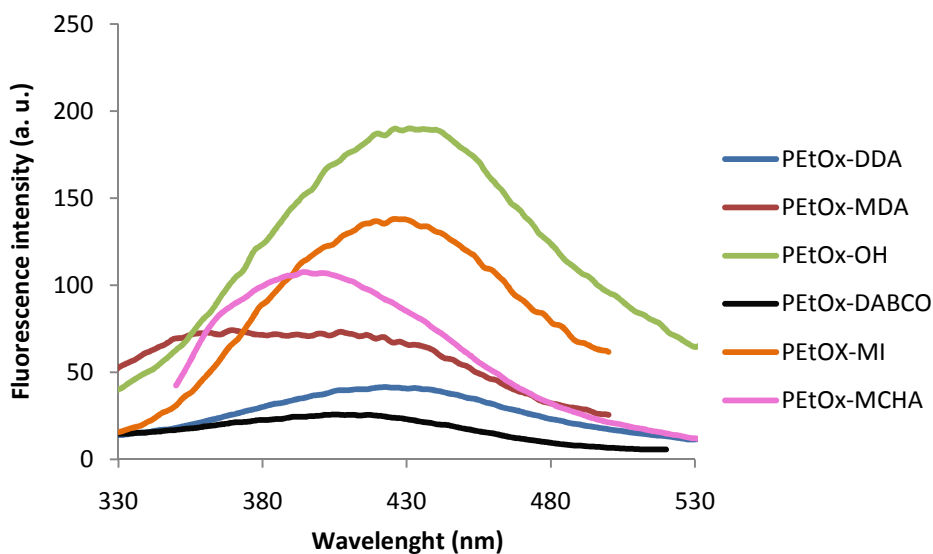


Figure 1.16 Fluorescence emission spectra of 2-ethyl-2-oxazoline-based polymers.

In figure 1.16, analyzing the fluorescence intensity of 2-ethyl-2-oxazoline-based polymers it can be seen that all polymers showed a similar emission.

- **2-phenyl-2-oxazoline-based polymers**

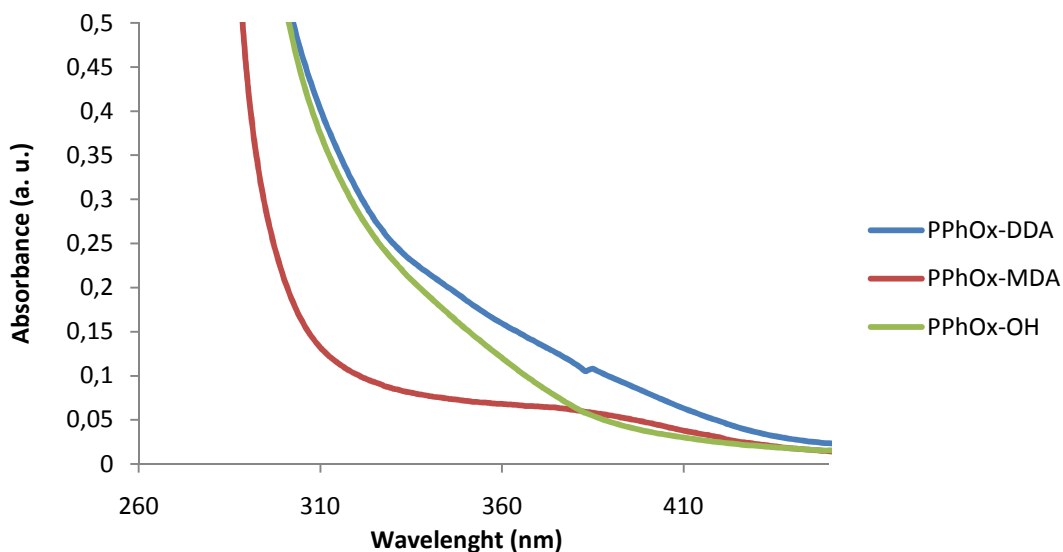


Figure 1.17 Absorption spectra of synthesized 2-phenyl-2-oxazoline-based polymers.

Figure 1.17 shows the absorption spectra of 2-phenyl-2-oxazoline-based polymers with a maximum at 370nm.

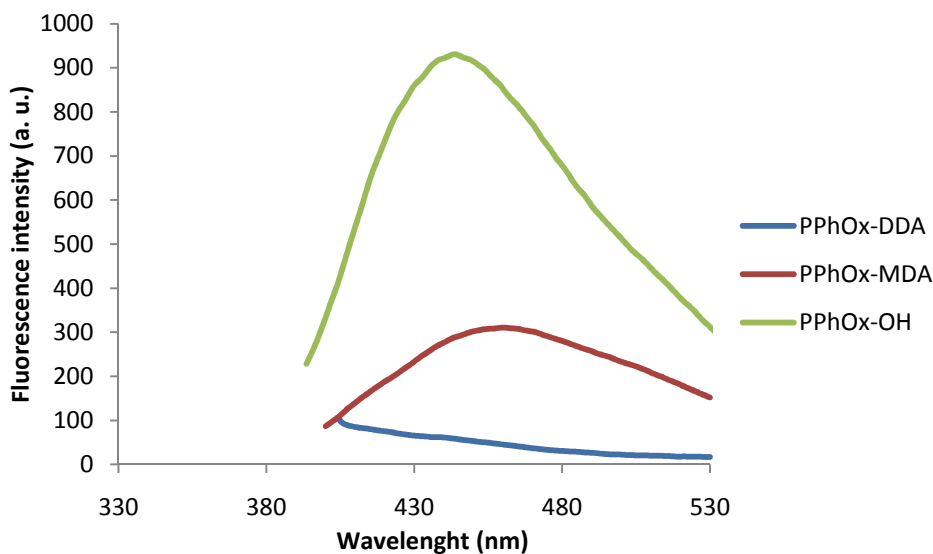


Figure 1.18 Fluorescence emission spectra of the 2-phenyl-2-oxazoline-based polymers.

In figure 1.18, it can be seen that 2-phenyl-2-oxazoline polymers have higher fluorescence intensities than the 2-alkyl-substituted polyoxazolines, fact that can be justified with the presence of aromatic groups in the polymer backbone.

- **bisoxazoline-based polymers**

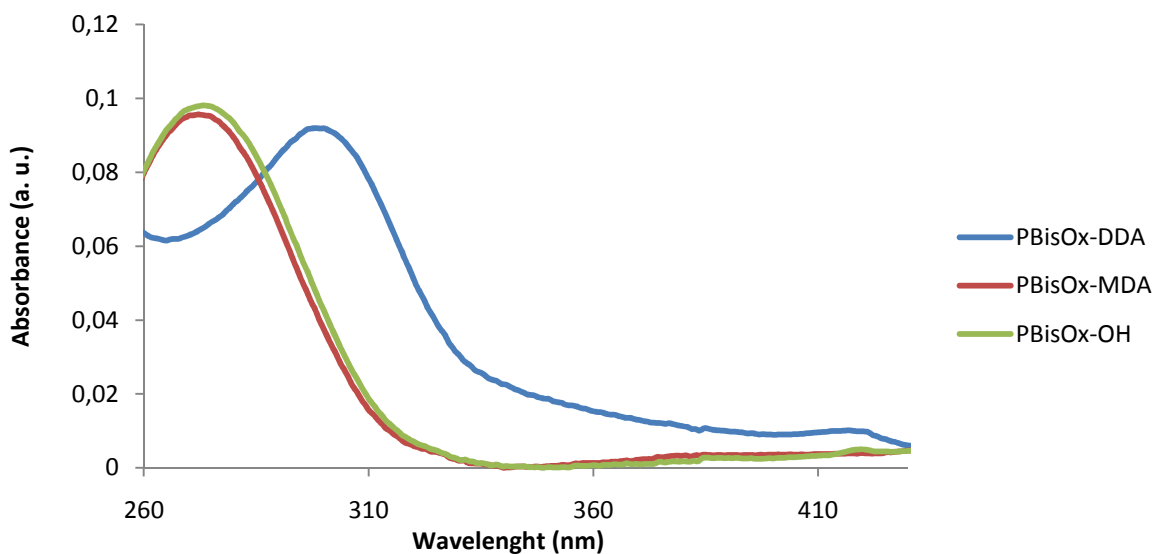


Figure 1.19 Absorption spectra of synthesized the bisoxazoline-based polymers.

The absorbance spectra of the bisoxazoline-based polymers (figure 1.19) show two different absorption bands being coincident for PBisOx-MDA and PBisOx-OH at 275nm, while in the case of PBisOx-DDA the band is around 300nm.

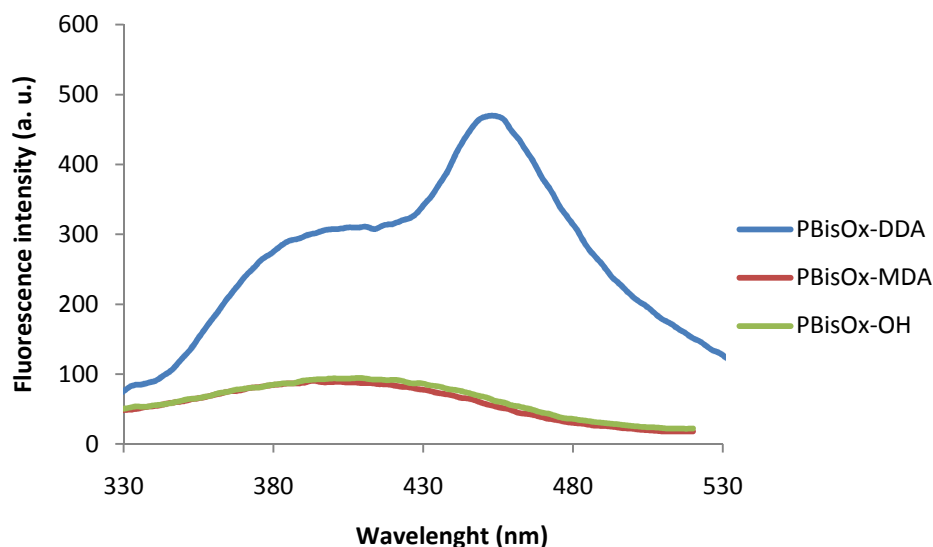


Figure 1.20 Fluorescence emission spectra of the bisoxazoline-based polymers.

In PBisOx-MDA and PBisOx-OH it can be observed an emission band around 400nm, while in the case of PBisOx-DDA a double emission is observed (at 400nm and 450nm). These two bands can be due to the existence of different three-dimensional conformations in the polymer (figure 1.20).

It can be concluded that the presence of carbonyl groups are essential for the intrinsic fluorescence of the polymers and that aromatic groups in the polymer chain will enhance the fluorescence intensity. All polymers exhibit emission bands that vary from 350 to 475 nm, possibly related with the linear or branched backbone structure. Polymers end-capped with a hydroxyl group showed, in general, higher fluorescence intensity. The end-capping with different amine groups (even aromatic amine groups) does not influence the absorbance bands but can decrease the fluorescence intensity. These findings led us to conclude that the quaternary ammonium end groups could be involved in the fluorescence quenching mechanism.

This unusual property of 2-oxazoline-based polymers enlarges their potential applications. For instance, their use as fluorescent tags can be envisaged as a promising tool for fluorescence microscopy assays.

1.5 CONCLUSION

This chapter reports the synthesis of 2-oxazoline-based polymers in supercritical media under a CROP mechanism and the end-capping of the *living polymers* with different types of amines.

Using $^1\text{H-NMR}$, $^{13}\text{C-NMR}$ and FT-IR it was possible to characterize all the synthesized materials. The polymers were synthesized using four different types of monomers and were also further hydrolysed, for the obtention of the corresponding LPEI. Both synthesis and later end-capping were performed with success. Using a CROP methodology in supercritical carbon dioxide, low molecular weight polymers were obtained but with low polydispersivity.

The synthesis by a microwave-assisted polymerization was also performed in order to prepare higher molecular weight polymer, which will allow the evaluation of molecular weight effect on antimicrobial activity (chapter 2).

An intrinsic blue photoluminescence was observed for all synthesized polymers. Since no fluorophores are present it was concluded that this property should be related to the high concentration of carbonyl groups present in the backbone, conjugated in some cases (PBisOx) with a more rigid three-dimensional polymer network.

1.6 REFERENCES

- ¹ Macedo, C. V., Silva, M. S., Casimiro, T., Cabrita, E. J., Aguiar-Ricardo, A., *Boron trifluoride catalysed polymerisation of 2-substituted-2-oxazolines in supercritical carbon dioxide*. *Green Chem.*, **2007**. 9: 948-953.
- ² Kemmere, M., Meyer, T., *Supercritical Carbon Dioxide: in Polymer Reaction Engineering*, ed. Wiley. **2005**.
- ³ Hyde, J. R., Licence, P., Carter, D., Poliakoff, M., Continuous catalytic reactions in supercritical fluids. *Applied Catalysis A: General*, **2001**. 222: 119-131.
- ⁴ Cooper, A. I., *Polymer synthesis and processing using supercritical carbon dioxide*. *J. Mater. Chem.*, **2000**. 10: 207-234.
- ⁵ Leitner, W., *Supercritical carbon dioxide as a green reaction medium for catalysis*. *Acc. Chem. Res.*, **2002**. 35: 746-756.
- ⁶ Sheldon, R. A., *Green solvents for sustainable organic synthesis: state of the art*. *Green Chem.*, **2005**. 7: 267–278.
- ⁷ Beckman, E. J., *Supercritical and near-critical CO₂ in green chemical synthesis and processing*. *J. of Supercritical Fluids*, **2004**. 28: 121-191.
- ⁸ Kendall, J. L., Canelas, D. A., Young, J. L., DeSimone, J. M., *Polymerizations in Supercritical Carbon Dioxide*. *Chem. Rev.*, **1999**. 99: 543–563.
- ⁹ Adams, N., Schubert, U. S., *Poly(2-oxazolines) in biological and biomedical application contexts*. *Advanced Drug Delivery Reviews*, **2007**. 59: 1504-1520
- ¹⁰ Lobert, M., Kohn, U., Hoogenboom, R., Schubert, U. S., *Synthesis and microwave assisted polymerization of fluorinated 2-phenyl-2-oxazolines: the fastest 2-oxazoline monomer to date*. *Chem. Commun.*, **2008**. 12: 1458-1460.
- ¹¹ Mohammadpoor-Baltork, I., Moghadam, M., Tangestaninejad, S., Mirkhani, V., Hojati, S. F., *Environmental-friendly synthesis of oxazolines, imidazolines and thiazolines catalysed by tungstophosphoric acid*. *Catalysis Communications*, **2008**. 9: 1153-1161.
- ¹² Aoi, K., Okada, Masahiko, *Polymerization of Oxazolines*. *Prog. Polym. Sci.*, **1996**. 21: 151-208.
- ¹³ Zhang, C., Liao, L., Gong, S. S., *Recent developments in microwave-assisted polymerization with a focus on ring-opening polymerization*. *Green Chem.*, **2007**. 9: 303-314.
- ¹⁴ Wiesbrock, F., Hoogenboom, R., Leenen, M. A. M., Meier, M. A. R., Schubert, U.S., *Investigation of the living cationic ring-opening polymerization of 2-methyl-, 2-ethyl-, 2-nonyl-, and 2-phenyl-2-oxazoline in a single-mode microwave reactor*. *Macromolecules*, **2005**. 38: 5025-5034.

- ¹⁵ Shelton, R. S., van Campen, M. G., Tilford, C. H., Lang, H. C., Nisonger, L., Bandelin, F. J., Rubenkoenig, H. L., *Quaternary Ammonium Salts as Germicides. I. Non-acylated Quaternary Ammonium Salts Derived from Aliphatic Amines*. J. Am. Chem. Soc., **1946**. 68: 753–755.
- ¹⁶ Shelton, R. S., van Campen, M. G., Tilford, C. H., Lang, H. C., Nisonger, L., Bandelin, F. J., Rubenkoenig, H. L., *Quaternary Ammonium Salts as Germicides. III. Quaternary Ammonium Salts Derived from cyclic Amines*. J. Am. Chem. Soc., **1946**. 68: 757–759.
- ¹⁷ Waschinski, C. J., Barnet, S., Theobald, A., Schubert, R., Kleinschmidt, F., Hoffmann, A., Saalwachter, K., Tiller, J. C., *Insights in the Antibacterial Action of Poly(methyloxazoline)s with a Biocidal End Group and Varying Satellite Groups*. Biomacromolecules, **2008**. 9: 1764–1771.
- ¹⁸ Waschinski, C. J., Herdes, V., Schueler, F., Tiller, J. C., *Influence of Satellite Groups on Telechelic Antimicrobial Functions of Polyoxazolines*. Macromol. Biosci., **2005**. 5: 149–156.
- ¹⁹ Xie, M., Zhang, C., *Synthesis and characterization of side-chain liquid-crystalline poly(ethyleneimine)s with cyanobiphenyl groups*. Liquid Crystals, **2007**. 34: 1275-1283.
- ²⁰ Kumar, R. S., Arunachalam, S., *DNA binding and antimicrobial studies of polymer-copper(II) complexes containing 1,10-phenanthroline and L-phenylalanine ligands*. European Journal of Medicinal Chemistry, **2009**. 44: 1878-1883.
- ²¹ Griffiths, P. C., Alexander, C., Nilmini, R., Pennadam, S. S., King, S. M., Heenan, R. K., *Physicochemical characterization of thermoresponsive poly(N-isopropylacrylamide)-poly(ethyleneimine) graft copolymers*. Biomacromolecules, **2008**. 9: 1170-1178.
- ²² Weyts, K. F., Goethals, E. J., *New synthesis of linear polyethyleneimine*. Polymer Bulletin, **1988**. 19: 13-19.
- ²³ Lungwitz, Uta, *Polyethylenimine-derived Gene Carriers and their Complexes with plasmid DNA-design, synthesis and characterization*. Faculty of Chemistry and Pharmacy University of Regensburg, **2006**.
- ²⁴ Hilal, N., Kochkodan, V., Al-Khatib, L., Levadna, T., *Surface modified polymeric membranes to reduce (bio)fouling: a microbiological study using E.coli*. Desalination, **2004**. 167: 293-300
- ²⁵ Beyth, N., Hour-Haddad, Y., Baraness-Hadar, L., Yudovin-Farber, I., Domb, A. J., Weiss, E. I., *Surface antimicrobial activity and biocompatibility of incorporated polyethylenimine nanoparticles*. Biomaterials, **2008**. 29: 4157-4163.
- ²⁶ Witte, H., Seeliger W., *Cyclische Imidsaureester aus Nitrilen und Aminoalkoholen*. Liebigs Ann. Chem., **1974**. 996-1009
- ²⁷ Imamura, K., Shimizu, J., Nogami, T., *The Phase Transition of 1,4-Dialkyl-1,4-diazoniabicyclo[2.2.2]octane Dibromides, C_{n+2}-Br*. Bull. Chem. Soc. Jpn, **1986**. 59: 2699-2705.

- ²⁸ Yuan, J.-J., Jin, R.-H., *Multiply Shaped Silica Mediated by Aggregates of Linear Poly(ethyleneimine)*. *Adv. Mater.*, **2005**. 17: 885-888
- ²⁹ Lee, W. I., Bae, Y., Bard, A. J., *Strong blue photoluminescence and ECL from OH-terminated PAMAM dendrimers in the absence of gold nanoparticles*. *J. Am. Chem. Soc.*, **2004**. 126: 8358-8359.
- ³⁰ Wang, D., Imae, T., *Fluorescence emission from dendrimers and its pH dependence*. *J. Am. Chem. Soc.*, **2004**. 126: 13204-13205.
- ³¹ Lin, Y., Gao, J.-W., Liu, H.-W., Li, Y.-S., *Synthesis and characterization of hyperbranched poly(ether amide)s with thermoresponsive property and unexpected strong blue photoluminescence*. *Macromolecules*, **2009**. 42: 3237-3246.
- ³² Wu, Liu, Y., He, Goh, S. H., *Blue photoluminescence from hyperbranched poly(amino ester)s*. *Macromolecules*, **2005**. 38: 9906-9909.
- ³³ Cao, L., Yang, W., Wang, C., Fu, S., *Synthesis and striking fluorescence properties of hyperbranched poly(amido amine)*. *Journal of Macromolecular Science – Pure Appl. Chem.*, **2007**. 44: 417-424.

Chapter 2 – CHARACTERIZATION OF THE ANTIMICROBIAL EFFECT OF FUNCTIONALIZED 2- OXAZOLINE-BASED POLYMERS

2.1 OVERVIEW

This section describes the work that has been done in order to investigate the antimicrobial effect of the synthesized 2-oxazoline-based polymers (chapter 1).

The aim of this part of the work is to establish if the functionalized polyoxazolines produced in supercritical media display antimicrobial activity against different pathogenic, planktonic bacteria. The antimicrobial activity of quaternary ammonium groups is well documented, therefore it could be anticipated that the synthesized polymers would display activity against pathogenic microorganisms.

Staphylococcus aureus NCTC8325-4 and *Escherichia coli* AB1157 strains were the selected organisms to answer the following questions:

What molecules will have efficient antimicrobial activity?

Can different quaternary ammonium groups highly influence the antimicrobial activity?

Does the size of the polymer influence the antimicrobial activity?

How much time will the polymers take to highly reduce the viability of microorganisms?

Characterization of the antimicrobial effect of the polymers was evaluated by the determination of minimum inhibitory concentration (MIC) and of the killing curves of the polymers against *S.aureus* and *E.coli* and also by fluorescence microscopy for the assessment of bacterial viability.

2.2 INTRODUCTION

The introduction of penicillin in 1940 provided a main breakthrough in bacterial infection chemotherapy, significantly contributing to the increase in average life expectancy observed over the last decades. However, even before its use was widespread, the first cases of penicillin resistance were described.¹ Regrettably, bacteria soon developed resistance mechanisms against new antibiotics, making bacterial resistance a long established and widely studied health problem.² Antimicrobial resistance can also be seen as an inevitable

consequence of the misuse, overuse, and abuse of antibiotics. Therefore, it is critical to develop new antibiotics with novel modes of action.

2.2.1 Mechanisms of resistance to antibacterial agents

Bacteria may manifest resistance to antibacterial drugs through a variety of mechanisms. Of greater concern are cases of acquired resistance, where initially susceptible populations of bacteria become resistant to an antibacterial agent and proliferate under the selective pressure of use of that agent.

Several mechanisms of antimicrobial resistance are commonly found in a variety of bacterial genera: acquisition of genes encoding enzymes that destroy the antibacterial agent before it can act; acquisition of efflux pumps that expel the antibacterial agent from the cell before it can reach its target site; point mutations or acquisition of gene(s) that results in the alteration of the target (either enzymes or compounds such as cell wall); and alteration of the permeability of the cellular membrane, decreasing the access and binding of the antibiotic to the intracellular target.³

As a result, normally susceptible populations of bacteria may become resistant to antimicrobial agents through point mutations or by acquiring the genetic information that encodes resistance from other bacteria genes.

In all of these cases, strains of bacteria with the mutations that confer resistance are selected by the use of antimicrobial agents allowing their survival and growth.

Some bacteria have become resistant to multiple classes of antibacterial agents, and these bacteria with multidrug resistance constitute a serious concern, particularly in hospitals and other healthcare institutions where they tend to occur more frequently.

2.2.2 Mechanisms of action of antibacterial agents

Most antimicrobial agents used for the treatment of bacterial infections may be categorized according to their principal mechanism of action. There are four main modes of action: interference with cell wall synthesis, inhibition of protein synthesis, interference with nucleic acid synthesis, and inhibition of a metabolic pathway.³

Gram positive and gram negative bacteria have different susceptibilities to different class of antimicrobial compounds, mainly due to the presence of the outer membrane in gram negative bacteria.

Gram negative bacteria have two membranes: an inner membrane composed principally of phosphatidylethanolamine (PE) and phosphatidylglycerol and an outer membrane that contains lipopolysaccharides (LPS) on its outer leaflet. Gram positive bacteria have only one membrane composed mainly of phosphatidylglycerol and cardiolipin,⁴ to which lipoteichoic acids (LTA) can be attached (figures 2.1 and 2.2).

Nevertheless, it should keep in mind that the phospholipid composition of bacterial membranes varies widely among different species. Generally gram-negative bacteria contains both anionic and zwitterionic phospholipids, while many gram-positive bacteria contains predominantly anionic lipids, although there are some exceptions.

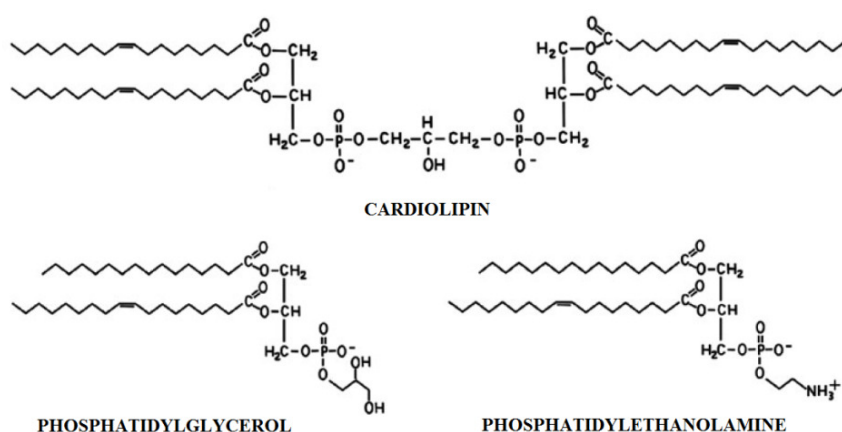


Figure 2.1 Chemical structures of the main phospholipid components of bacterial membranes.(adapted from ref. 4).

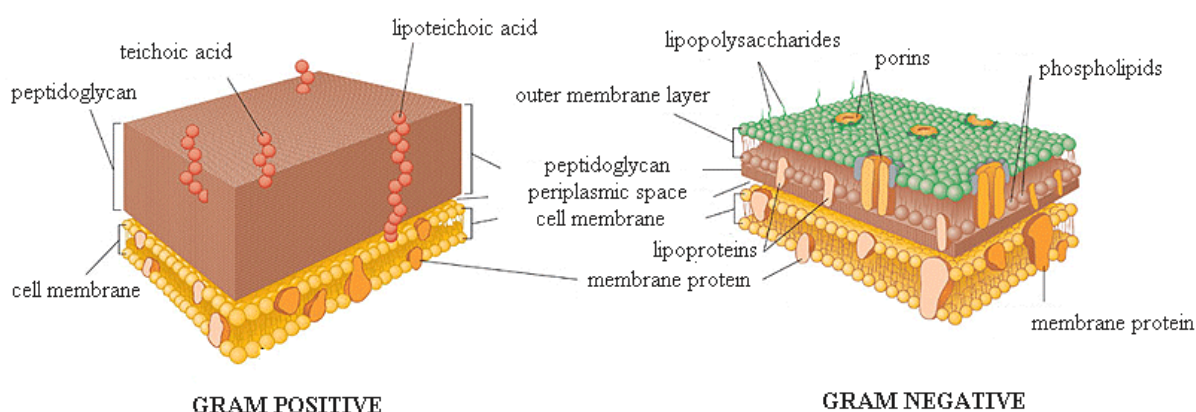


Figure 2.2 Molecular composition of gram positive and gram-negative bacteria. Main differences in evidence: peptidoglycan thickness and the presence of outer membrane (OM) in gram-negative bacteria (adapted from ref. 5).

Both gram-negative and gram-positive bacteria have a peptidoglycan layer outside of the cell membrane. Peptidoglycan (PG), also called murein, is a polymer that consists of long glycan chains cross-linked via flexible peptide bridges to form a strong but elastic structure which protects the cell from environmental stress or from lysis due to the high internal osmotic pressure.⁶ The glycan chain is built up of two different alternating subunits, β -1,4-linked *N*-acetylglucosamine (GlcNAc) and *N*-acetylmuramic acid (MurNAc).⁷ The chemistry of the glycan chains varies only slightly between different bacteria (figure 2.3).

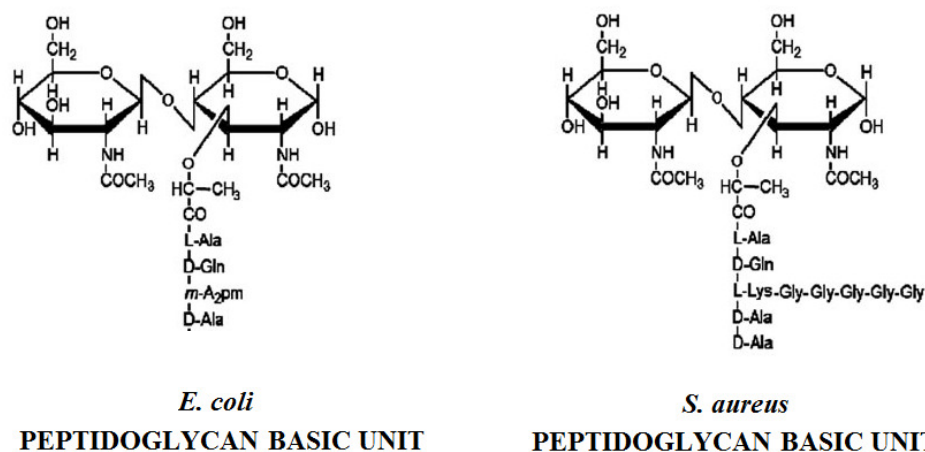


Figure 2.3 Structural differences between the *E.coli* and the *S.aureus* peptidoglycans. The basic unit of the peptidoglycan is composed by β -1,4-linked *N*-acetylglucosamine (GlcNAc) and *N*-acetylmuramic acid (MurNAc). (adapted from ref. 7).

Although the basic structure of the PG is very similar in gram-positive and gram-negative bacteria, its thickness is very different (figure 2.2), with the gram-positive wall much thicker (it has at least 10 to 20 layers) than the gram-negative wall (1 to 3 layers). In gram-negative bacteria, the thinner layer of PG is enough to maintain the mechanical stability of the cell and the PG is covalently attached to the outer membrane via lipoprotein. On the other hand, gram-positive bacteria, which do not have an outer membrane, have a thick cell wall that contains charged polymers covalently linked to it, such as teichoic acids, teichuronic acids, and proteins.⁷

The mechanisms of membrane disruption have been intensely studied. In general, membrane disruption is believed to occur mainly either via a detergent-like carpet mechanism (or carpeting mechanism),⁸ or through formation of discrete pores (figures 2.5 and 2.4, respectively).⁹ There is good experimental evidence for each of these processes, and different peptides may utilize different mechanisms to ultimately disrupt the microbial membrane. It may be that these mechanisms are not mutually exclusives: one process may

represent an initial or intermediate step and another may be its consequence. Additional factors such as the lipid-to-peptide ratio and the target membrane composition may also have an effect on the mechanisms of membrane disruption.

Regarding the pore formation mechanism, the antimicrobial agent can form a pore that acts as a conductance channel that disrupts the transmembrane potential and its ion gradients, leading to a leakage of cell components and consequently cell death. Dissipation of the transmembrane electrochemical gradient causes a loss of the bacterial cell's ability to synthesize ATP, and the increase in water and ion flow that accompanies loss of the permeability barrier leads to cell swelling and osmolysis. This mechanism requires the antimicrobial agent to be sufficiently long to traverse the hydrophobic core of the bilayer, and implies a direct contact between the antimicrobial agent molecules upon channel formation (figure 2.4).¹⁰

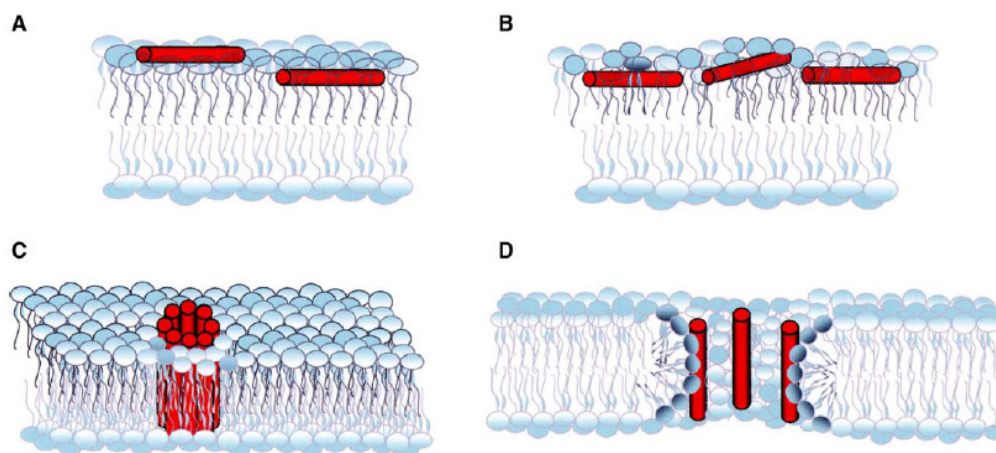


Figure 2.4 Models of transmembrane channel formation. Antimicrobial agent associates to the membrane surface (A) and accumulates (B). Once a critical antimicrobial agent/lipid ratio is reached, an insertion into the membrane is observed, with the formation of barrel-stave type pore (C) or formation of localized toroidal pores (D). (adapted from ref. 10)

On the other hand, in the carpeting mechanism, the antimicrobial agent accumulates at the bilayer surface like a carpet and, above a threshold concentration of the antimicrobial agent, the membrane is permeated and disintegrated in a detergent-like manner without the formation of discrete channels (figure 2.5).⁸

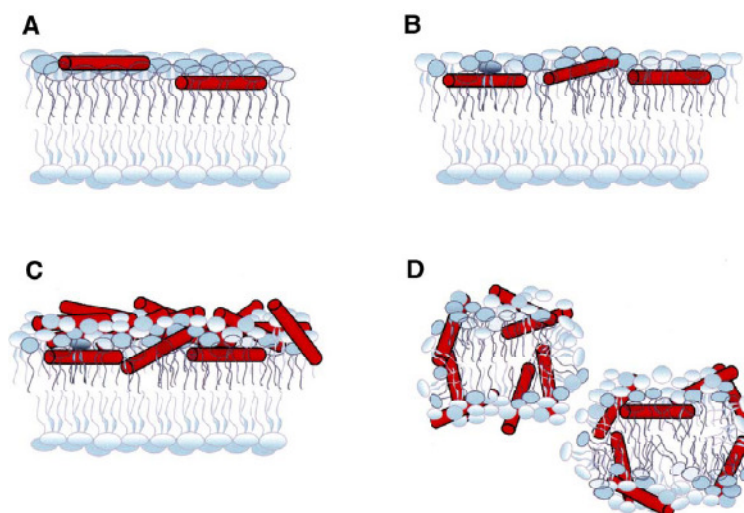


Figure 2.5 Model of membrane disruption by the carpet mechanism. The antimicrobial agent binds (A) and accumulates (B) in the membrane surface. Continued accumulation and covering (“carpeting”) of the bilayer (C) leads to a detergent-like disintegration (D) (adapted from ref. 10).

Possible mechanisms of action of functionalized 2-oxazoline-based polymers. There are some references in the literature about the possible mechanisms of action of polymers similar to the ones synthesized in this work, suggesting that the main target of these antimicrobial agents is the membrane.^{11,12} It is proposed that the antimicrobial mechanism of these polymers involves interaction with the membrane surface, which causes localized disruption of the bacterial phospholipid membrane by the linear end-capper group (figure 2.6).¹²

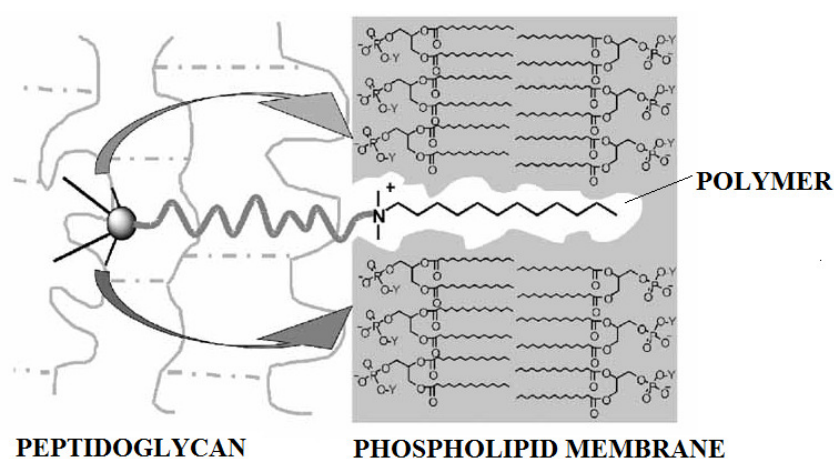


Figure 2.6 Proposed mechanism of membrane disruption by the polymers in the literature. (adapted from ref. 12)

2.2.3 Pathogenic relevance of *E.coli* and *S.aureus*

In this study two common pathogenic bacteria, the gram-negative *E.coli* and the gram-positive *S.aureus*, were used as model organisms.

Since 1883, *S.aureus* has been recognized as the most likely cause of wound infections. *S.aureus* infections are usually preceded by colonization, which occurs in about 30% of healthy people. It can cause common superficial infections, such as carbuncles, cellulitis, folliculitis, furuncles and impetigo but also primary bloodstream infections, or pneumonia.¹³ Bacterial infections are more common in hospital environments than elsewhere and *S.aureus* is most commonly passed on by direct contact. The spread of this type of infectious agents can be controlled effectively through a rigorous hygiene regime. Surfaces may act as reservoirs of microbes which could in turn lead to the spread of infection upon being touched, by either healthcare professionals or patients. Studies have shown the contamination of common hospital surfaces such as door handles, sterile packaging, ward fabrics and plastics, healthcare professionals pens, keyboards and taps, stethoscopes and telephones by potentially harmful microbes.^{14,15} Therefore, in hospitals, patients with open wounds, invasive devices, and weakened immune systems are at greater risk for infections than the general population.

E.coli is one of the best-known bacterial species and one of the most frequently isolated microorganisms from clinical specimens. *E.coli* can cause a wide variety of infections having a high incidence and associated morbidity and mortality. It can cause urinary, abdominal, pelvic and surgical site infections, pneumonia, meningitis and sepsis.¹⁶

New treatments and prevention measures are urgently needed for improved outcomes of bacterial infections and diminished disease.

2.2.4 Characterization of the antimicrobial effect

The success of the antimicrobial therapy is determined by complex interactions between an administered drug, a host and an infecting microorganism. In a clinical situation, the complexity of these interactions is usually reflected by a high variability in the dose-response relationship. Therefore, to minimize the dose-response variability and maximize antibiotics efficiency, key characteristics of the drug, host and microorganism should be taken in account.

Two methods that are frequently used to evaluate the antimicrobial activity are the determination of minimum inhibitory concentration (MIC) and of the killing-curves. Fluorescence methods can be used for the assessment of bacterial viability in the presence of the polymers.

Methods based on (MIC)s. The most common approach to antibiotic dosing is to adjust the doses to obtain antimicrobial concentrations in plasma that are above the MIC for the respective pathogenic microorganism during the dosing interval. MIC is defined as the lowest concentration of a specific antimicrobial agent that will completely inhibit the visible growth of a specific microorganism.^{17,18} This parameter is well known and allows the evaluation of the efficacy of antimicrobial agents. It is an extremely useful method due to its simplicity and reproducibility. However, this parameter has some limitations as it provides only limited information on the kinetics of the drug action. Since the MIC determination depends on the number of bacteria at a single time point, many different combinations of growth and kill rates can result in the same MIC. The different killing kinetics can be of extremely importance in therapeutics. MIC also represents *in vitro* threshold concentrations and not an *in vivo* scenario, where bacteria are not being exposed to constant but to constantly changing antimicrobial concentrations.¹⁹

Methods based on killing-curves. A different approach to assess the efficacy of antimicrobial agents is to follow microbial growth and killing as a function of time. These *in vitro* models provide more information about the time course of antimicrobial effect.

A typical bacterial growth curve (figure 2.7), in the absence of any antimicrobial compound, shows four characteristic phases: an initial lag phase, a phase of logarithmic growth called exponential phase, a stationary phase and, finally, a death phase. During the exponential phase, cells divide at a constant rate, which is dependent on the composition of the growth medium and conditions of incubation.

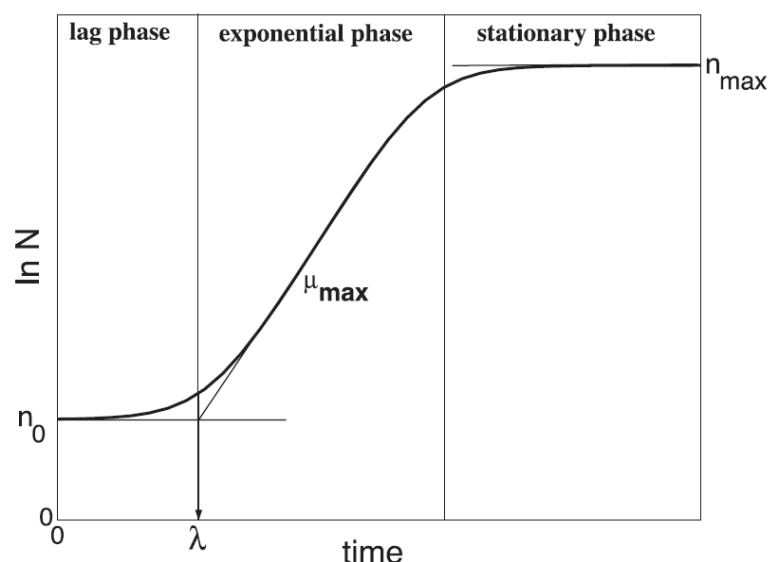


Figure 2.7 Typical bacterial growth curve at constant temperature conditions with three main phases shown. n_0 represents the initial population density, n_{max} the maximum population density, μ_{max} the maximum specific growth rate and λ the lag parameter (adapted from 20).

The effect of an antimicrobial agent can be evaluated by comparing the typical growth curve to the killing-curve performed in the presence of a constant concentration of the antimicrobial agent added in the exponential phase. Exposure to an antimicrobial compound while the bacteria are in the logarithmic phase will result in a change on the growth rate constant. A disadvantage of this type of approach is that, similarly to the MIC determination, it does not reflect the *in vivo* situation where a fluctuation of the concentration of the antimicrobial agent occurs.¹⁹

Fluorescent methods for assessment of bacterial viability. Classical methods for the determination of bacterial viability rely on the ability of cells to actively grow and form visible colonies on solid media. However, the number of viable cells can be underrepresented using these methods as viable bacteria may be unable to form a colony. Consequently, alternative methods for determining viability have been developed based on demonstration of cell integrity or metabolic activity. Alternatives include techniques like flow cytometry and fluorescent staining, the exploitation of physiological responsiveness or metabolic activity and nucleic acid-based analyses.^{21, 22, 23, 24}

The definition of bacterial cell death is quite controversial but, in this work, cells maintaining membrane integrity and retaining some metabolic activity will be considered viable.

The diagram on figure 2.8 represents some approaches used in the assessment of bacterial viability.

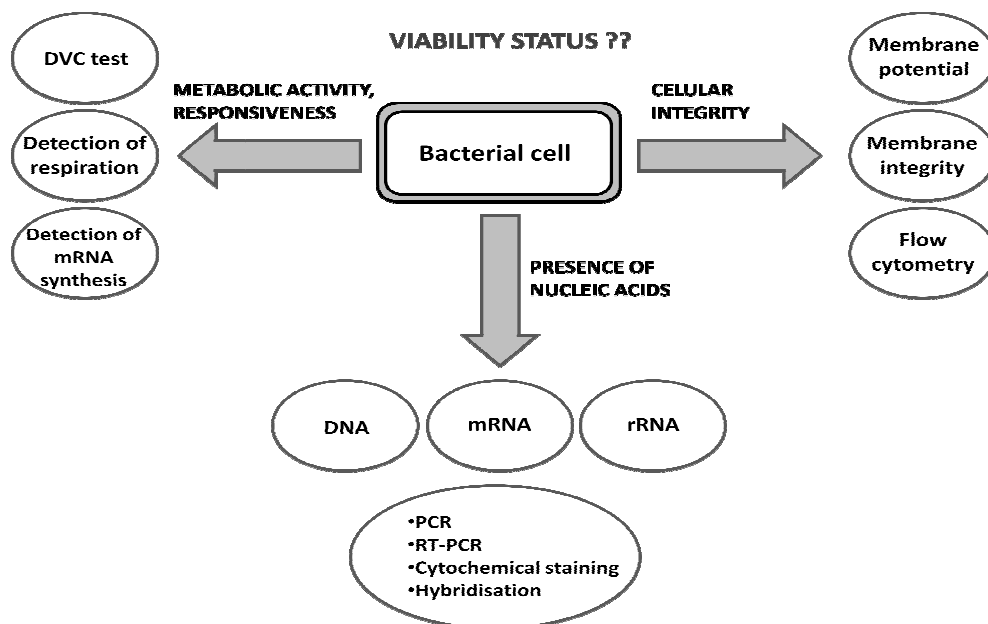


Figure 2.8 Schematic diagram that illustrates some approaches used in the assessment of bacterial viability (adapted from ref. 25).

In this work, a staining method was used for the assessment of bacterial viability based on monitoring the integrity of the membrane. For that purpose, it was used a fluorescent molecule, propidium iodide (PI, figure 2.9), that is the most commonly used dye to determine the bacterial viability.

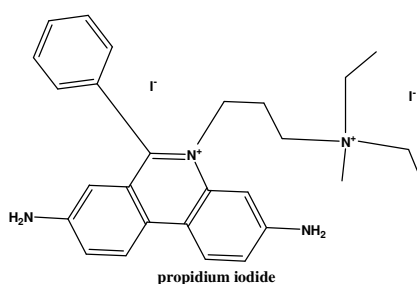


Figure 2.9 Chemical structure of PI.

Propidium iodide binds to DNA by intercalating between the bases, binding to the nucleotide pair guanine and cytosine. Once the dye is bound to the nucleic acids, its fluorescence is enhanced.²⁶ PI also binds to RNA, requiring treatment with nucleases to distinguish between RNA and DNA staining. PI is membrane impermeant and generally excluded from viable

cells. Therefore, PI only penetrates bacteria with compromised membrane and is commonly used to identify dead cells in a population.

2.3 EXPERIMENTAL METHODS

2.3.1 Bacterial strains and growth conditions. *Staphylococcus aureus* NCTC8325-4 and *Escherichia coli* AB1157 strains were used in all experiments and were grown in Mueller-Hinton broth medium (MHB, Oxoid). Cultures were grown overnight in broth at 37°C, diluted 1/200 and further incubated at 37 °C, with aeration and vigorous shaking to an optical density at 600nm of 0.5-0.6.

2.3.2 Disc diffusion technique. An initial test of antimicrobial activity of the synthesized polymers was made using disc diffusion technique. The tests were performed using 7 different microorganisms: *Staphylococcus aureus* ATCC 25923, *Enterococcus faecalis* ATCC 29212 (both gram-positive), *Escherichia coli* ATCC 25922, *Proteus mirabilis*, *Pseudomonas aeruginosa* ATCC 27853, *Klebsiella oxytoca* (all gram-negative) and *Candida albicans* ATCC MYA-2876 (fungi).

Cells were cultivated by adding 350µL of a stock solution of bacterial or fungi cells to a standard growth medium, Mueller-Hinton Agar (Merck, composition in g/L: meat infusion 2.0; starch 1.5; casein hydrolysate 17.5; agar 13.0).

Polymers were dissolved in water (all MetOx, EtOx and BisOx polymers) or in methanol (PhOx polymers).

Paper discs (BBL no. 231039, BD) were then impregnated with 15µL of polymer solution (of a concentration of 100mg/mL) and placed on the surface of the growth medium. The plates were incubated and the presence or absence of a zone of inhibition was evaluated. A negative control was set using a disc impregnated with water or methanol, according to the solvent used in the polymers solutions. Experiments were run in duplicate and the results obtained after incubation of 24 hours at 37°C for bacterial strains and 48 hours at 37°C for *Candida albicans*.

2.3.3 MIC determination. 2-oxazoline-based polymers were dissolved in the Mueller Hinton Broth medium. The polymers solutions were placed in a sterile 96-well microtiter plate and serially diluted. Then, 5 µL of culture (10^5 cells) were added to each well containing a volume of 100 µL of medium with a specific concentration of polymer (sequential 2 fold dilutions). Plates were incubated with shaking (100 rpm) at 37 °C overnight. Sterilization controls of the medium and polymer were also carried out. MIC results were determined after

24 hours of incubation. The tests were performed in duplicate and with both *S.aureus* and *E.coli* strains.

2.3.4 Killing Curves. A solution of polymer in growth medium with a concentration 5 or 2 times the obtained MIC value was added to *S.aureus* and *E.coli* cultures in exponential growth phase ($OD_{600nm} = 0,5-0,6$). Samples of the culture were taken before addition of polymer and 0, 2, 4, 6 and 10 minutes after the addition of PMetOx-DDA and PBisOx-DDA, and 0, 15, 30, 45, 60, 90, 120, 150, 180, 240 minutes after the addition of LPEI (see polymers reference at table **1.3**). Each sample was serially diluted to 10^0 , 10^{-2} and 10^{-4} in growth medium. 100 μ L of each dilution were plated on Mueller Hinton agar and incubated at 37 °C. After 24 hours, the number of viable colony was determined. Optical density was also measured during time assay. Killing curves were constructed by plotting colony-forming units (CFU) against time, in a log scale.

2.3.5 Fluorescence microscopy. A solution of polymer in a growth medium, with a concentration 5 times the obtained MIC value, was added to *S.aureus* and *E.coli* cultures in exponential phase ($OD_{600nm} = 0,5-0,6$). The incubation time used for each polymer solution was set according to the killing curve results obtained. Cultures were then labelled with propidium iodide (Molecular Probes, Invitrogen) during 5 minutes at room temperature, with agitation. Cells were visualized by phase-contrast and fluorescence microscopy in a Leica DRMA2 microscope coupled to a CoolSNAP HQ Photometrics camera (Roper Scientific).

2.4 RESULTS AND DISCUSSION

2.4.1 Disc diffusion technique

To have an initial idea of which polymers had antimicrobial activity, solutions of each 2-oxazoline-based polymer were placed on paper discs and were tested against different gram positive and negative bacteria as well as fungi. Microorganisms were incorporated in solid medium and solutions applied in paper discs.

The polymer solutions were highly concentrated to make sure that the quantity present was enough to inhibit the growth of the microorganism, if the polymer had antimicrobial activity. It should be noted that PBisOx-MDA and PBisOx-OH were only slightly soluble in water and methanol, the two solvents used in this test.

Table 2.1 Evaluation of the presence or absence of antimicrobial activity determined by disc diffusion technique (see polymers reference in table 1.3) Results of each polymer were identical to all 7 microorganism tested. ✓=presence of an inhibition halo; ✕= no inhibition halo present.

Polymer	Antimicrobial activity as determined by disc diffusion
PMetOX-DDA	✓
PMetOX-MDA	✓
PMetOX-OH	✕
PMetOX-DDA _{mw}	✕
PEtOX-DDA	✓
PEtOX-MDA	✓
PEtOX-DABCO	✕
PEtOX-MI	✕
PEtOX-MCHA	✕
PEtOX-OH	✕
PPhOx-DDA	✓
PPhOx-MDA	✓
PPhOx-OH	✕
PBisOx-DDA	✓
PBisOx-MDA	✕
PBisOx-OH	✕
LPEI	✓

This qualitative method allows the quick determination of the presence of antimicrobial activity (figure 2.10), although it may be considered less rigorous than the method based on MIC determination.

Polymers that showed antimicrobial activity, were efficient against all the 7 microorganisms tested, bacteria as well as fungi. The antimicrobial activity was observed for PMetOx-DDA, PMetOx-MDA, PEtOx-DDA, PEtOx-MDA, PPhOx-DDA, PPhOx-MDA, PBisOx-DDA, which

are end-capped with linear aliphatic amines *N,N*-dimethyldodecylamine (DDA) and *N*-methyldioctylamine (MDA) and that were obtained using four different oxazoline monomers (MetOx, EtOx, PhOx and BisOx); LPEI, the linear poly(ethyleneimine), also had antimicrobial activity. These results are in agreement with previous reports using similar polymers.^{11,12,27} Consequently, it may be concluded that the use of different oxazoline monomer will not highly influence the presence of antimicrobial activity.

The large size of the compound can explain the lack of activity of PMetOx-DDA_{mw} since this polymer is chemically identical to PMetOx-DDA but it has a higher molecular weight, which may limit diffusion.

Polymers end-capped with water, PMetOx-OH, PEtOx-OH, PPhOx-OH and PBisOx-OH showed no antimicrobial activity. These polymers were synthesized in order to evaluate if the antimicrobial activity was related with the presence of a quaternary ammonium salt end group. This result was predictable since the backbone of the 2-oxazoline-based polymer is not expected to have antimicrobial activity.

The functionalization of PEtOx-DABCO, PEtOx-MI and PEtOx-MCHA with non-linear amines (cyclic and aromatic amines) showed no antimicrobial activity, a result that might be related with the mechanism of membrane disruption proposed in the literature (figure 2.4),^{11,12} which seems to favor the insertion of linear amines in the membrane.

The lack of activity obtained for PBisOx-MDA, may be due to insufficient quantity of antimicrobial agent in the disc due to the low solubility of the polymer in the solvent used.

Negative results, in this type of test, can be due to the absence of antimicrobial activity but also to the incapacity of the polymer to diffuse from paper discs into the medium because of its size or solubility.

Due to the limitations of this technique, the antimicrobial activity was also tested using an alternative and quantitative method, the determination of the polymer's MICs.

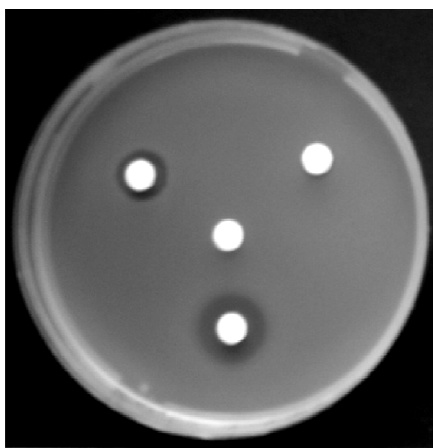


Figure 2.10 Disc diffusion test. Two polymers showing antimicrobial activity (with inhibition zones well defined) and two polymers that do not impair bacterial growth are shown in the image.

2.4.2 MIC determination

In this test, all 2-oxazoline-based polymers synthesized which are soluble in water were serially diluted and their antimicrobial effect was evaluated after 24 and 48 hours of incubation (table 2.2 and figure 2.11). The MIC values determined in duplicate are consistent in the range of 2-fold difference. This slight difference can be justified with different growth times of overnight cultures that led to different quantity of cells in the assays. The sterilization controls of medium and polymer showed no microbial growth.

Table 2.2 MIC determination of water soluble 2-oxazoline-based polymers.

Polymer	MIC value (mg/mL)	
	<i>S.aureus</i> NCTC 8325-4	<i>E.coli</i> AB1157
PMetOX-DDA *	1,5	0,75
	0,75	0,75
PMetOX-MDA	1,5	0,75
PMetOX-OH	> 25	> 25
PMetOX-DDA _{mw}	1,5	0,75
PEtOX-DDA	1,25	1,25
PEtOX-MDA	10	10
PEtOX-DABCO	5	> 25
PEtOX-MI	10	> 25
PEtOX-MCHA	10	> 25
PEtOX-OH	> 25	> 25
PBisOx-DDA *	0,37	0,37
	0,19	0,37
LPEI *	0,09	0,09
	0,05	0,19
CH ₃ -PMetOX ₅₃ -DDA ¹¹	1,03	2,49
CH ₃ -PMetOX ₂₂ -DDA ¹²	0,43	1,15

* MIC of these three polymers was determined in duplicate, once they were chosen to perform the rest of antimicrobial assays.

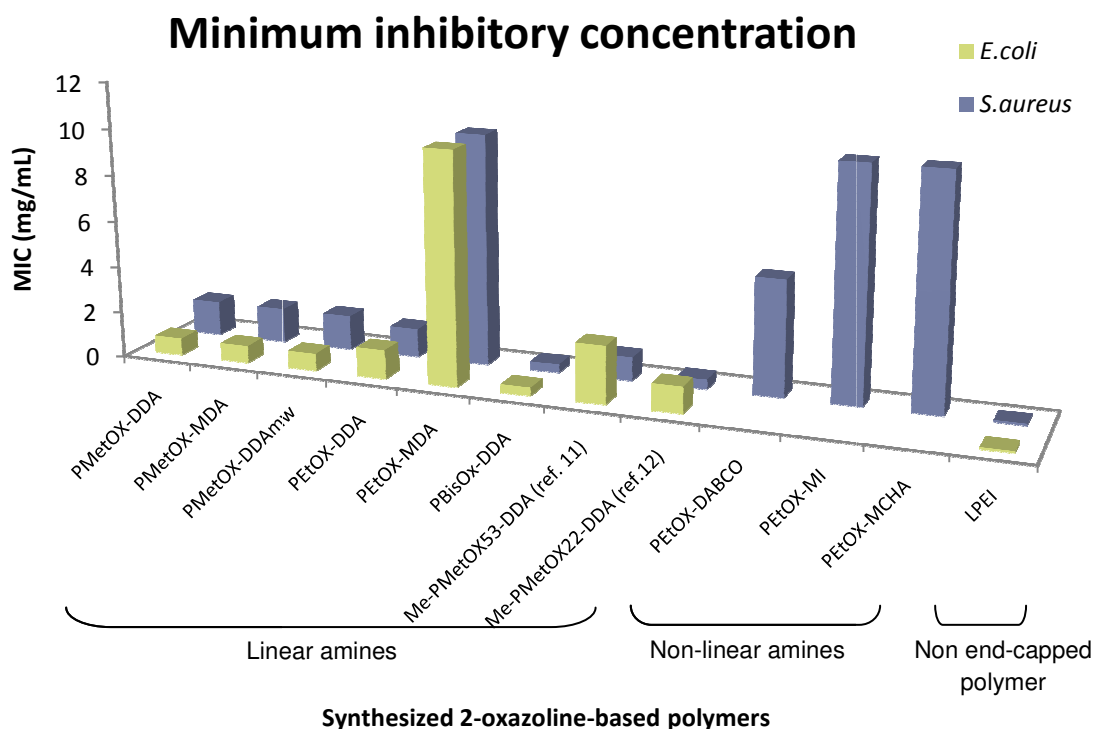


Figure 2.11 MIC of the water soluble 2-oxazoline-based polymers and also of two polymers referred in the literature, for *E. coli* and *S. aureus*.

MIC is the minimum inhibitory concentration that is necessary to inhibit the visible growth of a microorganism, therefore lower values obtained correspond to more efficient polymers.

Comparison of the MIC values obtained to the results of the inhibition halos shows that the polymers that showed antimicrobial activity by disc diffusion technique, are indeed efficient against *S. aureus* and *E. coli*. However, PMetOx-DDA_{mw}, PEtOx-DABCO, PEtOx-MI and PEtOx-MCHA that did not show antimicrobial activity by disc diffusion were shown to be active in liquid medium used for MIC determination. Hence, it can be confirmed that negative results obtained to the inhibition halos were not related with the absence of antimicrobial activity but with the size or solubility of the polymers, two parameters that can limit diffusion from the disc.

PMetOx-DDA_{mw} was as highly efficient as PMetOx-DDA. Both polymers are chemically identical but PMetOx-DDA_{mw} has a higher molecular weight, showing that the molecular weight does not influence the antimicrobial activity in the range tested (molecular weights between 1200-5000 g/mol). Similar polymers reported in the literature (references 11 and 12) also show an independence of MIC on molecular weight.

PEtOx-DABCO, PEtOx-MI and PEtOx-MCHA, end-capped with non-linear amines showed a higher MIC value to *S.aureus* than polymers end-capped with linear-amines and were not effective against *E.coli* in the concentration tested. It is described in the literature that the possible mechanisms of action of this type of compounds may involve a disruption of the membrane by a linear end-capper group.^{11,12} This may explain the requirement of a higher amount of antimicrobial compound end-capped with non-linear amines to inhibit bacterial growth. The lack of activity of these polymers against *E.coli* in the concentration range tested may result from the presence of an outer membrane.

Polymers with a hydroxyl end-capping group, (PMetOx-OH and PEtOx-OH) that were synthesized as a control, showed no biocidal activity. This proves that the antimicrobial activity is due to the presence of quaternary ammonium groups and that the backbone of the polymer does not influence its activity.

The polymers with a lowest MIC value were PBisOx-DDA and LPEI. The polymer PBisOx-DDA is poly(bisoxazoline) end-capped with *N,N*-dimethyldodecylamine, a branched polymer. This polymer is chemically similar to the 2-oxazoline-based polymers and the lowest MIC obtained can be related to the possibility of functionalization with more than one end group. The polymer LPEI does not have quaternary ammonium salt groups but the amine groups of its backbone become charged at physiological pH. According to the literature, the protonation of LPEI is obviously dependant of the pH of the assay. At pH 6.5-7.5 (the expected pH of the assays), the percentage of unprotonated amines may vary from 70 to 90%.²⁸ The polymer obtained was found to have a degree of polymerization (DP) of 12 by MALDI-TOF spectral analysis, and consequently it can contain 1 to 4 protonated amines. Therefore, LPEI can have 4 protonated amines in its chain, while PBisOx-DDA has the number of charges according with the number of end-capper groups in the polymer chain. These two polymers are the polymers with more positive charges per molecule, comparing to the rest of the synthesized polymers (that only have one charge per molecule since they have only one quaternary ammonium end-group).

The existence of positive charge may be an important requisite for the antimicrobial activity of the polymers and may play a key role in their mode of action, since the phospholipid composition of bacterial membranes has predominantly an anionic character. The cationic part of the polymer is believed to initiate electrostatic interactions with the negatively charged components of the membranes of microbes and to provide some degree of selectivity towards negatively charged microbial cell envelopes and cytoplasmatic membranes. Development of resistance to these type of antimicrobial polymers would then require bacteria to completely change their membrane structure, therefore this strategy could constitute a new and efficient alternative to conventional antimicrobial compounds.²⁹

In the literature, similar mechanisms are described as possible modes of action of polymers. For instance, it is believed that chitosan, a natural polycationic polymer, interacts with the negative charge on the surface of bacteria changing the permeability of the bacterial cell membrane. It is also described that the antimicrobial activity of this polymer is dependent of the pH of the assay. Chitosan is effective at pH 6.0 but ineffective at pH above 7.0 as a consequence of the deprotonation of amine groups of the polymer in basic conditions.³⁰

To perform the next microbiological tests, PMEtOx-DDA, PBisOx-DDA and LPEI were chosen. PBisOx-DDA and LPEI were selected because of their lowest MIC value and PMEtOx-DDA as representative of a 2-oxazoline-based and functionalized polymer. Moreover, PMEtOx-DDA is a linear polymer, PBisOx-DDA is a branched one and LPEI is a non-functionalized amine-based polymer.

2.4.3 Killing curves

In this test, microbial killing by three chosen polymers was followed as function of time. A solution of the polymer (PMEtOx-DDA, PBisOx-DDA or LPEI), with concentrations higher than the MIC value obtained (2 or 5 times) was added to the *E.coli* and *S.aureus* exponentially growing cultures. Samples were taken over time and plated to assess cell viability. OD_{600nm} was also measured. Assays were done in duplicate.

Optical density (OD) measures turbidity directly and the turbidity of a suspension of cells is directly related with the cell quantity. However, this measure does not differentiate between viable and death cells. Samples were therefore plated at different time points to assess viability since dead cells will not form any colonies.

• *E.coli*

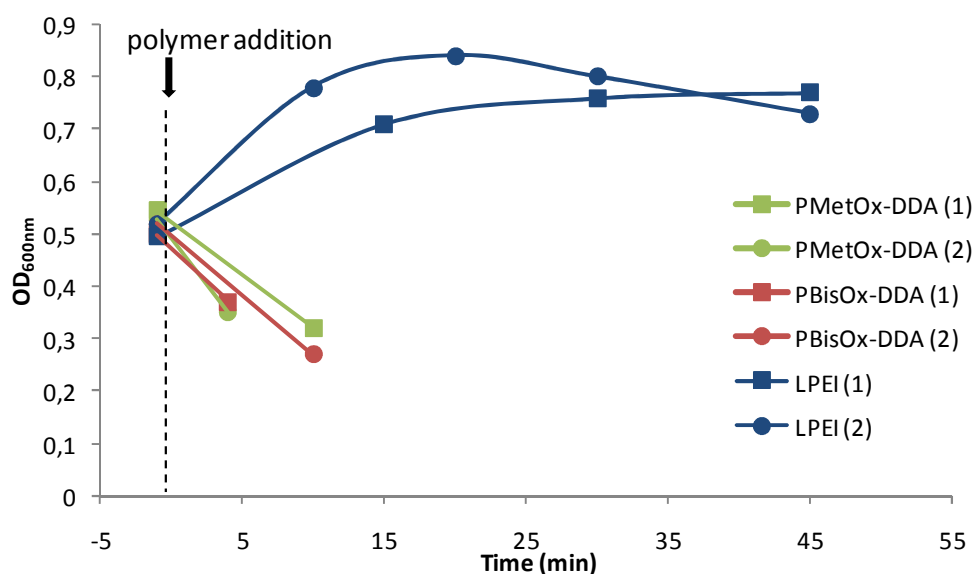


Figure 2.12 Bacterial growth after the addition of the polymers. The decrease in the optical density (600 nm) of *E.coli* in the presence of PMetOx-DDA and PBisOx-DDA after 4 and 10 minutes and stabilization of the bacterial growth during 45 minutes in the presence of LPEI can be seen. Time t=0 minutes represents the addition of the polymer. Assays were done in duplicate (1 and 2 for each polymer).

In figure 2.12, after the addition of PMetOx-DDA and PBisOx-DDA the optical density of *E.coli* cultures decreased indicating that the cells are dying after only 4 minutes in the presence of the polymers.

After the addition of LPEI, the optical density of *E.coli* continues to increase in the first 20-30 minutes and then stabilizes.

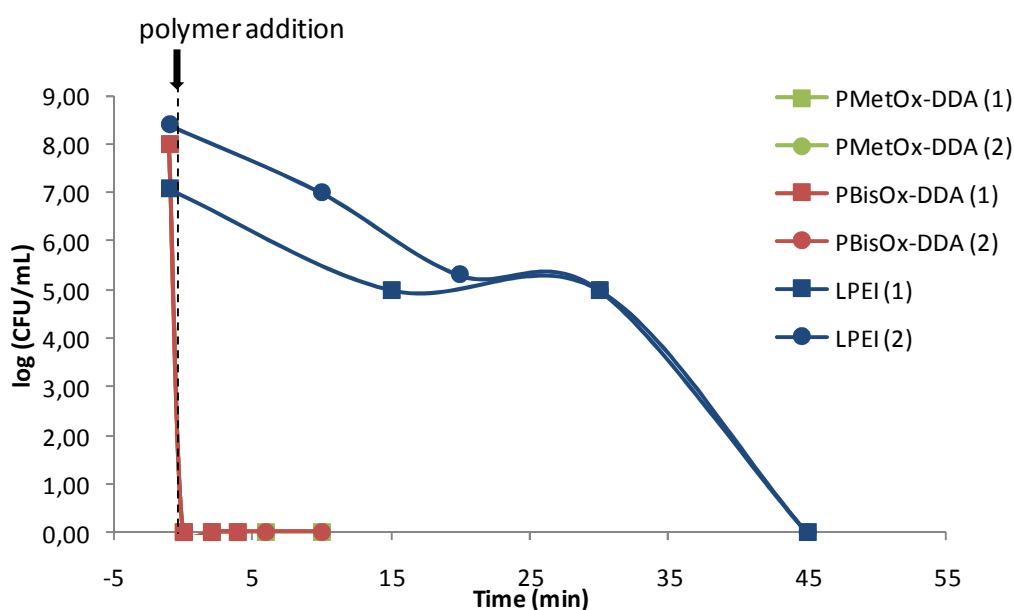


Figure 2.13 Number of viable cells per mL after the addition of the polymers. The reduction in the number of viable *E.coli* in the presence of PMetOx-DDA and PBisOx-DDA during 10 minutes and LPEI during 45 minutes of assay can be seen in a logarithmic scale. PMetOx-DDA and PBisOx-DDA assays are overlapped in the graph, showing identical behaviour. The value of the initial viable cells (10^8 cells) is an estimated value. Time t=0 minutes represents the addition of the polymer. Assays were done in duplicate (1 and 2 for each polymer).

Immediately after the addition of PMetOx-DDA and PBisOx-DDA there is a quick decrease in the number of colony-forming units. In fact, just after the addition of the polymer all cells are killed (figure 2.13).

After the addition of LPEI, viable cells of *E.coli* started to decrease but only achieved zero CFU after 45 minutes of incubation with LPEI.

PMetOx-DDA and PBisOx-DDA showed to have faster killing rates comparatively to LPEI.

- ***S.aureus***

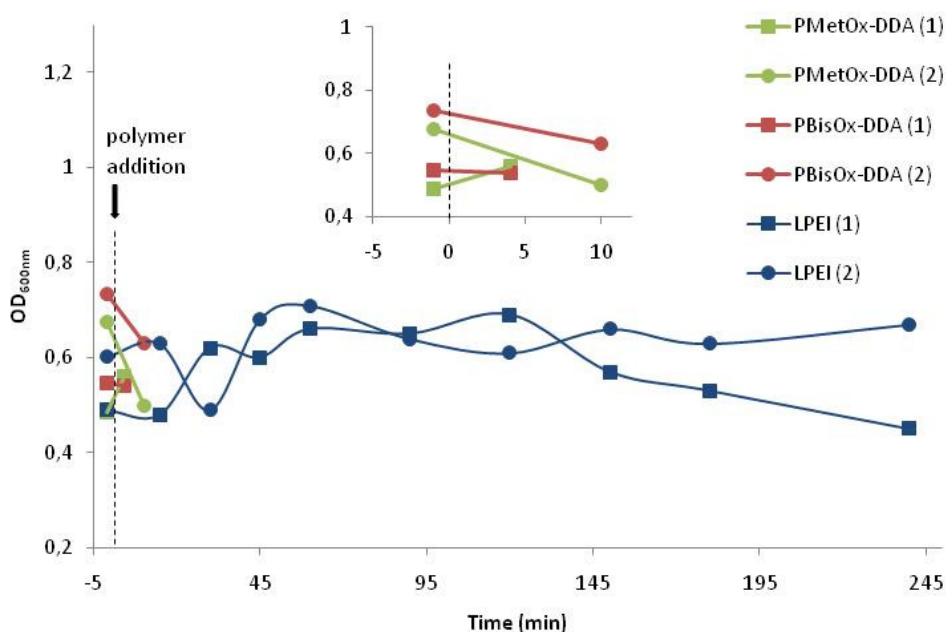


Figure 2.14 Bacterial growth after the addition of the polymers. The reduction in the optical density (600 nm) of *S.aureus* in the presence of PMetOx-DDA and PBisOx-DDA after 4 and 10 minutes and the stabilization of the bacterial growth during 240 minutes in the presence of LPEI can be seen. Inset shows PMetOx-DDA and PBisOx-DDA assays in detail. Time t=0 minutes represents the addition of the polymer. Assays were done in duplicate (1 and 2 for each polymer).

Figure 2.14 shows a slight reduction in the optical density after the addition of PMetOx-DDA and PBisOx-DDA. Both polymers caused a decrease in O.D. 10 minutes after their addition to a *S.aureus* culture.

LPEI caused a halt in exponential growth but no decrease in O.D. was observed during the 4 hours assay.

Similarly to *E.coli*, PMetOx-DDA and PBisOx-DDA were more effective at inhibiting growth of *S.aureus* than LPEI.

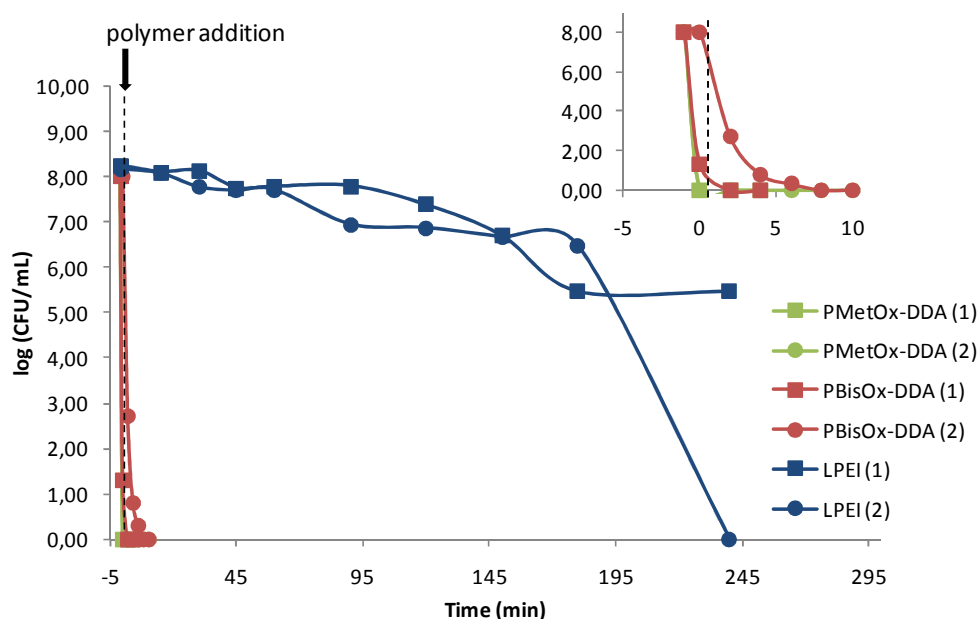


Figure 2.15 Number of viable cells per mL after the addition of the polymers. The reduction in the number of viable *S.aureus* in the presence of PMetOx-DDA and PBisOx-DDA during 10 minutes and of LPEI during 240 minutes of assay can be seen in a logarithmic scale. PMetOx-DDA and PBisOx-DDA assays are overlapped in the graph, showing identical behaviour. The value of the initial viable cells (10^8 cells) is an estimated value. Inset shows PMetOx-DDA and PBisOx-DDA assays in detail. Time $t=0$ minutes represents the addition of the polymer. Assays were done in duplicate (1 and 2 for each polymer).

Figure 2.15 shows that addition of PMetOx-DDA and PBisOx-DDA caused a fast decrease of total viable *S.aureus* cells.

LPEI took 240 minutes to kill all ($\geq 10^8$ cells) *S.aureus* cells.

The end-capping with *N,N*-dimethyldodecylamine of poly(2-methyl-2-oxazoline) and poly(bisoxazoline) led to materials with higher MIC values but fast killing rates: less than 5 minutes to achieve 100 % killing for both bacterial species. On the other hand, LPEI, the polymer with lower MIC value, achieved 100 % killing after 45 minutes in contact with *E.coli* and after 4 hours in contact with *S.aureus*.

This difference in the biocidal behavior (MIC and killing rates) can possibly indicate some differences in the mode of action of these polymers. Polymers with higher MIC value and faster killing rates may act in the bacterial membrane by a carpeting mechanism. Polymer accumulates in the membrane until reaches a required concentration and then, the

membrane disintegrates. Therefore, it is expected that the amount of antimicrobial agent will be higher than the amount required to form discrete pores. The polymer with a lower MIC value is expected may act through a pore formation mechanism, taking more time to act in the membrane.

Hence, PMetOx-DDA and PBisOx-DDA could possible act by a carpeting mechanism. The polymer accumulates, acts in the membrane rapidly and lyses the bacterial cells, without making a distinction between *E.coli* and *S.aureus*, leading to similar behaviors of both strains (rapid killing rates and the immediate reduction in O.D. confirming that the cells are, in fact, being lysed).

On the other hand, LPEI may act as a proton sponge that causes ion influx and leads to membrane rupture, or can act in the membrane by forming pores. In this second type of mechanism, cell lysis does not occur immediately as the cells first lose their membrane potential, components and the ability to divide. This fact can justify the stabilization of the O.D. during the assays since cells are no longer dividing but are not yet lysed. Comparing the results for both strains, a large difference in the killing rates can also be noted. Growth of *E.coli* can be inhibited by disrupting just the outer membrane,³¹ justifying the need of 30 minutes to reduce the viable cells. In case of *S.aureus*, the polymer must diffuse through the thicker peptidoglycan to be effective at the inner membrane.³²

2.4.4 Fluorescence microscopy

Propidium iodide dye was used for cell labeling, followed by fluorescence microscopy to assess viability of *S.aureus* and *E.coli* strains in the presence of the three better studied polymers: PMetOx-DDA, PBisOx-DDA and LPEI (figures **2.16** and **2.17**). Cells were incubated in the presence of the polymers for variable times, chosen in agreement of the killing curves obtained for each polymer (figures **2.13** and **2.15**).

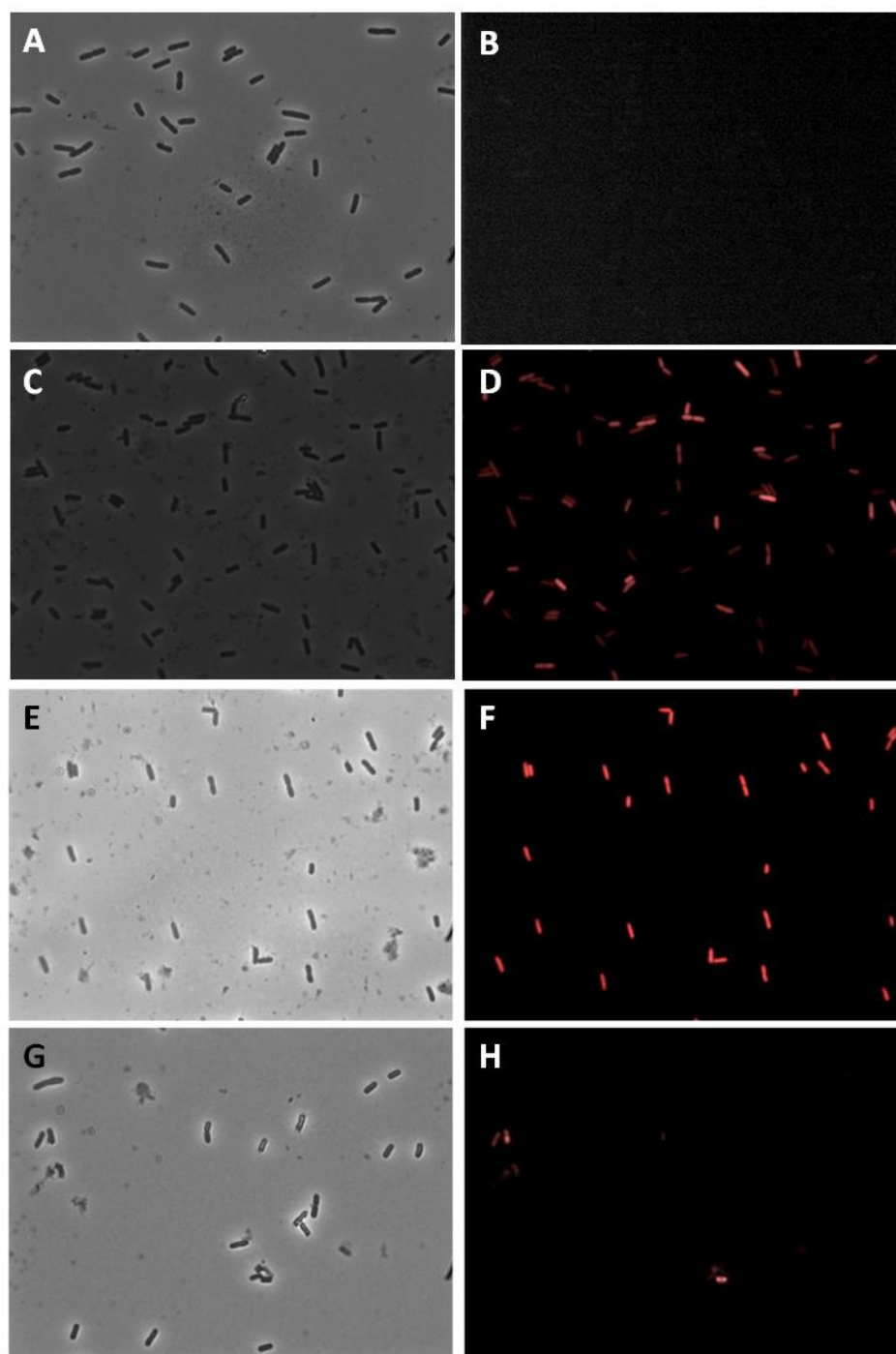


Figure 2.16 Fluorescence labeling with propidium iodide for assessment of cell viability. **A** and **B**: cells of *E.coli* AB1157 visualized by phase-contrast and fluorescence microscopy using Texas Red filter, respectively, in the absence of any polymer. **C** and **D**: same cells incubated with PMEtOx-DDA during 5 minutes. **E** and **F**: same cells incubated with PBisOx-DDA **4a** during 5 minutes. **G** and **H**: same cells incubated with LPEI during 30 minutes. Dead cells are seen as fluorescent on right panels.

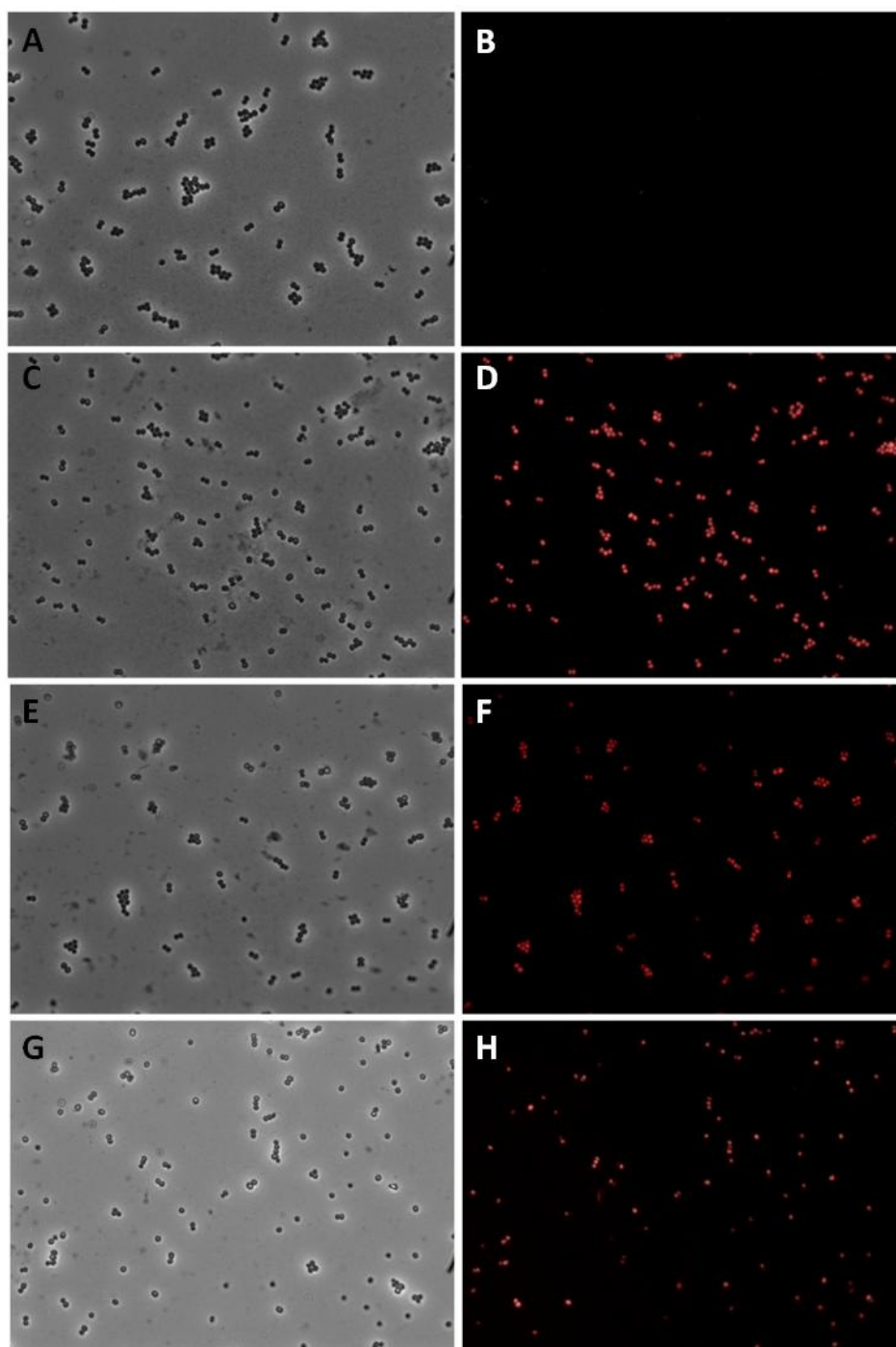


Figure 2.17 Fluorescence labeling with propidium iodide for assessment of cell viability. **A** and **B**: cells of *S.aureus* NCTC 8325-4 visualized by phase-contrast and fluorescence microscopy using Texas Red filter, respectively, in the absence of any polymer. **C** and **D**: same cells incubated with PMEtOx-DDA during 5 minutes. **E** and **F**: same cells incubated with PBisOx-DDA during 5 minutes. **G** and **H**: same cells incubated with LPEI during 240 minutes. Dead cells are seen as fluorescent on right panels.

The results obtained in this test are in accordance with the results obtained in the killing-curves for each polymer. Both *E.coli* and *S.aureus* become fluorescent after the addition of each polymer indicating that cells are in fact being killed.

In figure **2.16H** the cells were not all stained with propidium iodide, but on the other hand some unstained lysed cells in the picture can be seen. Lysed cells are dead cells with membrane integrity compromised and that had released the cellular contents. Moreover, accordingly to the results obtained in the killing-curves of *E.coli*, after 30 minutes in the presence of the LPEI, the presence of viable cells can be still observed.

This method is reliable, easy to perform and a good alternative to assess the viability, since viable cells are not underrepresented in this method.

2.5 CONCLUSION

The library of the synthesized 2-oxazoline-based polymers was characterized by microbiological techniques.

A initial quick and qualitative test and a later rigorous method for the determination of minimum inhibitory concentrations (MIC) values of each polymer, lead to the conclusion that 2-oxazoline-based polymers functionalized with different types of amines as well as LPEI have a broad antimicrobial activity as well as antifungal activity.

The four different types of 2-substituted oxazoline monomers used in the polymers' synthesis as well as the difference in the molecular weight between chemically identical polymers do not highly influence their antimicrobial activity.

Besides MIC, killing curves of the synthesized polymers against *S.aureus* and *E.coli* were also determined. The end-capping with *N,N*-dimethyldodecylamine of poly(2-methyl-2-oxazoline) and poly(bisoxazoline) *living polymers* led to materials with higher MIC values but fast killing rates (less than 5 minutes) than LPEI, a polymer which had a lower MIC value, but took longer to kill both *E.coli* and *S.aureus* cells. LPEI achieved 100% killing after 45 minutes in contact with *E.coli* and after 4 hours in contact with *S.aureus*.

The presence of positive charge in the polymers might play a significant role in the initial binding of the polymers to the cell membrane and, therefore, in the mode of action since the phospholipid composition of bacterial membranes has predominantly an anionic character. In a second step, it is believed that polymers will induce membrane permeation either via pore formation or membrane disintegration, accompanied by a loss of bacterial membrane potential.^{33,34}

The differences observed in the biocidal behavior (MIC and killing rates) of different polymers may be an indication of differences in their mode of action. Polymers with higher MIC values and faster killing rates possibly act in the bacterial membrane by a carpeting mechanism, while LPEI, the polymer with a lower MIC value and slower killing rate, may act through the formation of pores in the membranes.

Further studies are being performed to elucidate these mechanisms of action.

2.6 REFERENCES

-
- ¹ Abraham, E. P., Chain, E., *An enzyme from bacteria able to destroy penicillin*. Rev. Infect. Dis., **1940**. 10: 677-678.
- ² Russel, A. D., *Bacterial resistance to disinfectants: present knowledge and future problems*. Journal of Hospital Infection, **1998**. 43: S57-S68.
- ³ Tenover, F.C., *Mechanisms of Antimicrobial Resistance in Bacteria*. The American Journal of Medicine, **2006**. 199: S3-S10.
- ⁴ Epand, R.M., Epand, R.F., *Domains in bacterial membranes and the action of antimicrobial agents*. Mol. BioSyst., **2009**. 5: 580-587.
- ⁵ Betsy, T., Keogh, J., *Microbiology Demystified*. McGraw-Hill Publishing, **2005**.
- ⁶ Schleifer, K. H., Kandler, O., *Peptidoglycan types of bacterial cell walls and their taxonomic implications*. Bacteriol. Rev., **1972**. 36: 407–477.
- ⁷ Scheffers, D.J., Pinho, M.G., *Bacterial cell wall synthesis: new insights from localization studies*. Microbiology and Molecular Biology Reviews, **2005**. 69: 585-607.
- ⁸ Y. Shai, *Mode of action of membrane active antimicrobial peptides*. Biopolymers, **2002**. 66: 236–248.
- ⁹ H.W. Huang, *Action of antimicrobial peptides: two-state model*. Biochemistry, **2000**. 39: 8347–8352.
- ¹⁰ Sato, H., Feix, J.B., *Peptide-membrane interactions and mechanisms of membrane destruction by amphipatic α -helical antimicrobial peptides*. Biochimica et Biophysica Acta, **2006**. 9: 1245-1256.
- ¹¹ Waschinski, C. J., Barnert, S., Theobald, A., Schubert, R., Kleinschmidt, F., Hoffmann, A., Saalwachter, A., Tiller, J. C., *Insights in the antibacterial action of poly(methyloxazoline)s with a biocidal end group and varying satellite groups*, Biomacromolecules **2008**. 9: 1764–1771.
- ¹² Waschinski, C. J., Herdes, V., Schueler, F., Tiller, J. C., *Influence of satellite groups on telechelic antimicrobial functions of polyoxazolines*, Macromol. Biosci. **2005**. 5: 149–156.
- ¹³ Smith, T. L., Jarvis, W. R., *Antimicrobial resistance in Staphylococcus aureus*. Microbes and Infection, **1999**. 1: 795-805.
- ¹⁴ Page, K., Wilson, M., Parkin, I. P., *Antimicrobial surfaces and their potential in reducing the role of the inanimate environment in the incidence of hospital-acquired infections*. J. Mater. Chem., **2009**. 19: 3819-3831.

- ¹⁵ Ferreira, L., Zumbuehl, A., *Non-leaching surfaces capable of killing microorganisms on contact*. Journal of Materials Chemistry, **2009**. 134: 7796-7806.
- ¹⁶ Russo, T. A., Johnson, J.R., *Medical and economic impact of extraintestinal infections due to Escherichia coli: focus on an increasingly important endemic problem*. Microbes and Infection, **2003**. 5: 449-456.
- ¹⁷ Andrews, J. M., *Determination of minimum inhibitory concentrations*. Journal of Antimicrobial Chemotherapy, **2001**. 48: S1, 5-16.
- ¹⁸ National Committee for Clinical Laboratory Standards. *Methods for Dilution Antimicrobial Susceptibility Tests for Bacteria that grow aerobically*. 4th. ed. Approved Standard. NCCLS Publication No. M7-A4. National Committee for Clinical Laboratory Standards, Villanova, Pa. **1997**.
- ¹⁹ Muller, M., de la Pena, A., Derendorf, H., *Issues in Pharmacodynamics of Anti-Infective Agents: Kill Curves versus MIC*. Antimicrobial Agents and Chemotherapy, **2004**. 48: 369-377.
- ²⁰ Swinnem, I. A. M., Bernaerts, K., Dens, E. J. J., Geeraerd, A. H., Van Impe, J.F., *Predictive modeling of the microbial lag phase: a review*. International Journal of Food Microbiology, **2004**. 94: 137-159.
- ²¹ Caron, G.N., Stephens, P., Badley, R.A., *Assessment of bacterial viability status by flow cytometry and single cell sorting*. J.Appl. Microbiol., **1998**. 84: 988– 998.
- ²² Turner, K., Porter, J., Pickup, R., Edwards, C., *Changes in viability and macromolecular content of long-term batch cultures of Salmonella typhimurium measured by flow cytometry*. J. Appl. Microbiol., **2000**. 89: 90–99.
- ²³ Kogure, K., Simidu, U., Taga, N., *A tentative direct microscopic method for counting living marine bacteria*. Can. J. Microbiol., **1979**. 25: 415– 420.
- ²⁴ Sheridan, G. E. C., Masters, C. I., Shallcross, J. A., Mackey, B. M., *Detection of mRNA by reverse transcription-PCR as an indicator of viability in Escherichia coli cells*. Appl. Environ. Microbiol., **1998**. 64: 1313– 1318.
- ²⁵ Keer, J. T., Birch, L., *Molecular methods for the assessment of bacterial viability*. Journal of Microbiological Methods, **2003**. 53: 175-183.
- ²⁶ Suzuki, T., Fujikura, K., Higashiyama, T., Takata, K., *DNA staining for fluorescence and laser confocal microscopy*. The Journal of Histochemistry & Cytochemistry, **1997**. 45(1): 49-53.
- ²⁷ Beyth, N., Hour-Haddad, Y., Baraness-Hadar, L., Yoduvin-Farber, I., Domb, A. J., Weiss, E. I., *Surface antimicrobial activity and biocompatibility of incorporated polyethylenimine nanoparticles*. Biomaterials, **2008**. 29: 4157-4163.
- ²⁸ Suh, J., Paik, H.-J., Hwang, B. K., *Ionization of Poly(ethylenimine) and Poly(allylamine) at various pH's*. Bioorganic Chemistry, **1994**. 22: 318-327.

- ²⁹ Zasloff, M., *Antimicrobial Peptides, Innate Immunity, and the normally sterile urinary tract*. Journal of the American Society of Nephrology, **2007**. 18: 2810-2816.
- ³⁰ Rabea, E. I., Badaway, M. E., Stevens, C. V., Smagghe, G., Steurbaut, W., *Chitosan as antimicrobial agent: applications and mode of action*. Biomacromolecules, 2003. 4:1457-1465.
- ³¹ Vaara, M., *Outer membrane permeability barrier to azithromycin, clarithromycin, and roxithromycin in gram-negative enteric bacteria*. Antimicrobial Agents and Chemotherapy, **1993**. 37: 354-356.
- ³² Tiller, J. C., Liao, C.-J., Lewis, K., Klibanov, A. M., *Designing surfaces that kill bacteria on contact*. PNAS, **2001**. 98: 5981:5985.
- ³³ Brogden, K. A., *Antimicrobial peptides: pore formers or metabolic inhibitors in bacteria?*. Nat. Rev. Microbiol., **2005**. 3: 238–250.
- ³⁴ Yeaman, M. R., Yount, N. Y., *Mechanisms of antimicrobial peptide action and resistance*. Pharmacol. Rev., **2003**. 55: 27–55.

FUTURE WORK

In order to achieve a better understanding of the polymers killing mechanisms and also to explore their fluorescence properties further work is required.

It is essential to fully understand the mechanisms of action of PMetOx-DDA, PBisOx-DDA and LPEI in *E.coli* and *S.aureus*, through the use of microbial cell biology techniques, with the aim of confirming the membrane as the target.

It is very important to study the precise local of polymers action in order to understand their mechanism of action. To assess if the polymers permeabilize either inner (IM) or outer membrane (OM), a reported method will be used, through the use of *E.coli* ML 35p. This *E.coli* strain constitutively expresses cytoplasmic β -galactosidase but lacks its permease. In the presence of β -galactosidase substrate, ONPG (*o*-nitrophenyl- β -D-galactopyranoside), the production of *o*-nitrophenyl (ONP) over time is going to be monitored spectrophotometrically at 420nm. The production of ONP indicates that β -galactosidase was released from the cytoplasm and that IM was damaged. OM permeabilization will be assessed using the same strain and by 1-*N*-phenyl-naptylamine (NPN) uptake. This hydrophobic probe strongly interacts in phospholipid layer but only weakly in an aqueous environment. Usually, intact OM excludes hydrophobic molecules, but through the usage of permeabilizers, the phospholipids become accessible and allow NPN access into the phospholipid layer. By this way, increased fluorescence in NPN-containing bacterial suspensions will indicate OM damage.

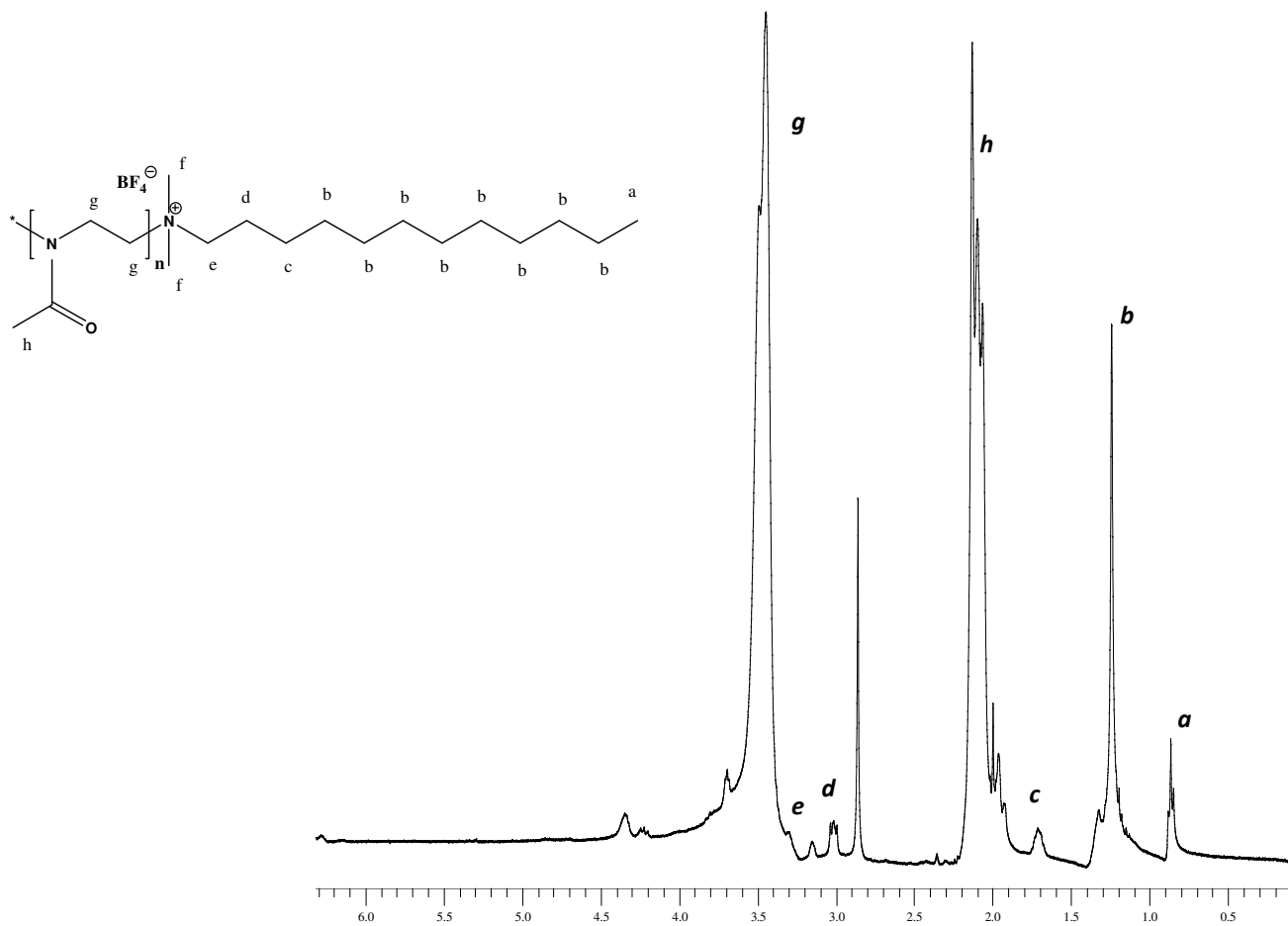
It is also fundamental to study the cytotoxicity of the synthesized polymers. If their toxicity to mammalian cells is proved to be minimal, it would be interesting to exploit some applications: development of scaffolds with antimicrobial activity for cell growth; immobilization, coating or incorporation of the polymers in medical devices like catheters, for example; the development of antimicrobial gels for topic use; among many others.

Testing the antibiofouling activity of the polymers is also envisaged, once that the formation of biofilms is also a major problem in the spread of infections, exhibiting extreme resistance to antibiotics.

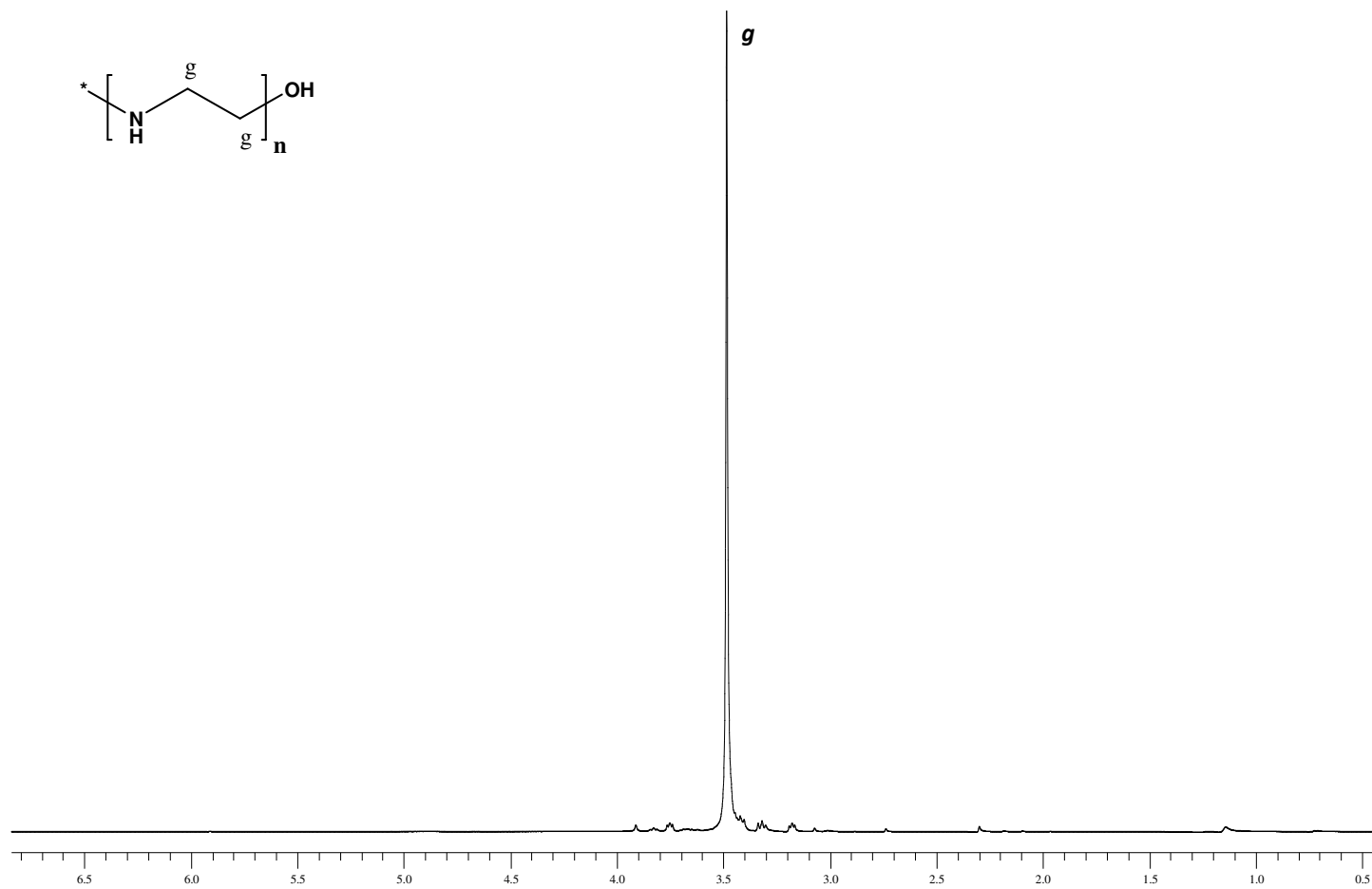
It would be also interesting to promote the growth of bacterial cells with sub-MIC quantities of polymers and assess if the cells become polymer resistant and then study the resulted mutations to better understand the mechanisms of resistance associated with polyoxazolines and to exploit alternatives to the development of this resistance.

Taking advantage of the intrinsic fluorescence of 2-oxazoline-based polymers, it would be fascinating to optimize the assays conditions to examine the localization of polymers while interacting with bacteria without the use of any staining molecules.

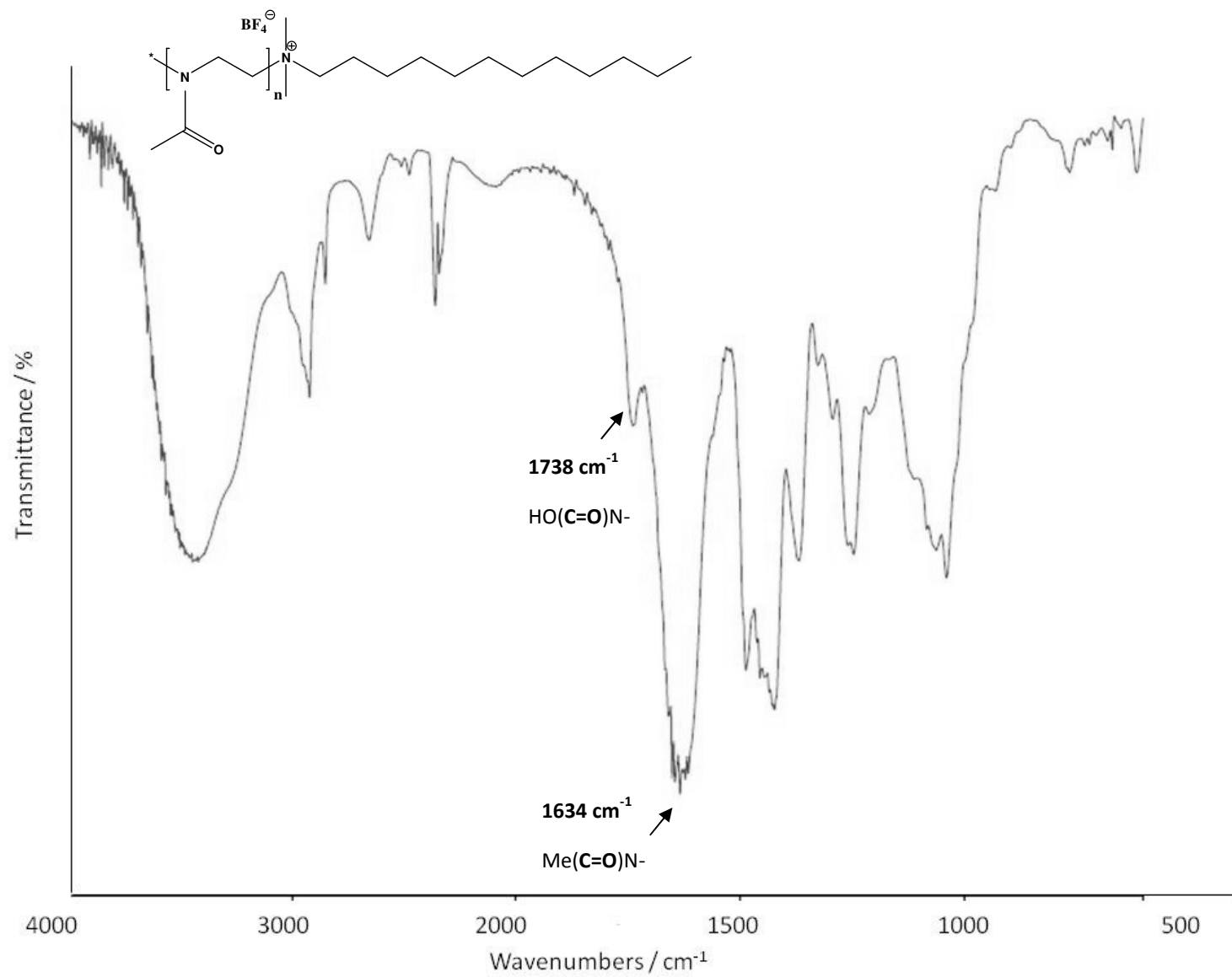
APPENDIX SECTION



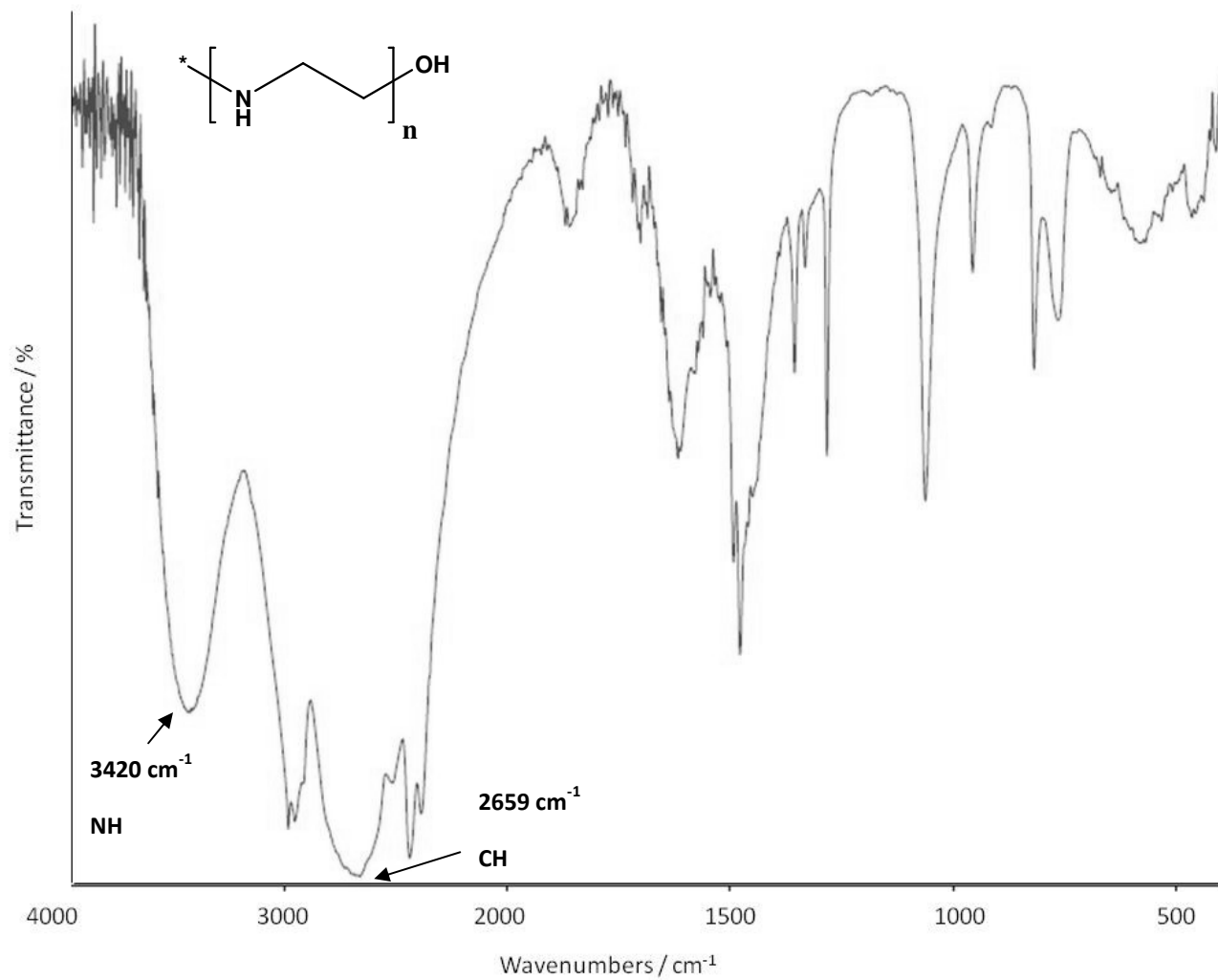
Appendix 1 ¹H-NMR spectrum (400 MHz, CDCl₃) of PMetOx-DDA.



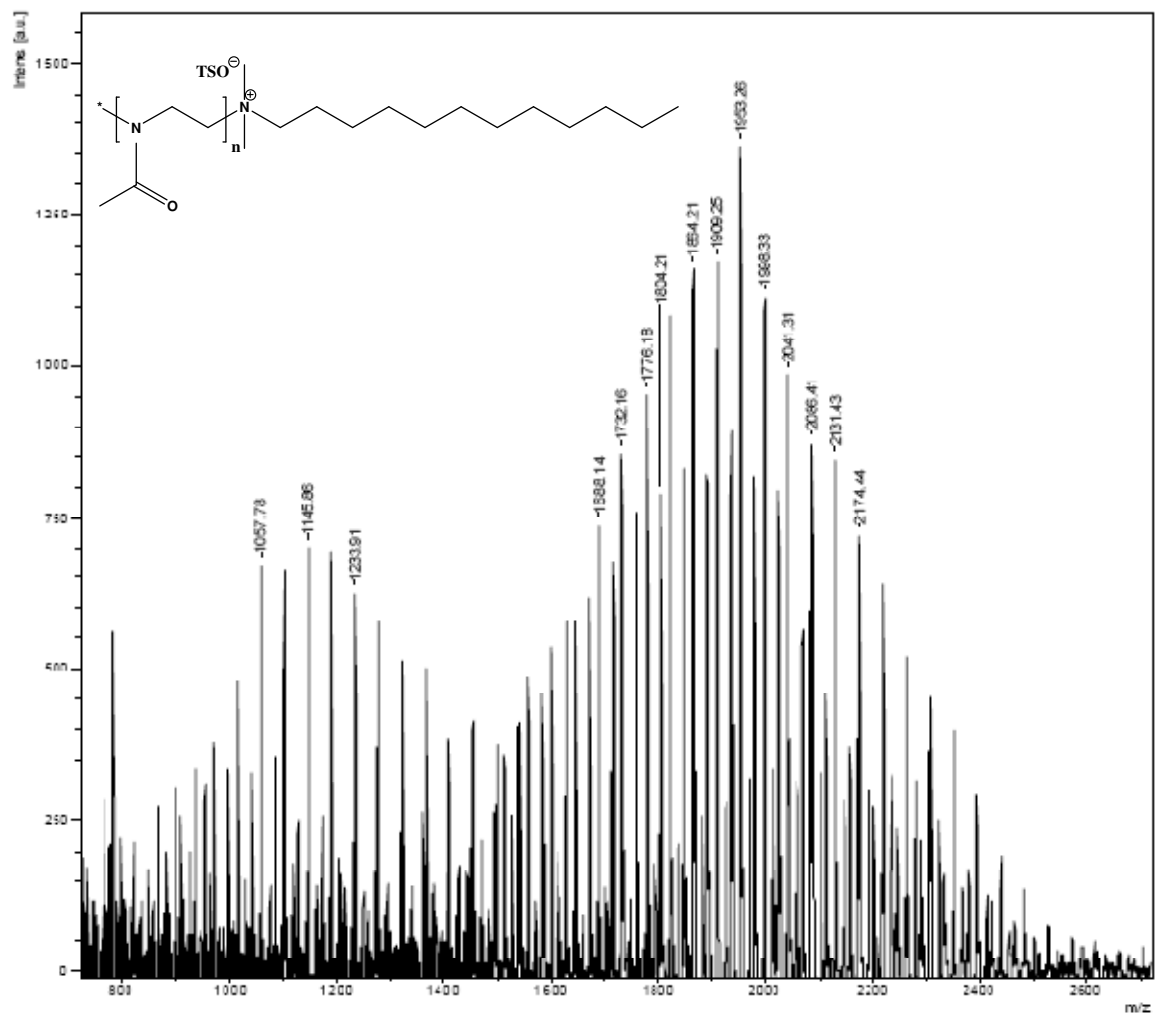
Appendix 2 ¹H-NMR spectrum (400 MHz, D₂O) of LPEI.



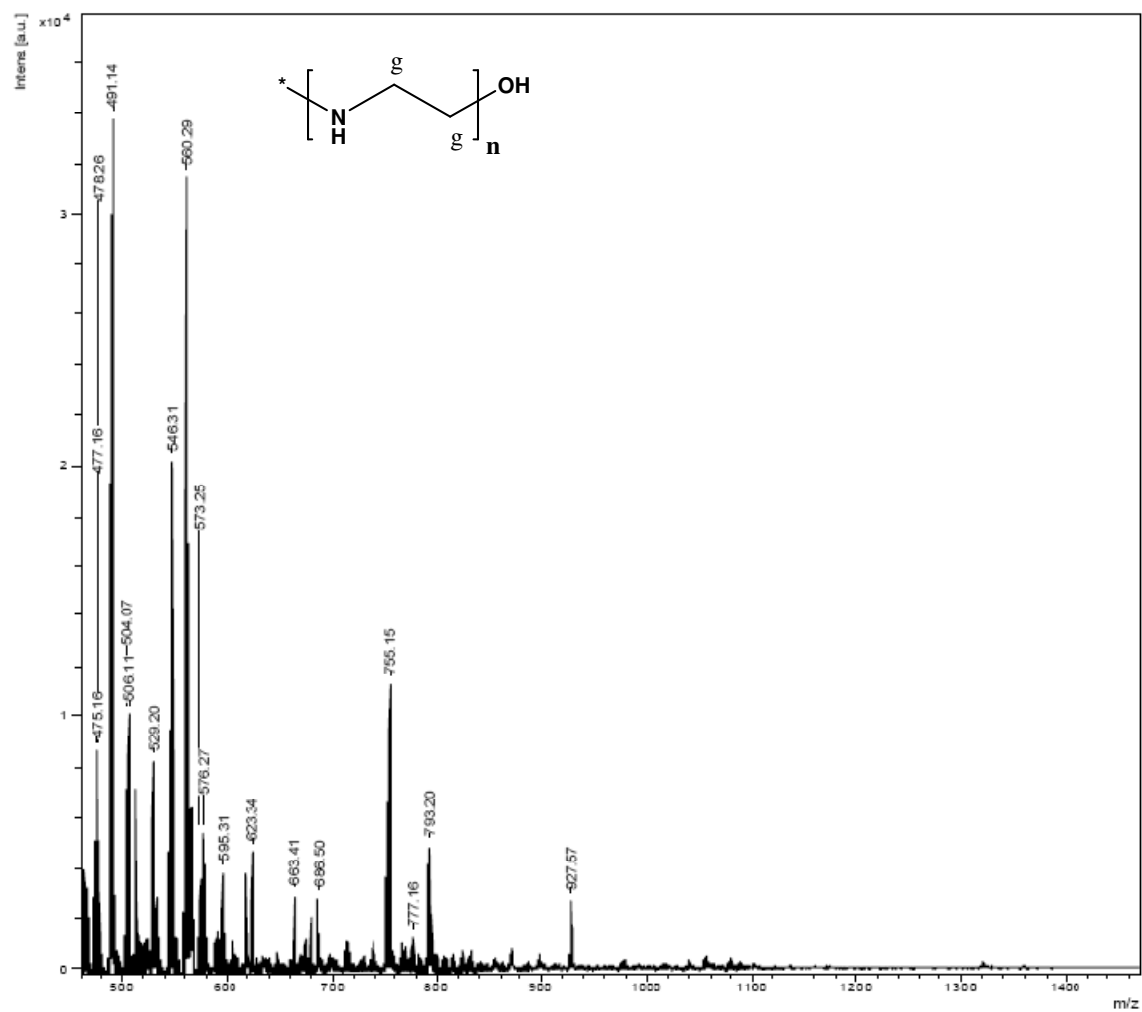
Appendix 3 FT-IR spectrum (NaCl) of PMetOx-DDA.



Appendix 4 FT-IR spectrum (NaCl) of LPEI.



Appendix 5 MALDI-TOF spectrum (dithranol) of PMetOx-DDA_{mw}.



Appendix 6 MALDI-TOF spectrum (dithranol) of LPEI.